

UCRL-6759 (Vol. 1) (Rev. 1)

UCRL-6759-Vol 1  
Rev 1

F  
D-5

Reproduced From  
Best Available Copy

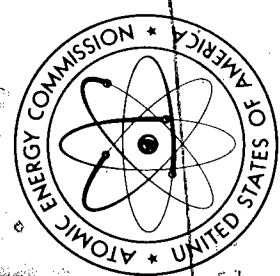
High Explosive Handbook, Volume 1  
Revision 1

Lawrence Radiation Laboratory

# Facsimile Report

DTIC VALUE INSPECTED 4  
20000908 158

Reproduced by  
**UNITED STATES  
ATOMIC ENERGY COMMISSION**  
Division of Technical Information  
P.O. Box 62 Oak Ridge, Tennessee 37830



LOVELACE

DOCUMENT

29411  
NOV 30 1967

# NEFO

# LER

706576

# REVIEWS



MICROCOPY RESOLUTION TEST CHART  
NATIONAL BUREAU OF STANDARDS-1963-A

AUG 2 1967

MASTER

COST PRICE

H.C. \$3.00; R.N. 65

Lawrence Radiation Laboratory  
UNIVERSITY OF CALIFORNIA  
LIVERMORE

UCRL-6759 (Revision 1)  
HIGH EXPLOSIVES HANDBOOK  
(Title: Unclassified)  
VOLUME 1  
Device Engineering Division  
Mechanical Engineering Department  
July 1967

BLANK PAGE

LEGAL NOTICE

This report was prepared as an account of Government sponsored work. Neither the United States, nor the Commission, nor any person acting on behalf of the Commission, makes any warranty or representation, expressed or implied, with respect to the accuracy, completeness, or usefulness of the information contained in this report, or that the use of any information herein may not infringe upon privately owned rights or otherwise cause damage to property or for damages resulting from the use of the information. As used in the above, "person acting on behalf of the Commission" includes any employee or contractor of the Commission, or employee or contractor of any person acting on behalf of the Commission, or provides access to, any information pursuant to his employment or contract with the Commission, or his employment with such contractor.

DISTRIBUTION OF THIS DOCUMENT IS UNLIMITED

This High Explosives Handbook (UCRL-6759, Revision 1) provides information related to the design of nuclear systems. This volume (Volume I of two volumes) contains information on

Primary Explosives  
High Explosives  
Squibs and Primacord  
Adhesives, Fillers, and Coatings used with Explosives  
Solid Propellant Gas Generators

The handbook is issued by the Device Engineering Division of the Mechanical Engineering Department. All inquiries concerning this handbook should be made at the Device Engineering Division Office, Room 2111, Building 170 (New No. 131). This handbook will be updated as new data becomes available.



Richard Stone  
Division Head  
Device Engineering Division  
Mechanical Engineering Department

# SAFETY FIRST

All explosives handling must be in accordance with LRL safety regulations. These are given in:

- 1) Safety and Operational Manual - Site 300
- 2) LRL-Nevada Test Site Safety Manual

These manuals can be obtained at the Hazards Control Office at Site 300. Advice on situations not clearly explained in the manual should be obtained at the same office.

## CONTENTS

	Page No.
<b>PRIMARY EXPLOSIVES</b>	
I General . . . . .	PE-1
II Properties of Primary Explosives . . . . .	PE-1
<b>HIGH EXPLOSIVES</b>	
I General . . . . .	HE-1
IA Definition of High Explosives . . . . .	HE-1
IB Manufacture of High Explosives . . . . .	HE-1
IC Molecular Weights and Atomic Compositions . . . . .	HE-1
II Properties of High Explosives . . . . .	HE-2
IIA Thermodynamic, Physical, and Compatibility Properties . . . . .	HE-2
IIB Mechanical Properties . . . . .	HE-4
IIB1 Mechanical Properties for High Explosives under Short-Duration Loads . . . . .	HE-4
IIB2 Mechanical Properties of High Explosives under Intermediate-Duration Loads . . . . .	HE-13
IIB3 Mechanical Properties of High Explosives under Long-Duration Loads . . . . .	HE-21
IIC Failure Properties of High Explosives . . . . .	HE-22
IC1 Failure Properties of LX-04-1 . . . . .	HE-24
IC2 Failure Properties of PBX 9404 . . . . .	HE-24
IID Thermal Properties of High Explosives . . . . .	HE-25
ID1 Thermal Stability . . . . .	HE-25
ID2 Thermal Stability of Larger Explosive Charges . . . . .	HE-25
IIE Detonation Properties of High Explosives . . . . .	HE-26
IE1 Detonation Velocity Equations . . . . .	HE-26
IE2 Detonation Velocities of High Explosives . . . . .	HE-26
IE3 Chapman-Jouguet Detonation Pressure . . . . .	HE-26
IE4 Cylinder Test Measurements of Explosive Energy . . . . .	HE-27
IE5 Heats of Detonation . . . . .	HE-27
IIF Miscellaneous Properties of High Explosives . . . . .	HE-28
IF1 Melting Points, Boiling Points, and Vapor Pressures of Various High Explosives . . . . .	HE-28
IF2 Solubility of HMX in Various Solvents . . . . .	HE-28
IIG Impact Sensitivities of High Explosives . . . . .	HE-28
IG1 Drop Weight Machine Impact Sensitivities . . . . .	HE-28
IG2 Susan Impact Sensitivities . . . . .	HE-28
IG3 Sliding Impact Sensitivities . . . . .	HE-30
IG4 Gap Test Sensitivities . . . . .	HE-31
III Special Tests and Properties of High Explosives . . . . .	HE-32
IIIA Mechanical Simulation of High Explosives with Mock High Explosives . . . . .	HE-32
IIIB Coefficients of Friction of High Explosives and Mock High Explosives . . . . .	HE-37
IV Special Studies of High Explosives . . . . .	HE-41
IVA LX-04-1 Aging Study . . . . .	HE-41
IVB PBX 9404 Aging Study . . . . .	HE-43
IVC Studies of Viton and HMX . . . . .	HE-44
IVD Stress and Strain Concentrations in High Explosives . . . . .	HE-46
IIE Fracture Surface Pictures . . . . .	HE-46

# BLANK PAGE



## PRIMARY EXPLOSIVES

## I GENERAL

Primary explosives are metastable substances extremely sensitive to ignition by heat, shock, and electrical discharge. Their defining characteristic is that ignition goes instantaneously to high order detonation even in milligram quantities. As a result, they are commonly used in detonators (non-ABC) as starting materials. They also find considerable use in squibs.

Because of their extremely sensitive nature, especially to electrical discharge, great care must be taken in handling primary explosives. In general, the smallest amount possible should be handled and all personnel and equipment must be grounded. Primary explosives should be stored under a suitable liquid in a special magazine and should be dried only in the amount required.

II PROPERTIES OF PRIMARY EXPLOSIVES:  
Table II-1.

Table II-1. Properties of primary explosives.

Property	Lead azide	Lead styphnate	Mercury fulminate
Molecular formula	$PbN_6$	$PbC_6H_3N_3O_8$	$C_2N_2O_2Hg$
Molecular weight	291.3	430.3	284.6
Physical state	Solid	Solid	Solid
Melting point	(a)	(a)	(a)
Density, g/cc	4.8	3.1	4.4
Heat of formation (kcal/mole)	-101	-41	-60
Thermal conductivity (cal/°C cm sec)	$1.55 \times 10^{-4}$	5200 at $\rho = 2.9$	$1 \times 10^{-4}$
Detonation velocity (m/sec)	367	457	5000 at $\rho = 4.0$
Heat of detonation (cal/g)	9	8	427
Impact sensitivity $H_{50}$ (cm)			
Thermal stability			
50-63s (STP)			
g-48 hr			

(a) All explode on heating before melting.

## HIGH EXPLOSIVES

## I

**GENERAL.** All currently available mechanical and physical properties of high explosives (HE) commonly used in weapon designs are presented in this section.

The information in Section II, "FAILURE PROPERTIES OF HIGH EXPLOSIVES," contains much less data than is desired. On the other hand, failure points in the data of other parts can be used as part of the overall failure results. Our goal was to present a set of failure properties to predict failure under arbitrary load histories. The difficulty is that no universally proven failure theory exists. We are trying to find the one most applicable to HE among the many existing theories.

The information given in Section IV, "SPECIAL STUDIES OF HIGH EXPLOSIVES," is presented to enlighten the understanding of the mechanical behavior of HE. The results are interesting and may be of some help to design engineers.

Several discussions and tables of chemistry information, including information on mock explosives, are presented that may be of help to the designer. This information was obtained from the HE section of the Chemistry Department.

The "HIGH EXPLOSIVES" section is concluded with a list of references that are obtainable from the Weapons Division, Chemistry Department, or the Technical Information Department.

## DEFINITION OF HIGH EXPLOSIVES

High explosives are metastable compounds that can react rapidly to give gaseous products at high temperature and pressure. The subsequent expansion of these products is the mechanism by which explosives do useful work. As with primary explosives, reaction can be initiated by shock and heat. High explosives, however, differ from primaries in that:

- 1) Small, unconfined charges, even though ignited, will not usually detonate high order.
- 2) Electrostatic ignition is very difficult (except in explosive dust clouds).
- 3) Considerably larger shocks are required for ignition.

## IB

## MANUFACTURE OF HIGH EXPLOSIVES

Pure explosives are usually synthesized by a sulfuric-nitric acid nitration of organic compounds. The product is separated from the mixed acids by filtration and then worked free of impurities and dried.

TNT is one of the few pure explosives that can be fabricated directly by melting and casting into a desired shape. Most other materials must be diluted either with TNT (thereby unstable) or with plastic (thereby

pressable) before they can be fabricated into useful shapes.

The procedure used for fabricating castable, TNT-containing formulations is as follows: TNT is melted and the desired solid ingredients are added to the melt and stirred. The melt is precrystallized into a slurry, and vacuum is applied just before pouring the slurry into a mold. By carefully controlling the cooling rate, cracking, and density and composition spreads are minimized.

Plastic-bonded explosives (PBX) are pressed from "molding" powders, which may be produced in several ways. A typical preparation is by the slurry technique: Powdered explosive and water are agitated in a container equipped with a cover, condenser, and stirrer. A lacquer composed of the plastic (together with a suitable solvent is added to the slurry. The solvent is removed by distillation, causing the plastic phase to precipitate out on the explosive. The plastic-explosive agglomerates into beads as the stirring and solvent removal are continued. Finally, water is removed from the beads by filtration and drying the resultant product is the molding powder. Good molding powders have a high bulk density and are free-flowing and dustless.

PBX molding powder can be pressed into usable shapes by two methods: compression molding with steel dies, or hydrostatic or isostatic pressing. In the latter method, the explosive is placed in rubber sacks and subjected to fluid pressure. With either method, consolidation of the molding powder into reasonable densities (97% of theoretical) is obtained at pressures between 12,000 and 20,000 psi and molding temperatures between 25 and 120°C. An important and necessary feature of molding is the use of vacuum. The molding powder is normally evacuated to a pressure of less than 1,000  $\mu$  before pressing.

Both pressed and cast explosives are normally machined to final shape. Many intricate forms have been cut successfully. As a rule, machining explosives is similar to machining a conventional plastic except that water is used as a cutting-tool coolant. New explosives are machined remotely until their behavior under machining conditions has been carefully evaluated.

## MOLECULAR WEIGHTS AND ATOMIC COMPOSITIONS

For explosives that are pure chemical compounds, Table IC-1 gives the molecular formula. For explosives that are mixtures, an arbitrary molecular weight

## IC

of 100 was assigned, and an empirical formula corresponding to this weight is cited. For such mixtures, the weight

percentage of an element is given by the product of the atomic weight and empirical formula subscript.

Table IC-1. Molecular weights and atomic compositions of HMX, LX-02-1, LX-04-1, LX-07-2, and NTX 8003.

Explosive	Molecular weight	Subscripts in the molecular or empirical formula $C_aH_bN_cO_dF_eCl_fBr_gI_hSi_kBa_m$				
		a	b	c	d	Other subscripts
HMX	296.2	4	8	8	8	
LX-02-1	100	2.76	4.87	0.83	2.99	k = 0.03
LX-04-1 <sup>a</sup>	100	1.55	2.58	2.30	2.30	e = 0.52
LX-07-2 <sup>a</sup>	100	1.48	2.62	2.43	2.43	e = 0.35
PHX 9404	100	1.40	2.75	2.57	2.69	h = 0.01, f = 0.03
NTX 8003	100	1.50	3.64	1.01	3.31	k = 0.27

<sup>a</sup>LX-07-2 differs from LX-07-1 in particle size. Mechanical properties should be similar.

## II PROPERTIES OF HIGH EXPLOSIVES

### IIA THERMODYNAMIC, PHYSICAL, AND COMPATIBILITY PROPERTIES

The coefficients of expansion, thermal conductivity, and estimated heat capacities of various explosives, explosive mixtures, and binders are presented in Table IIA-1. Thermal expansion data were obtained with two pieces of equipment: a bulk dilatometer and a linear expansion apparatus. The two pieces of equipment produce comparable results where checks have been made. Thermal conductivity measurements were obtained on an apparatus similar to that used by the National Bureau of Standards.

Engineering Note ENW-334, dated Sept 10, 1964, describes this equipment. Heat capacities were estimated by D. Miller of the Chemistry Department using the Kopp-Joules rule. The estimates

of the estimates listed are believed accurate within  $\pm 10\%$ .

The results of studies made on the compatibility of various explosives with materials of interest are presented in Table IIA-2. D. Seaton of the Chemistry Department provided much of this information. Classified compatibility data not presented here may be obtained from Mr. Seaton.

$$C_{PT} = C_{P70} \left[ \frac{C_{PT} \text{ of RDX}}{C_{P70} \text{ of RDX}} \right]$$

Table IIA-1 Thermodynamic and physical properties of various high explosives, explosives mixes, and binders.

Material	Composition, wt %	Linear coefficient of thermal expansion		Estimated heat capacity		Thermal conductivity		Density, g/cc	G. point, °F
		Temp., °F	Temp., °F	Temp., °F	Temp., °F	Temp., °F	Temp., °F		
LX-04-1	HMX: 85 Viton: 15	-65 to -18 -18 to 165	23.5 39.5	70	0.28	-65 0 70 120 165	0.23 0.23 0.22 0.22 0.21	1.860 to 1.870	-13
PHX 9404	HMX: 94 NC <sup>20</sup> : 3 CEP <sup>20</sup> : 3	-65 to -29 -29 to 165	28.1 32.2	70	0.28	-65 0 70 120 165	0.28 0.26 0.25 0.23 0.22	1.828 to 1.842	-29
LX-07-1	HMX: 90 Viton: 10	-65 to -18 -18 to 165	26.7 34.8	70	0.28	-56 -25 -12 72 130	0.25 0.25 0.24 0.23 0.22	1.860 to 1.870	-18
LX-02-1	PETN: 73.5 RDX: 17.6 Acetyl-tributyl citrate: 6.9 Cab-O-Sil: 2.0	-4 to 122	71.5	70	0.29	NA	NA	1.44	None above -4
XTX 8003	PETN: 80 Sylgard: 20	-22 to 158	76.6	70	0.27	NA	NA	1.544	NA
HMX	Not applicable	-65 to 165	22.0	70	0.28	NA	NA	1.894	None
PETN	Not applicable	-4 to 158	46.1	NA	NA	NA	NA	1.776	None
Viton	Fluoro-elastomer	165 to 165	135	NA	NA	NA	NA	1.819	-18
Sylgard	Silicone rubber	165 to 165	180	NA	NA	NA	NA	NA	None above -65
LM-04-0	Cyanuric acid: 59.7 tronic mock for LX-04-1: 23.3	-65 to -18 -18 to 66	21.2 33.7	NA	NA	-76 -40 14 68 134 131	0.72*** 0.68 0.65 0.62 0.58 0.56	1.705 to 1.715	-18
LX-04-1	Viton: 16.8	66 to 165	40.0	81 to 109	0.23	70	0.67	1.870 to 1.880	NA
RM-04-0	Cyanuric acid: 70.5 RG (Mech. prop. mock for LX-04-1): 14.5	-22 to 165	36.9	109 to 140	0.23	100	0.66	1.880	NA
90010	Peric: 48.0 Barium prop. nitrate: 48.0 mock for RDX: 4.0 CEP <sup>20</sup> : 3.3	-65 to 68	20.8	140 to 174	0.24	172	0.66	1.842	NA

\* Nitrocellulose.

\*\* Tris(2-chloroethyl) phosphate.

\*\*\* Thermal conductivity values were obtained by R. Cornwell, Engineering Test Section, Support Engineering Division.

NA: No data available.



Table IIA-2. Chemical compatibilities of various structural materials with high explosives.

Structural material	LX-04-1	PBX 9404	LX-07-1	PBX 9007	LX-02-1	NTX-8003
D 38	C	C	C	C	C	C
Nickel	A	A	A	A	A	A
Dow Corning 200 and Dow Corning 4	A	A	A	A	A	A
Polycarbonate	A	A	A	A	A	A
Polypropylene	A	A	A	A	A	A
Asbestos filled diallyl phthalate,	A	A	A	A	A	A
diallyl phthalate	A	A	A	A	A	A
Polyvinyl chloride	A	A	A	A	A	A
Cellulose acetate butyrate	A	A	A	A	A	A
Polyethylene	A	A	A	A	A	A
Polyurethane foam	B 1	B 1	B 1	B 1	B 1	B 1
Polystyrene foam	A	A	A	A	A	A
Cellular silicone	B 1	B 1	B 1	B 1	B 1	B 1
RTV 501, 521, 93009, 93029	A	A	A	A	A	A
Neoprene	A	A	A	A	A	A
Fiberglass	A	A	A	A	A	A

A Compatibility OK for long term storage.

B Compatibility OK for short term storage (less than 30 days).

C Specific authorization needed for use.

1 OK for device applications. Each foam must be evaluated if subjected to long term storage.

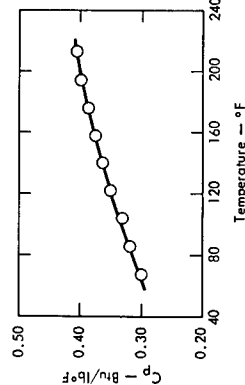


Fig. IIA-1. Specific heat of RDX.

## IIB

## MECHANICAL PROPERTIES

High explosives are nonlinear, viscoelastic materials. To describe completely the mechanical properties of a nonlinear, viscoelastic material would require a very long time and a large effort. Since no immediate need exists for a complete description, we concentrated on properties of immediate usefulness. A small part of our continuing effort is being spent on nonlinear properties in anticipation of future needs and to improve our knowledge of HE mechanical behavior.

W-Division problems were drawn upon for guidance on the type of properties to be measured. All major design problems in W-Division fall into one of three categories: short-duration loads, intermediate-duration loads, and long-duration loads.

The short-duration loads include those imposed by shock and vibration, and nuclear countermeasures. Intermediate-duration loads include the thermally

induced loads and the transportation preloads. Dead weight and assembly preloads in storage constitute the long-duration loads. Problems belonging to the short-duration time regime subject to the conditions given in the opening statement of Section IIB1 can be safely treated as purely elastic since the creep mechanisms in the HE's essentially do not operate during the short duration of the load. The other two load categories are inherently viscoelastic; however, a viscoelastic fluid description may be adequate for the long-duration behavior under constant loads. We are considering this and other simplifying possibilities.

## IIB1

## Mechanical Properties for High Explosives under Short-Duration Loads

Short-duration loads include those induced by shock and vibration, and nuclear countermeasures. At any temperature, any load whose duration or cyclic period is below the curve of Fig. IIB1-1 is considered short-duration. In these short time spans, the creep mechanisms do not have a chance to operate, thereby rendering an elastic behavior. In addition, if the load is less than the maximum given in Fig. IIB1-2, then the present data indicate that LX-04-1 and PBX 9404 may be considered isotropic, linear, elastic materials. A similar statement can be made for LX-07-1, and we speculate that the maximum load curve will be close to that for LX-04-1 in Fig. IIB1-2. However, this needs to be experimentally verified. The moduli presented on mechanical properties are known to apply to HE's which have had no prior load history (i.e., virgin HE's) or to HE's which have recovered from any prior load history.

However, even with the lack of sufficient data, we feel the moduli can be safely used for nonvirgin HE's under most circumstances.

Amorphous materials such as the binders in HE's respond in two ways under short-duration loadings: quasistatically and ultrasonically. A plausible explanation is that the quasistatic moduli characterize the instantaneous motions between the chain molecules, whereas the ultrasonic moduli characterize the atomic motions of the atoms in the molecules. The ultrasonic moduli are much higher than the quasistatic moduli. Both deformation mechanisms always exist, but their relative degree of existence depends on the duration and magnitude of the load. High pressure impact loads lasting for only a few milliseconds produce mainly the ultrasonic responses. Low frequency vibrations excite mainly the quasistatic responses.

All available quasistatic and ultrasonic moduli for LX-04-1, PBX 9404, and LX-07-1 are presented in this subsection. All ultrasonic data were obtained by H. L. Duregan and B. A. Kuhn of Support Engineering Division.

## IIB1a

## Properties of LX-04-1 under Short-Duration Loads

Properties in this section are as follows:  
LX-04-1 initial longitudinal modulus: Fig. IIB1a-1.  
LX-04-1 initial Poisson's ratio: Fig. IIB1a-2.  
LX-04-1 initial shear modulus: Fig. IIB1a-3.  
LX-04-1 initial bulk modulus: Fig. IIB1a-4.  
Uniaxial tensile fast load rate for LX-04-1: Fig. IIB1a-5.  
Uniaxial tension properties of LX-04-1: Fig. IIB1a-6.  
LX-04-1 uniaxial tensile stress strain under high rate loading: Fig. IIB1a-7.  
Ultrasonic longitudinal velocity of LX-04-1: Fig. IIB1a-8.  
Ultrasonic shear modulus of LX-04-1: Fig. IIB1a-9.  
Ultrasonic Young's modulus of LX-04-1: Fig. IIB1a-10.  
Ultrasonic Poisson's ratio of LX-04-1: Fig. IIB1a-11.  
Ultrasonic shear velocity of LX-04-1: Fig. IIB1a-12.

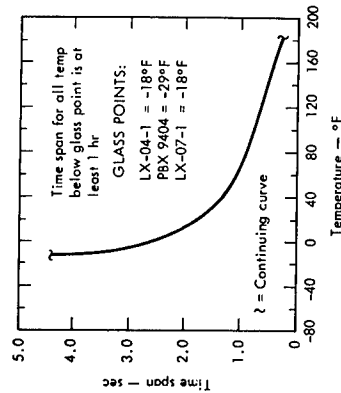


Fig. IIB1-1. Approximate time span for short-duration loads vs temperature for LX-04-1, PBX 9404, and LX-07-1.

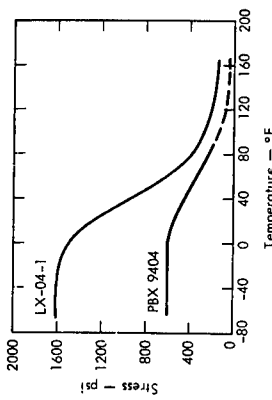


Fig. IIB1-2. Maximum allowable stress for isotropic linear elastic theory to hold under short-duration loads.

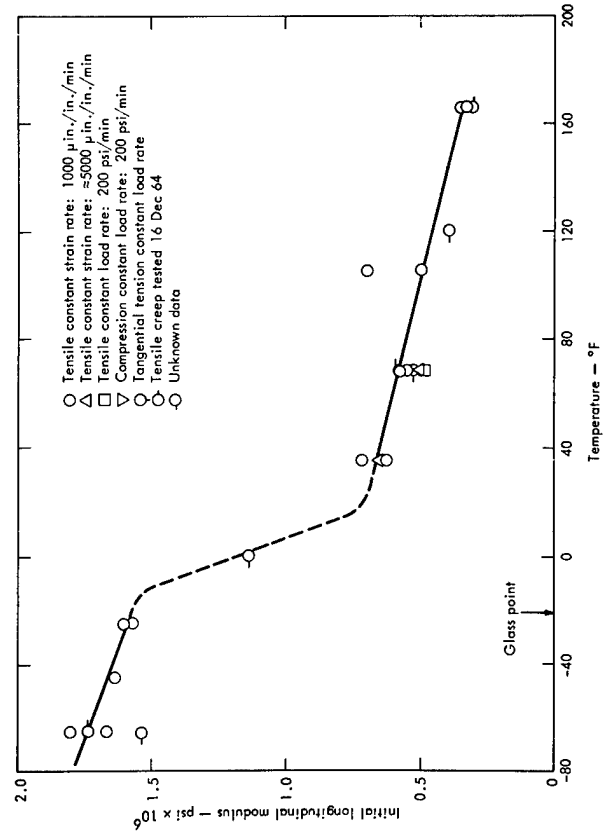


Fig. IIB1a-1. LX-04-1 initial longitudinal modulus.

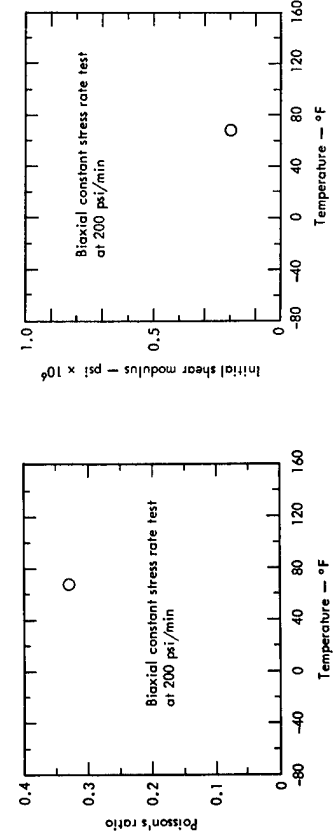


Fig. IIB1a-2. LX-04-1 initial Poisson's ratio.

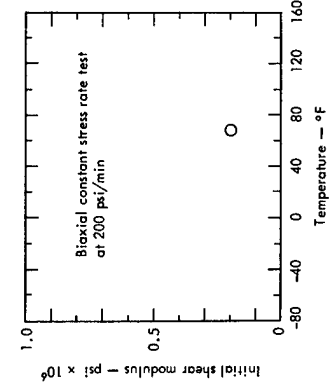


Fig. IIB1a-3. LX-04-1 initial shear modulus.

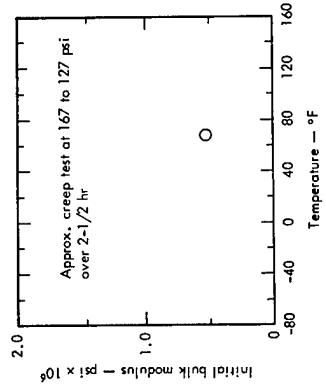


Fig. IIB1a-4. LX-04-1 initial bulk modulus.

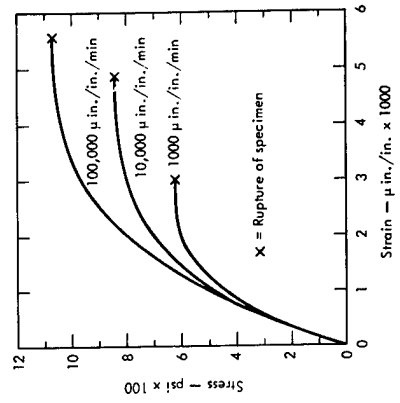


Fig. IIB1a-6. Uniaxial tension properties of LX-04-1. Constant strain rate. Test temperature, 35°F.

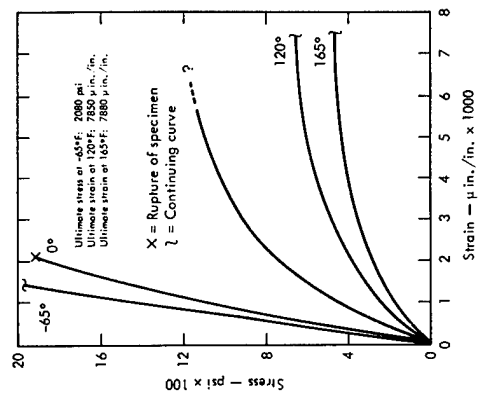


Fig. IIB1a-5. Uniaxial tensile, fast load rate for LX-04-1 (Rate: 11,000  $\text{psi/sec}$ ).

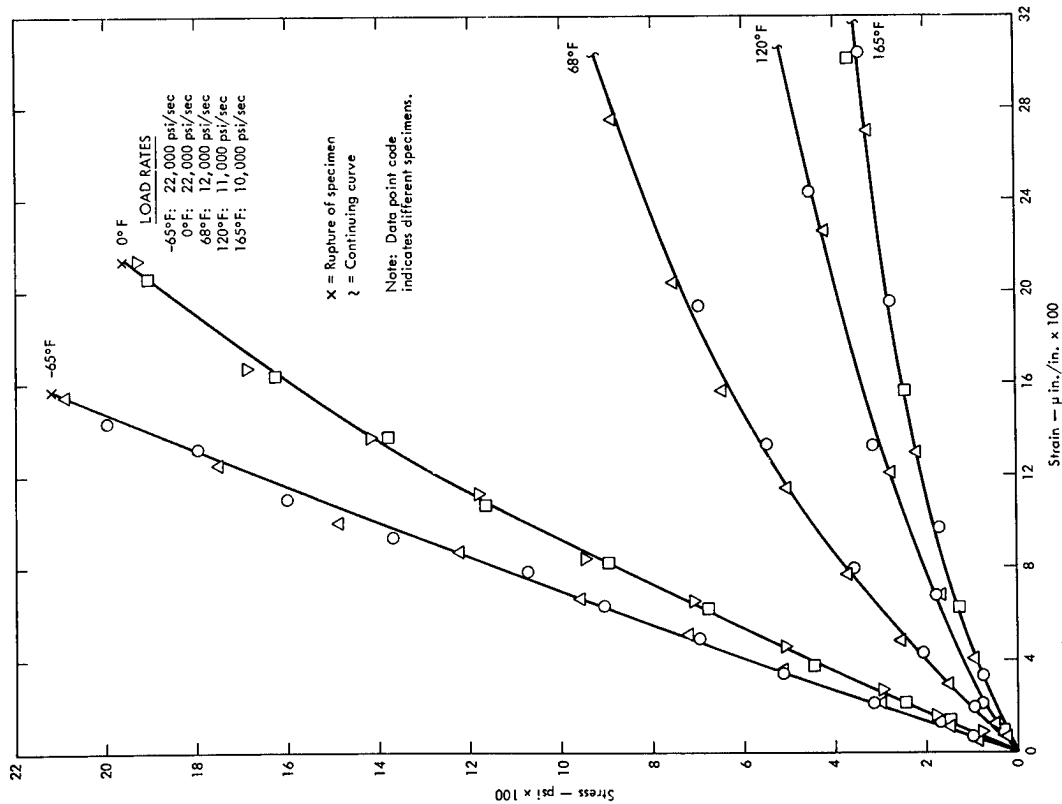


Fig. IIB1a-7. Uniaxial tensile stress-strain for LX-04-1 under high rate loading.

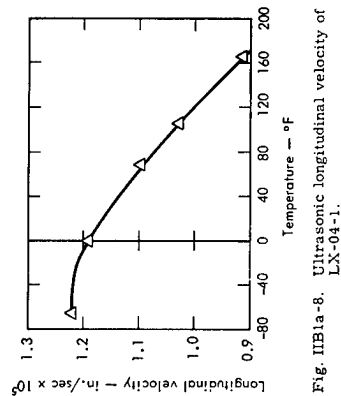


Fig. IIB1a-8. Ultrasonic longitudinal velocity of LX-04-1.

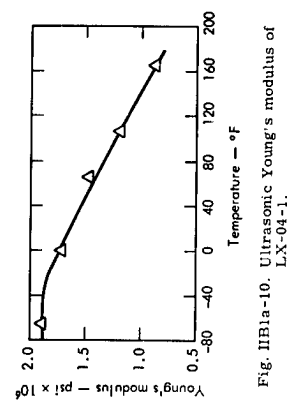


Fig. IIB1a-10. Ultrasonic Young's modulus of LX-04-1.

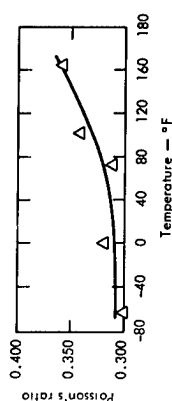


Fig. IIB1a-11. Ultrasonic Poisson's ratio of LX-04-1.

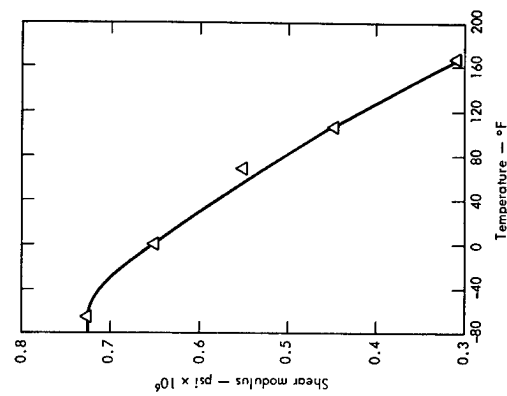


Fig. IIB1a-9. Ultrasonic shear modulus of LX-04-1.

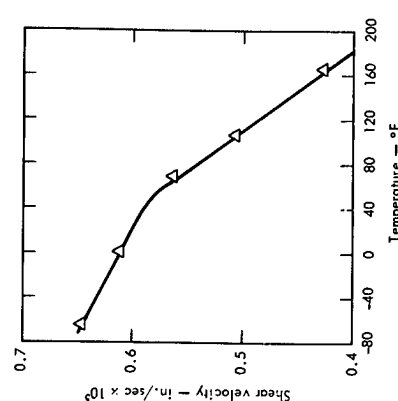


Fig. IIB1a-12. Ultrasonic shear velocity of LX-04-1.

IIB1b Properties of PBX 9404 under Short-Duration Loads  
Properties in this section are as follows:

- PBX 9404 initial longitudinal modulus: Fig. IIB1b-1.
- PBX 9404 initial longitudinal modulus upon unloading: Fig. IIB1b-2.
- PBX 9404 initial Poisson's ratio: Fig. IIB1b-3.

- Ultrasonic longitudinal velocity of PBX 9404: Fig. IIB1b-4.
- Ultrasonic shear velocity of PBX 9404: Fig. IIB1b-5.
- Ultrasonic Young's modulus of PBX 9404: Fig. IIB1b-6.
- Ultrasonic Poisson's ratio of PBX 9404: Fig. IIB1b-7.
- Ultrasonic shear modulus of PBX 9404: Fig. IIB1b-8.

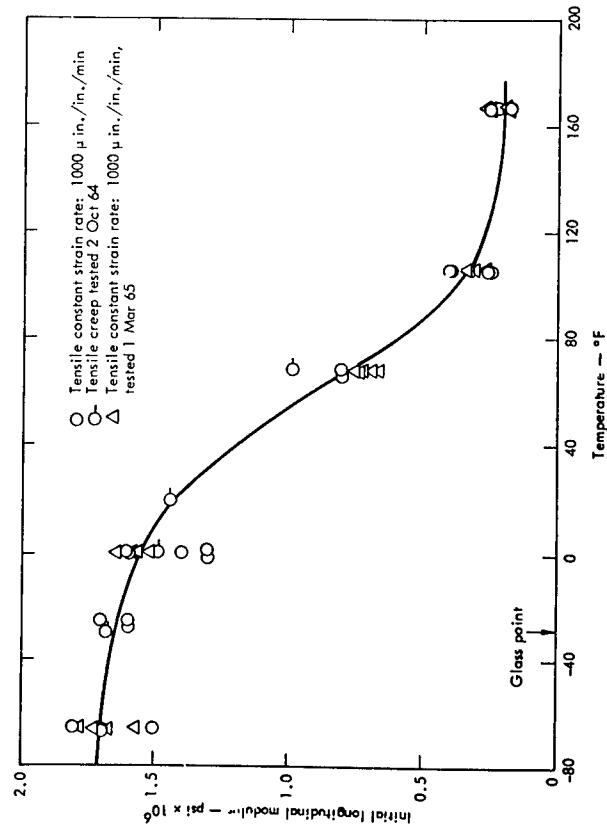


Fig. IIB1b-1. Initial longitudinal modulus of PBX 9404.

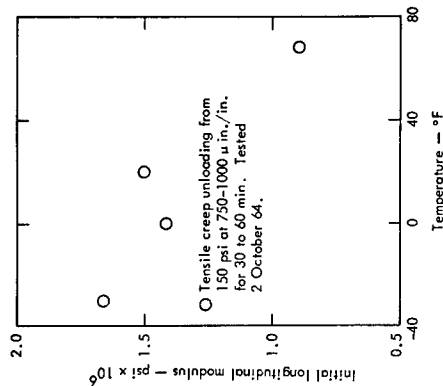


Fig. IIB1b-2. Initial longitudinal modulus of PBX 9404 upon unloading.

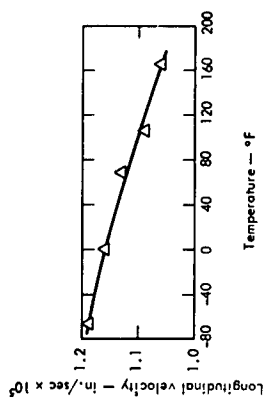


Fig. IIB1b-4. Ultrasonic longitudinal velocity of PBX 9404.

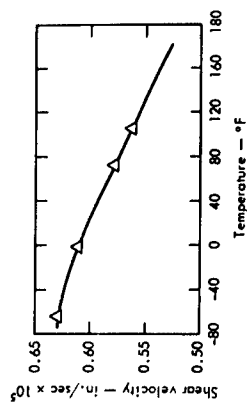


Fig. IIB1b-5. Ultrasonic shear velocity of PBX 9404.

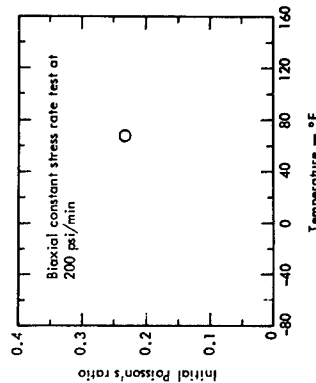


Fig. IIB1b-3. Initial Poisson's ratio of PBX 9404.

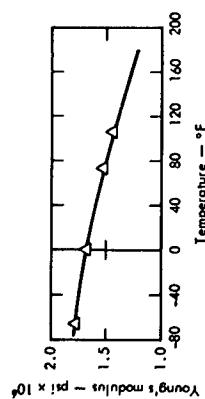


Fig. IIB1b-6. Ultrasonic Young's modulus of PBX 9404.

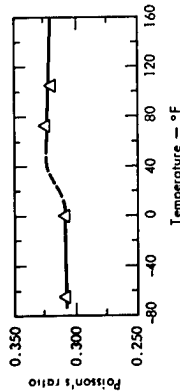


Fig. IIB1b-7. Ultrasonic Poisson's ratio of PBX 9404.

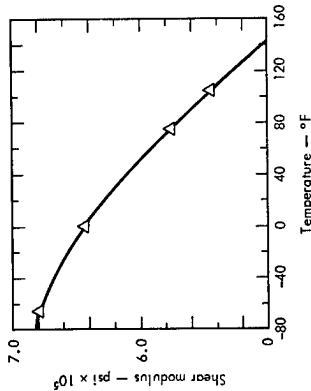


Fig. IIB1b-8. Ultrasonic shear modulus of PBX 9404.

# IIB1c Properties of LX-07-1 under Short-Duration Loads

Properties in this section are as follows:  
LX-07-1 initial longitudinal modulus:  
Fig. IIB1c-1.

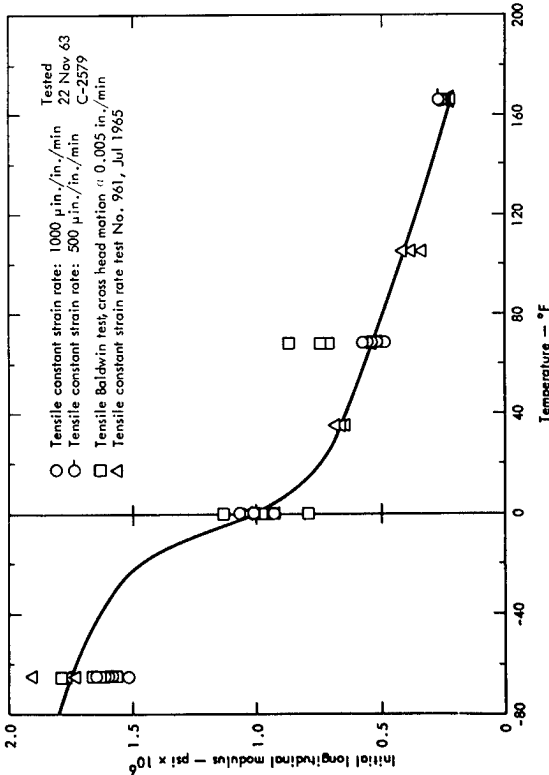


Fig. IIB1c-1. Initial longitudinal modulus of LX-07-1.

## IIB2 Mechanical Properties of High Explosives under Intermediate-Duration Loads

Intermediate-duration loads are those induced by the usual temperature changes experienced by a weapon and by the dead weight of the weapon during any transportation. A nonlinear, viscoelastic description is generally needed for these loads above the glass-transition temperature, if the load is very low, below 20 psi say, a linear viscoelastic description may be adequate. This needs to be further verified, but for an analytical solution to a boundary-value problem with very low loads, a linear, viscoelastic analysis should give a fair first approximation of the actual behavior. Below the glass-transition temperature, a linear elastic description is adequate, and the appropriate data under short-duration loads can be used.

Because of the nonlinearity and the viscoelasticity of the HE's behavior under most intermediate-duration loads, the use of intermediate-duration data must be sure that the data he uses involves a load and a duration approximately the same as those of his problem. Otherwise, a wrong prediction can result especially with respect to the failure point.

At the present time, we do not have enough data to completely characterize the nonlinear, viscoelastic behavior. We strove mainly to provide a good indication of the extent of nonlinearity and sufficient information on which to base engineering judgements for a large range of load conditions.

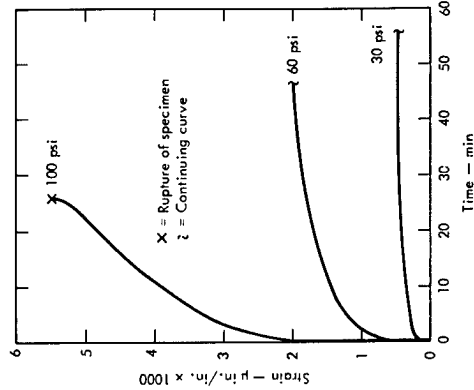


Fig. IIB2a-1. Uniaxial tension creep of LX-04-1 at 165°F. Sixty minute plot.

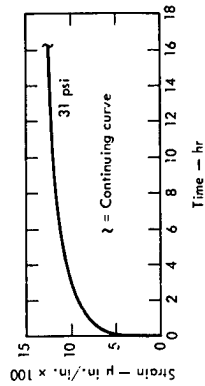


Fig. IIB2a-2. Uniaxial tension creep of LX-04-1 at 165°F. Sixteen hour plot.

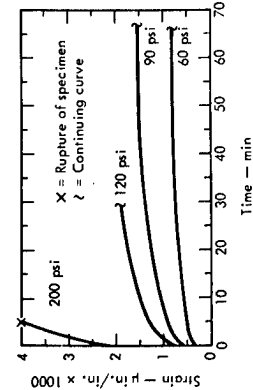


Fig. IIB2a-3. Uniaxial tension creep of LX-04-1 at 120°F. Sixty minute plot.

## IIB2a Properties of LX-04-1 under Intermediate-Duration Loads

Properties in this section are as follows:  
LX-04-1 uniaxial tension creep: temp 165°F; 60 min plot: Fig. IIB2a-1.  
LX-04-1 uniaxial tension creep: temp 165°F; 16 hr plot: Fig. IIB2a-2.  
LX-04-1 uniaxial tension creep: temp 120°F; 60 min plot: Fig. IIB2a-3.  
LX-04-1 uniaxial tension creep: temp 120°F; 60 hr plot: Fig. IIB2a-4.  
LX-04-1 uniaxial tension creep: temp 68°F; 60 min plot: Fig. IIB2a-5.  
LX-04-1 uniaxial tension creep: temp 68°F; 16 hr plot: Fig. IIB2a-6.  
LX-04-1 uniaxial tension creep: temp 0°F; 60 min plot: Fig. IIB2a-7.  
LX-04-1 uniaxial tension creep: temp -65°F; 60 min plot: Fig. IIB2a-8.  
LX-04-1 uniaxial constant strain rate tensile test: Fig. IIB2a-9.  
LX-04-1 constant rate cross-head deflection test: Fig. IIB2a-10.

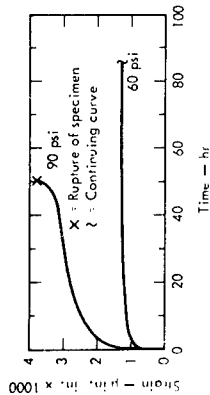


Fig. IIB2a-4. Uniaxial tensile creep of LX-04-1 at 120°F. Fifty hour plot.

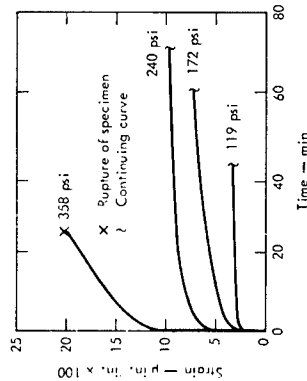


Fig. IIB2a-5. Uniaxial tension creep of LX-04-1 at 60°F. Sixty minute plot.

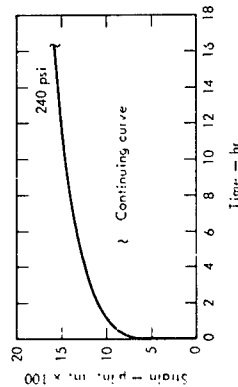


Fig. IIB2a-6. Uniaxial tension creep of LX-04-1 at 68°F. Sixteen hour plot.

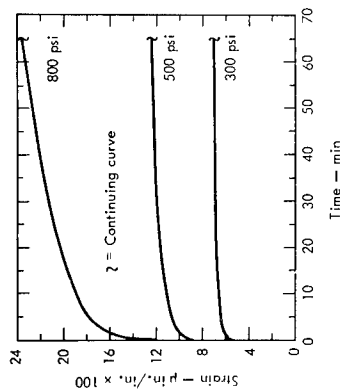


Fig. IIB2a-7. Uniaxial tension creep of LX-04-1 at 0°F. Sixty minute plot.

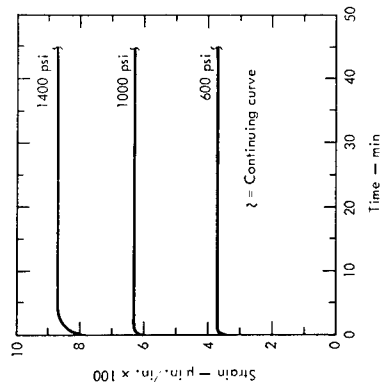


Fig. IIB2a-8. Uniaxial tension creep of LX-04-1 at -65°F. Sixty minute plot.

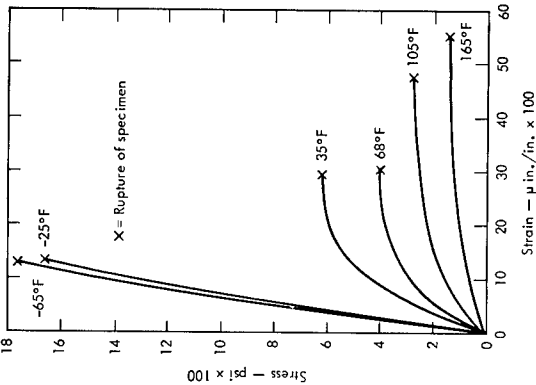


Fig. IIB2a-9. Uniaxial constant strain rate tensile test of LX-04-1. Strain rate equals 1000 in./in./min.

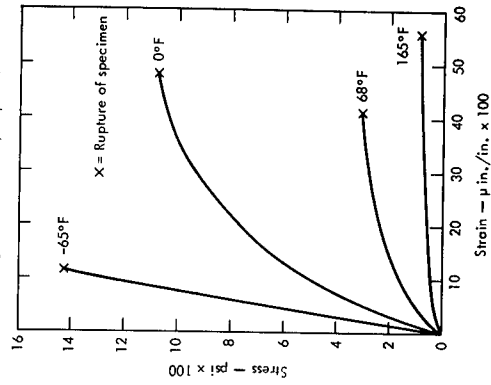


Fig. IIB2a-10. Constant rate cross-head deflection test of LX-04-1. Rate = 0.005 in./min.

IIB2b Properties of PBX 9404 under Intermediate-Duration Loads  
Properties in this section are as follows:  
PBX 9404 uniaxial tension creep; temp 68°F; 60 min plot; Fig. IIB2b-1.  
PBX 9404 uniaxial tension creep; temp 20°F; 60 min plot; Fig. IIB2b-2.  
PBX 9404 uniaxial tension creep; temp 0°F; 60 min plot; Fig. IIB2b-3.  
PBX 9404 uniaxial tension creep; temp -28°F; 60 min plot; Fig. IIB2b-4.  
PBX 9404 uniaxial constant strain rate tensile test; Fig. IIB2b-5

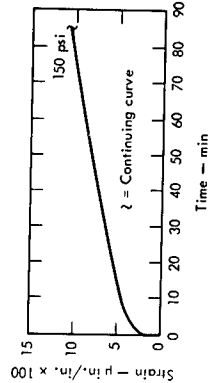


Fig. IIB2b-1. PBX 9404 uniaxial tension creep at 68°F. Sixty minute plot.

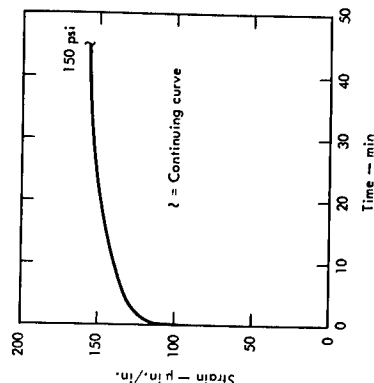


Fig. IIB2b-2. PBX 9404 uniaxial tension creep at 20°F. Sixty minute plot.

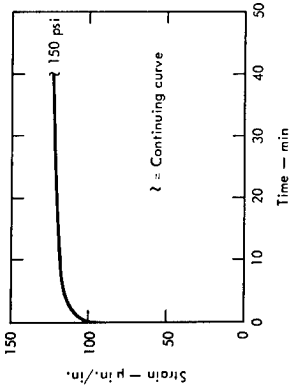


Fig. IIB2b-3. PBX 9404 uniaxial tension, creep at 0°F. Sixty minute plot.

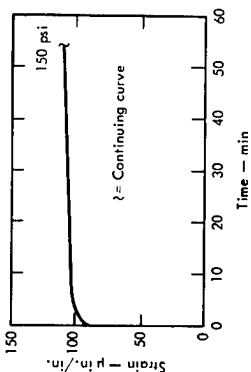


Fig. IIB2b-4. PBX 9404 uniaxial tension creep at -28°F. Sixty minute plot.

IIB2c Properties of LX-07-1 under Intermediate-Duration Loads  
Properties in this section are as follows:  
Uniaxial constant strain rate tensile test of LX-07-1: Fig. IIB2c-1.  
IIB2c-2 10% tensile creep, temp 68°F: Fig. IIB2c-3.  
LX-07-1 tensile creep, temp 105°F: Fig. IIB2c-4.  
LX-07-1 tensile creep, temp 120°F: Fig. IIB2c-5.  
LX-07-1 tensile creep, temp 165°F: Fig. IIB2c-6.  
LX-07-1 tensile creep, temp 68°F: Fig. IIB2c-7.  
LX-07-1 tensile creep, temp 105°F: Fig. IIB2c-8.  
LX-07-1 tensile creep, temp 120°F: Fig. IIB2c-9.

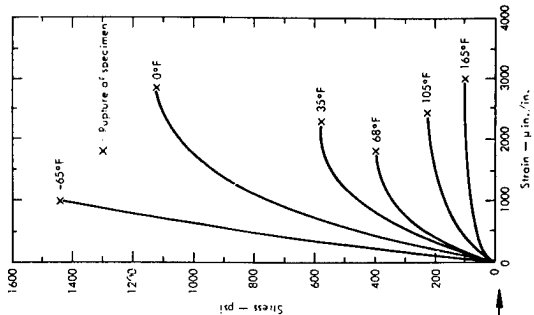


Fig. IIB2c-1. Uniaxial constant strain rate tensile test of LX-07-1. Strain rate equals 1000 μ in./in./min. Typical of Lot A377.

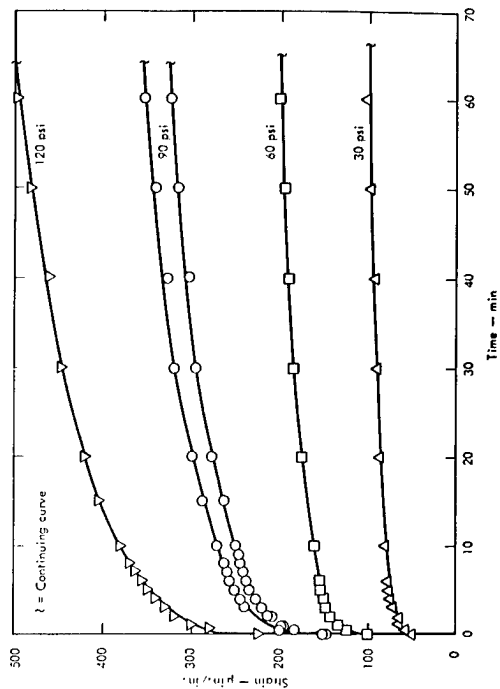


Fig. IIB2c-2. Tensile creep of LX-07-1 at 68°F. Sixty minute plot.

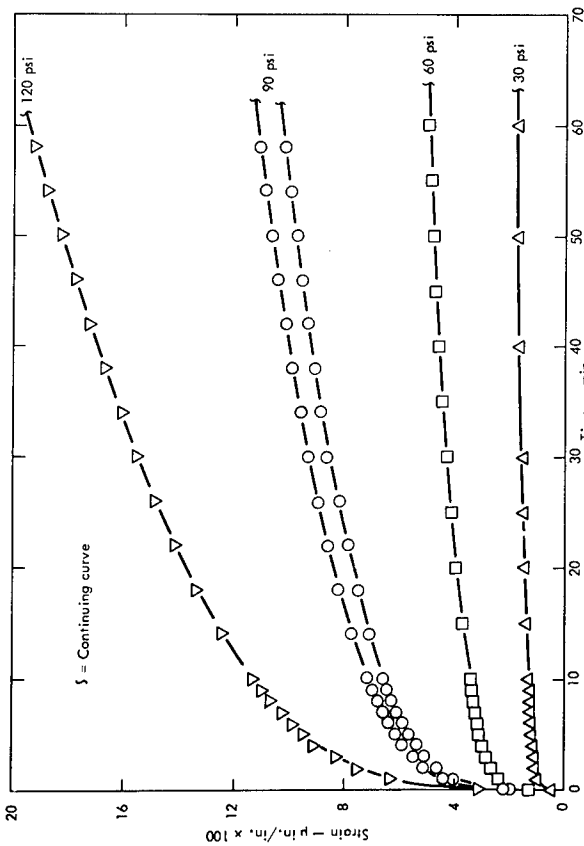


Fig. IIB2c-3. Tensile creep of LX-07-1 at 105°F. Sixty minute plot.

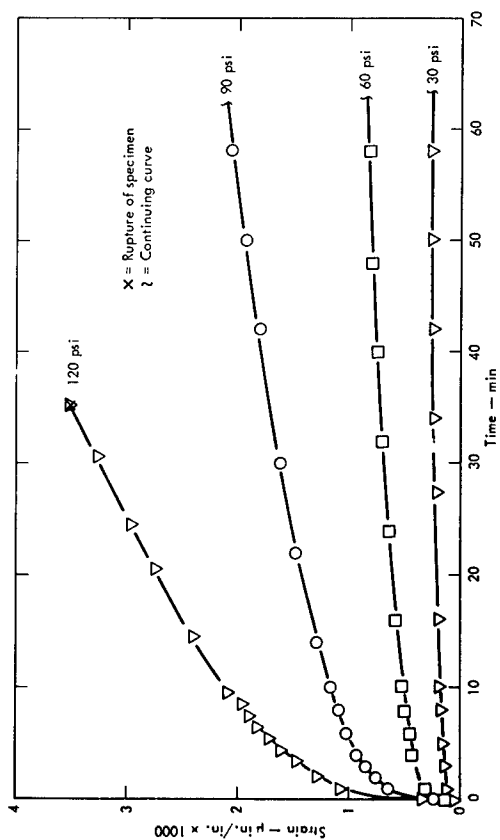


Fig. IIB2c-4. Tensile creep of LX-07-1 at 120°F. Sixty minute plot.

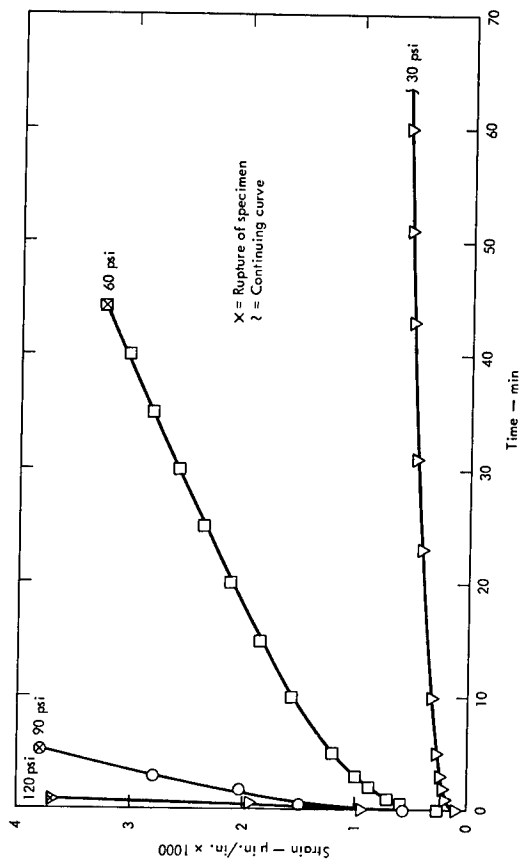


Fig. IIB2c-5. Tensile creep of LX-07-1 at 165°F. Sixty minute plot.

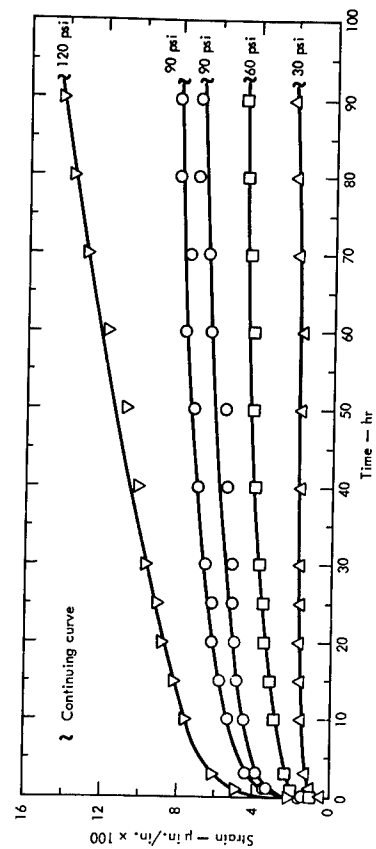


Fig. IIB2c-6. Tensile creep of LX-07-1 at 68°F. Sixty hour plot.



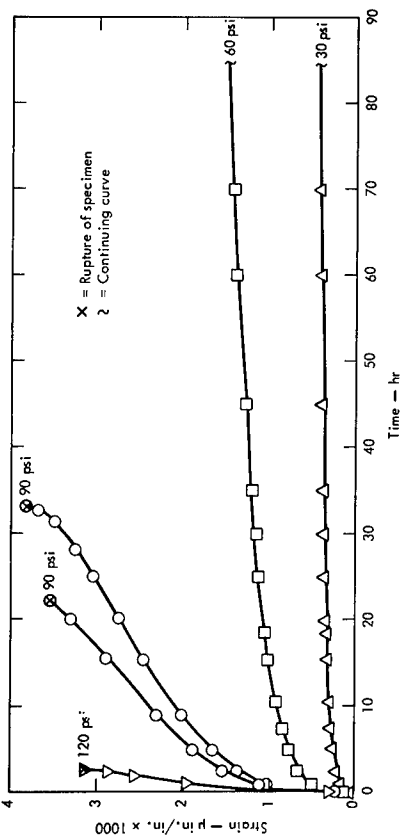


Fig. IIB2c-7. Tensile creep of LX-07-1 at 105°F. Sixty hour plot.

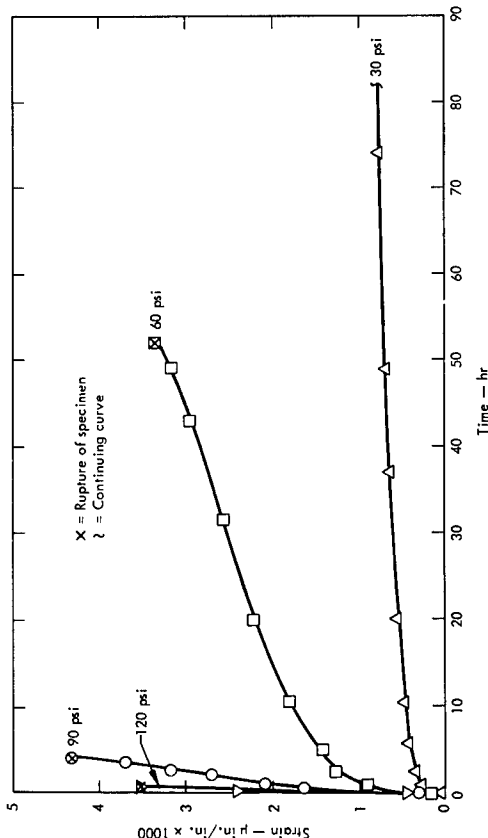


Fig. IIB2c-8. Tensile creep of LX-07-1 at 120°F. Sixty hour plot.

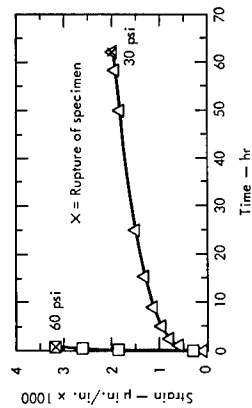


Fig. IIB2e-9. Tensile creep of LX-07-1 at 165°F. Sixty hour plot.

### IIB3 Mechanical Properties of High Explosives under Long-Duration Loads

The weight of the weapon during storage constitutes the only significant long-duration load. High explosives behave nonlinearly and viscoelastically under this load at temperatures above the glass-transition temperature. Assuming that the loads remain constant throughout storage, two approximate descriptions of actual behavior are possible, an equilibrium elastic description or a very viscous fluid description. (An equilibrium elastic modulus is not the same as the initial elastic modulus since the former is usually an order of magnitude lower than the latter.) Experimental data supports more strongly the very viscous fluid description, and so does the fact that the binders (for LX-04-1, PBX 9404, and LX-07-1) are noncrosslinked thermoplastics. This implies that complete confinement of HE is advisable to avoid large deformations and eventual rupture when subjected to large long-duration loads, and it is advisable to avoid sustained large loads whenever possible.

Below the glass-transition temperature, the HE's can be treated as linear elastic materials, and the appropriate results in Subsection IIB2a can be used.

### IIB3a

Properties of LX-04-1 under Long-Duration Loads  
Properties in this section are:  
LX-04-1 uniaxial compressive creep;  
LX-04-1 uniaxial tensile creep;  
LX-04-1 tensile creep, temp 120°F;  
Fig. IIB3a-2.

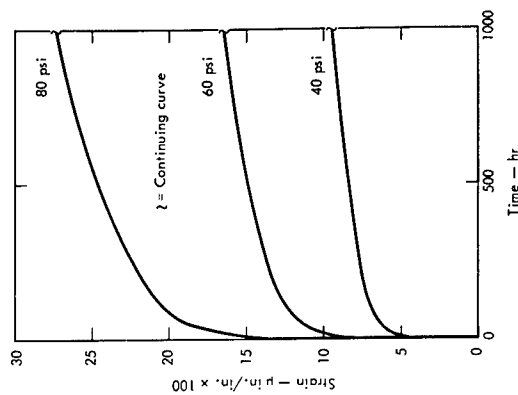


Fig. IIB3a-1. Uniaxial compressive creep of LX-04-1 at 135°F. One thousand hr plot.

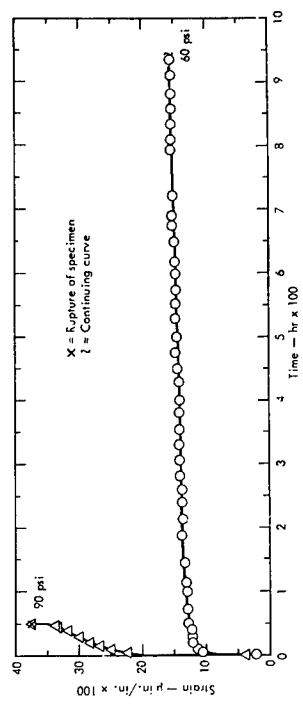


Fig. IIB3a-2. Tensile creep of LX-04-1 at 120°F.

The results shown in Figs. IIB3a-1, IIB3a-2, IIB3b-1 and IIB3b-2 are from tests of 1000 hr or longer.

**IIIB3b** Properties of PBX 9404 under Long-Duration Loads  
Properties in this section are as follows:  
PBX 9404 uniaxial compressive creep;  
temp 70°F; 1000 hr plot; Fig. IIB2b-1.  
PBX 9404 uniaxial compressive creep;  
temp 115°F; 3000 hr plot; Fig. IIB3b-2.

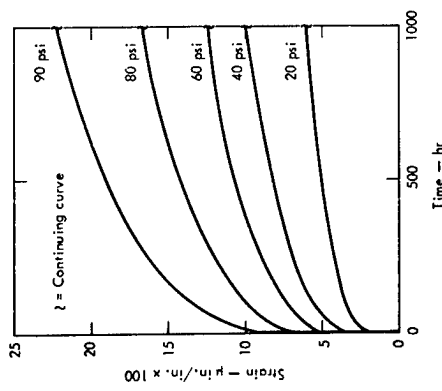


Fig. IIB3b-1. Uniaxial compressive creep of PBX 9404 at 70°F. One thousand hr plot.

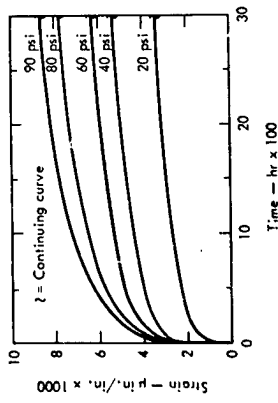


Fig. IIB3b-2. Uniaxial compressive creep of PBX 9404 at 115°F. Three thousand hr plot.

### FAILURE PROPERTIES OF IIHG EXPLOSIVES

The mechanical failure of HE's is dependent on the load history. Rapid loadings or low temperatures result in a high ultimate stress and a low ultimate strain. Conversely slow loadings or high temperatures give a low ultimate stress and a high ultimate strain. The user of the handbook must be sure that the load and duration involved in the data being used are approximately the same as those of his actual problem. Otherwise a wrong prediction can result.

The primary mode of failure for HE's is on a plane normal to the maximum tensile stress. If tensile stresses are absent or very low, failure will occur in shear. Therefore, shear failure can be expected under totally compressive loads.

Failure stresses and strains for biaxial and triaxial states of stress are different from those for a uniaxial state of stress. In general, a biaxial failure stress is lower than a uniaxial failure stress, whereas a biaxial failure strain will be higher or lower than a uniaxial failure strain. The effects of biaxial states of stress on LX-04-1 and PBX 9404 are illustrated in Secs. IIC1 and IIC2, respectively.

The span of observed ultimate tensile strains vs temperature is presented in Fig. IIC-1 to show the variability of failure and to illustrate its dependence on the load history.

Some effects of age on failure stress and strain for LX-04-1 and PBX 9404 under a constant strain rate of 1000  $\mu\text{in./in./min}$  can be seen in Sections IVA and IVB, respectively.

All existing data express failure under increasing loads. The failure stresses and strains will be lower under multi-cycle loading. Multi-cycle loading tests will be carried out in the near future, and the data will eventually be provided in a revision to this handbook.

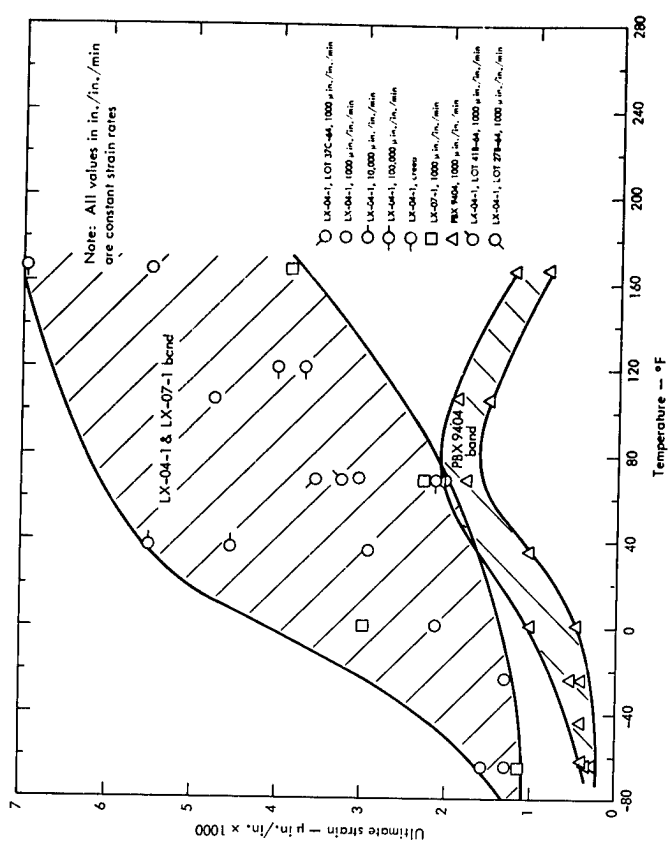


Fig. IIC-1. Observed failure region for LX-04-1, LX-07-1, and PBX 9404.

IIC1 Failure Properties of LX-04-1

Failure properties in this section are as follows:  
LX-04-1 stress biaxial failure envelope for one kind of history: Fig. IIC1-1.  
LX-04-1 strain biaxial failure envelope for one kind of history: Fig. IIC1-2.

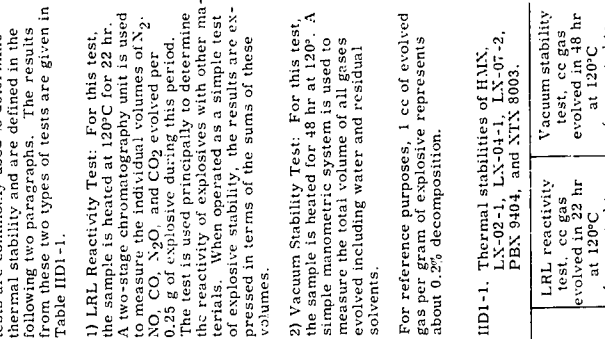


Fig. IIC1-1. Stress biaxial failure envelope for one kind of history with LX-04-1. Effective rate 200 psi/min.

IIC2 Failure Properties of PBX 9404

Failure properties in this section are as follows:  
PBX 9404 stress biaxial failure envelope for one kind of history: Fig. IIC2-1.  
PBX 9404 strain biaxial failure envelope for one kind of history: Fig. IIC2-2.

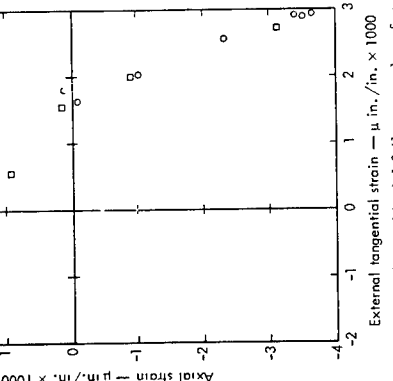


Fig. IIC2-1. Stress biaxial failure envelope for one kind of history with LX-04-1. Effective rate 200 psi/min.

IIC2 Thermal Stability of Larger Explosive Charges

For large amounts of explosive there is a critical safe temperature. This temperature is the point where thermal energy from slow chemical decomposition is given off at a rate greater than it can be dissipated. The temperature is

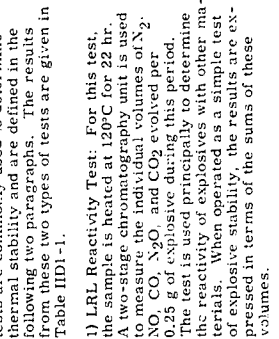


Fig. IIC2-1. Stress biaxial failure envelope for one kind of history with PBX 9404. Effective rate 200 psi/min.

Explosive	LRL reactivity test, cc gas evolved in 52 hr at 120°C (corrected to cc gas STP/0.25 g)	Vacuum stability test, cc gas evolved in 48 hr at 120°C (corrected to cc gas STP/g)
HMX	<0.01	0.07
LX-02-1	0.3-0.6	NA
LX-04-1	0.3-0.06	NA
LX-07-2	0.03-0.06	NA
PBX 9404	0.36-0.40	3.2-4.9
NTX 8003	<0.02a	NA

a. Measured at 100°C.  
NA: No data available.

IIC2 Thermal Stability of Larger Explosive Charges

For large amounts of explosive there is a critical safe temperature. This temperature is the point where thermal energy from slow chemical decomposition is given off at a rate greater than it can be dissipated. The temperature is

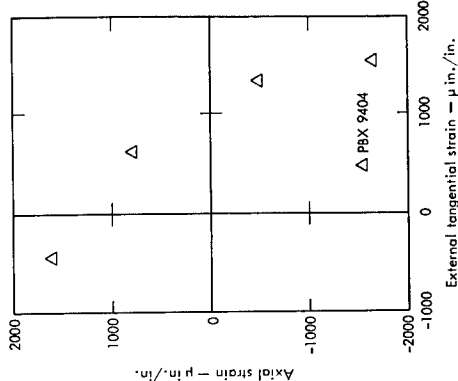


Fig. IIC2-2. Strain biaxial failure envelope for one kind of history with PBX 9404. Effective rate 200 psi/min.

IIC2 Thermal Stability of Larger Explosive Charges

For large amounts of explosive there is a critical safe temperature. This temperature is the point where thermal energy from slow chemical decomposition is given off at a rate greater than it can be dissipated. The temperature is



Fig. IIC2-1. Stress biaxial failure envelope for one kind of history with PBX 9404. Effective rate 200 psi/min.

Explosive	LRL reactivity test, cc gas evolved in 52 hr at 120°C (corrected to cc gas STP/0.25 g)	Vacuum stability test, cc gas evolved in 48 hr at 120°C (corrected to cc gas STP/g)
HMX	<0.01	0.07
LX-02-1	0.3-0.6	NA
LX-04-1	0.3-0.06	NA
LX-07-2	0.03-0.06	NA
PBX 9404	0.36-0.40	3.2-4.9
NTX 8003	<0.02a	NA

a. Measured at 100°C.  
NA: No data available.

IIC2 Thermal Stability of Larger Explosive Charges

For large amounts of explosive there is a critical safe temperature. This temperature is the point where thermal energy from slow chemical decomposition is given off at a rate greater than it can be dissipated. The temperature is



# HF MISCELLANEOUS PROPERTIES OF HIGH EXPLOSIVES

## HF1 Melting Points, Boiling Points, and Vapor Pressures of Various High Explosives

Table HF1-1. Melting points, boiling points, and vapor pressures of HMX, LX-02-1, LX-04-1, LX-07-2, PBX 9404, and LX-04-03.

Explosive	Melting point (°C)	Boiling point (mm Hg)	Vapor pressure (mm Hg)
HMX	285-287	NA	NA
LX-02-1	(a)	NA	NA
LX-04-1	(b)	NA	NA
LX-07-2	(b)	NA	NA
PBX 9404	(c)	NA	NA
TXN 8003	(c)	NA	NA

(a) Putty-like material, no fixed melting point.  
(b) Solid composite material, melts at about 280°C with decomposition.  
(c) Melts with decomposition at 129-135°C.  
NA: No data available.

## HF2 Solubility of HMX in Various Solvents

Table HF2-1.

Table HF2-1. Solubility of HMX in various solvents.

Solvent	HMX
Acetone	soluble
Benzene	soluble
Carbon disulfide	soluble
Carbon tetrachloride	soluble
Chloroform	soluble
Dimethylformamide	soluble
Dimethylsulfoxide	soluble
Ethanol	soluble
Ethyl acetate	soluble
Ethyl ether	soluble
Pyridine	soluble
Water	soluble

i: INSOLUBLE: less than 0.1 g dissolved at ambient temperature per 100 ml of solvent.  
sl s: SLIGHTLY SOLUBLE: 0.1-5 g dissolved at ambient temperature per 100 ml of solvent.  
s: SOLUBLE: more than 5 g dissolved at ambient temperature per 100 ml of solvent.

## IIG IMPACT SENSITIVITIES OF HIGH EXPLOSIVES

### IIG1

#### Drop Weight Machine Impact Sensitivities: Table IIG1-1

The drop weight machine, or drop hammer, is one means of evaluating impact sensitivity. In the drop hammer test, a 2-1/2 to 5-lb weight is dropped from a preset height onto a small sample of explosive. A series of drops from different heights is made, recording for each height whether the material explodes. (The criterion for explosion is an arbitrarily set level of sound which

must be produced by the explosive when impacted.) The result of the test is summarized as a height in cm (H<sub>50</sub>) where there is 50% probability that the material will explode. Values given in the table were determined on machines patterned after the original design of World War II. Because of the extremely complicated process involved in initiation by impact, these drop hammer numbers serve only as approximate indications of sensitivity. The numbers are quite dependent on anvil surface. Two surfaces are normally used: sandpaper (type 120) and roughened steel (type 12B tooling). In general, explosion-height values below 25 cm on either type of surface for an unknown material usually indicate a material of moderate sensitivity that possibly can be handled in accordance with standard procedures, values above 70 cm usually indicate a material which, with a fairly high degree of probability, will prove to be relatively insensitive to impact.

The sensitivity indications provided by the drop hammer are always verified by large scale testing for any material which is to be handled in large quantities.

Table IIG1-1. Drop weight machine impact sensitivities of HMX, LX-02-1, LX-04-1, LX-07-2, PBX 9404, and TXN 8003.

Explosive	50% probability of explosion height (cm)	
	LRL machine	LASL machine
	12B tools	12B tools
HMX	30	40
LX-02-1	80	NA
LX-04-1	41	55
LX-07-2	38	NA
TXN 8003	25 (uncured)	23
	21	NA

NA: No data available

### IIG2

**Susan Impact Sensitivities**  
The Susan Impact Sensitivity Test is a projectile impact test with the projectile shown in Fig. IIG2-1 shot from a special type gun. The weight of explosive in the projectile head is about 1 lb. The target is armor-plate steel. The results of the test are expressed in terms of a relative "sensitivity" curve in which the relative point-source detonation energy released by the explosive as a result of the impact is plotted against the velocity of the projectile. The relative point-source detonation energy is derived from a constant time measurement of the air shock wave from the impact point to a measuring point 10 ft away.

Three explosives were tested by means of the Susan test: LX-04-1, LX-07-2, and PBX 9404-03. The results are plotted in

ignition of LX-04-1 in the Susan test does not lead to any reaction of consequence and, in fact, the fire appears to go out before the pinch stage of the impact is reached. This would indicate that LX-04-1 is not likely to build to a detonation from a rather minor ignition when there is little or no confinement.

LX-04-1 has frequently been observed to detonate high order in other impact test geometries where the effective confinement is rather good and the explosive well is pulverized to give a lot of surface area at the time of the detonation.

LX-04-1 can be ignited in drilling "over-tests."

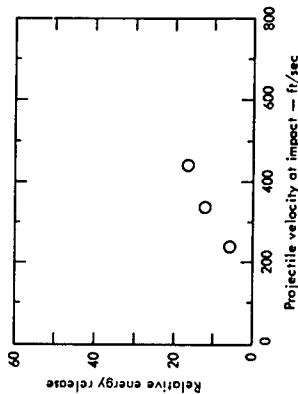


Fig. IIG2-1. Susan projectile (scaled drawing; high explosive head is 4 in. long X 2 in. in diameter.)

Figs. IIG2-2, IIG2-3, and IIG2-4, respectively. In the subsequent calculation it was assumed that the air shock is generated by a point source. The energy scale was adjusted to vary from zero for no chemical reaction to approximately 100 for the most violent detonation-like reaction (all explosive consumed). Burning reactions which appear to consume all of the explosive give values on the scale of about 40-50. Comments are also made on the details of the impact process which seem to have a bearing on the impact safety of an explosive.

Special terms are used in describing the results of Susan tests. These are "early detonation stage" and "pinch stage." The "early" or "forerun" stage refers to the first inch of crushing and shearing of the projectile nose cap and the contained explosive. "Pinch stage" refers to the terminal stage of the impact when the nose cap has been completely split open longitudinally and peeled back to the steel projectile body, which is rapidly being brought to a halt.

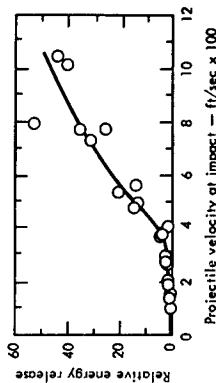


Fig. IIG2-2. Susan sensitivity curve for LX-04-1.

The threshold velocity for chemical reaction in a Susan test on LX-04-1 is about 140 to 150 ft/sec. LX-04-1 also lights in the early deformation stage of the test. This type of behavior is defective from a safety point of view because LX-04-1 can easily be ignited by a small amount of mechanical energy. Fortunately, the early deformation stage

The threshold velocity for chemical reaction in a Susan test on LX-07-2 is not definitely known, but it appears to be less than that for LX-04-1. LX-07-2 also lights in the early deformation stage of the impact. This impact behavior of LX-07-2 is defective from a safety point of view because LX-07-2 can easily be ignited by a small amount of mechanical energy.

The propagation behavior of LX-07-2 after ignition at the early deformation stage is defective from a safety point of view because the fire continues to burn right up to the pinch stage. This indicates that a rather minor ignition could easily build to a major ignition and possibly a detonation if enough explosive were present.

The general features of the Susan sensitivity curve are quite border line for LX-07-2. In particular, the velocity for reaction levels greater than 10 energy units is quite low. This would indicate that LX-07-2 could quite easily be ignited to rather violent reactions. Note should be taken of the Skid test results.

Fig. IIG2-3. Susan sensitivity curve for LX-07-2.

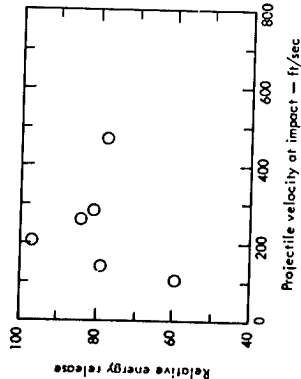


Fig. IIC2-4. Susan sensitivity curve for PBX 9404-03.

Susan test results indicate that PBX 9404-03 is easily ignited by small amounts of mechanical energy. Ignition occurring at threshold velocities of about 105 ft/sec. Ignition occurs during the early deformation stage of the impact and persists to the pinch stage, whereupon a violent reaction is observed. As can be seen from the curve, this reaction is apparently independent of velocity. Thus, PBX 9404 has a very large probability of building to a violent deflagration of detonation from any accidental ignition.

**Sliding Impact Sensitivity**  
A valuable test for evaluating the plant-handling safety of explosives is the Sliding Impact Test (also known as skid test) with large hemispherical billets of explosive. The test was developed at the Great Britain Atomic Weapons Research Establishment in England.

In the LRL-Pantex version, the test billet, supported on a pendulum device, is allowed to swing down from a preset height and strike at an angle on a sand-coated steel-target plate. Impact angles employed are 14° and 45° (defined as the

angle between the line of billet travel and the horizontal). The spherical surface of the billet serves to concentrate the force of the impact in a small area, the pendulum arrangement gives the impact both a sliding and a striking component, and a vertical axis. The results of the test are expressed in terms of the type of chemical event produced by the impact as a function of impact angle and vertical drop. Chemical events are defined as follows:

Scale	Reaction
0	No reaction. Charge retains integrity.
1	Burn or scorch marks on HE or target. Charge retains integrity.
2	Puff of smoke, but no flame or light visible in high speed photography. Charge may retain integrity or may be broken into large pieces.
3	Mild low-order reaction with flame or light. Charge broken up and scattered.
4	Medium low-order reaction with flame or light. Major part of HE consumed.
5	Violent deflagration. Virtually all HE consumed.
6	Detonation.

The importance of the sliding impact test to plant handling safety is that the drop heights and impact angles used in the test are quite within the limits that might be found during the accidental dropping of an explosive billet. The test is used not only to determine the sensitivity of different explosives to being detonated but also to evaluate the effect that typical plant floor coverings have in producing detonations.

Results of sliding impact testing to determine the sensitivity of various explosives to being detonated are presented in Table IIG3-1. Results of sliding impact testing to determine the effect that various plant floor coverings have in producing detonation are presented in Table IIG3-2.

Table IIG3-1. Relative detonation sensitivity of various high explosives to sliding impact (LRL-Pantex Test, sand-coated steel reference surface).

Explosive	Weight of charge, lb	Vertical drop height, (ft)	Impact angle	Scale of chemical event
LX-04-1a	25	1.75	14°	0
	25	2.5	14°	2
	25	14.1	14°	1
	25	14.1	14°	2
	25	14.1	14°	2
LX-07-0	25	3.5	45°	0
	25	5.0	45°	3
	25	7.1	45°	1
	25	10.0	45°	2
	25	14.1	45°	3
PBX 9010	25	1.75	14°	0
	25	2.5	14°	4
	25	3.5	14°	4
	25	1.75	45°	0
	25	2.5	45°	3
PBX 9404	25	3.5	45°	6
	25	0.88	14°	0
	25	1.25	14°	6
	25	2.5	45°	0
	25	3.5	45°	6
PBX 9404	25	1.25	14°	6
	25	1.75	14°	6
	25	3.5	45°	0
	25	5.0	45°	6
	25	5.0	45°	6

<sup>a</sup>The effect of temperature on the sensitivity of an LX-04 formulation (LX-04-0) was tested. For a 45° impact angle, minimum heights where a reaction was observed were:  
-57°F, No. 2 reaction at 3.5 ft (25 lb)  
60°F, No. 3 reaction at 5.0 ft (25 lb)  
230°F, no reaction up to 14 ft (50 lb)

#### IIG4

**Gap Test Sensitivity:** Table IIG4-1  
The gap test gives a measure of the shock sensitivity of an explosive. The values are obtained by measuring the thickness of inert spacer material which will just produce a 50% probability of detonation in the test explosive when the spacer is placed between the test explosive and a plant floor covering. The values in Table IIG4-1 are the most recent obtained by GMA-2 (LRL) using their small scale test. Accidents have occurred with pellets 1/2 in. in diameter and 1-1/2 in. long. Spacers were 0.010-in. brass shims; donors were

Table IIG3-2. Relative effect of plant floorings in producing detonations in PBX 9010 (LRL-Pantex Test with 50 lb hemisphere of PBX 9010 and 45° impact angle).

Floor material	Vertical drop height, (ft)	Scale of chemical event
Sanded steel	1.75	0
	2.5	6
	2.5	6
Vinyl	5.0	0
	5.0	0
	7.1	6
	7.1	6
Polyurethane (5/64 in. Adiprene L-100)	7.1	0
	14.1	0
	21.0	0
Linoleum, 1/8 in. thick	7.1	0
	10.0	0
	14.1	0
	20.0	0
Corrugated rubber floor covering: Against grain	10	0
	10	0
With grain	20	0
Urapol floor covering 3/32 in. thick	10	0
	14.1	0
	20	0
	10	0
	14.1	0
	20	0
Torginal (Torga-Deck) 1/16 in. thick	14.0	0
	20.0	6
	20.0	6
3/16-1/4 in. thick	28.0	1

Thicknesses of at least 1/8 in. were used where the dimension of the plant flooring is not indicated.

modified SE-1 detonators with PBX 9407 pellets 0.300 in. in diameter and 0.207 in. long. Detonation of the acceptor charge was ascertained by the dent produced in a steel witness plate.

In general, the larger the spacer gap, the more shock sensitive is the explosive. The numbers, however, depend on test size, geometry, method of preparation of the explosive, and percent voids in the explosive. They are, therefore, only approximate indications of relative shock sensitivity.

Table IIG4-1. Gap test sensitivities of LX-04-1, PBX 9404-03, and GTX 8003.

Explosive	Preparation	Density (g/cc)	% voids	Mean gap (mils)	±lg5 (mils)
LX-04-1	Hot pressed	1.868	1.1	70	8
PBX 9404-03	Hot pressed	1.854	NA	86	6
GTX 8003	Uncured	NA	NA	174	11

NA: No data available.

### III SPECIAL TESTS AND PROPERTIES OF HIGH EXPLOSIVES

#### III A MECHANICAL SIMULATION OF HIGH EXPLOSIVES WITH MOCK HIGH EXPLOSIVES

LX-04 and RM-04-BG are the most commonly used mocks among the various mocks for LX-04-1. LM-04 was developed as a composition mock, however, it has sometimes been used as a mock-up of mechanical properties as well. RM-04-BG was recently developed as a strength mock. Preliminary results showed that it behaves slightly more similar to LX-04-1 than LX-04 does, but its uniaxial tensile failure stress and strain tend to be higher than those of LX-04-1. Although RM-04-BG is a slightly more realistic mechanical mock, LM-04 is a reasonable mechanical mock when composition mock-up is more important than mechanical-properties mock-up.

90010 was developed as a strength mock for PBX 9404, and it is the most commonly used mock for this HE.

All ultrasonic data contained in this subsection were provided by H. L. Duneagan and B. A. Kuhn of Support Engineering Division.

Information on the formulations of mock explosives, on their mechanical properties, and on their miscellaneous properties, are presented in Tables IIIA-1, IIIA-2, and IIIA-3, respectively.

Test data on LM-04, RM-04-BG, and 90010 is presented in the following figures:

Fig. IIIA-1: RM-04-BG initial longitudinal modulus.  
Fig. IIIA-2: LM-04 initial longitudinal modulus.  
Fig. IIIA-3: Ultrasonic longitudinal velocity of LM-04 and LX-04-1.  
Fig. IIIA-4: Ultrasonic shear velocity of LM-04 and LX-04-1.  
Fig. IIIA-5: Ultrasonic Young's modulus of LM-04 and LX-04-1.  
Fig. IIIA-6: Ultrasonic shear modulus of LM-04 and LX-04-1.  
Fig. IIIA-7: Ultrasonic Poisson's ratio of LM-04 and LX-04-1.  
Fig. IIIA-8: Constant rate cross-head deflection test for RM-04-BG.  
Fig. IIIA-9: Constant rate cross-head deflection test for LM-04.  
Fig. IIIA-10: 90010 initial longitudinal modulus.

Fig. IIIA-11: Ultrasonic longitudinal velocity of 90010 and PBX 9404.  
Fig. IIIA-12: Ultrasonic shear velocity of 90010 and PBX 9404.  
Fig. IIIA-13: Ultrasonic Young's modulus of 90010 and PBX 9404.  
Fig. IIIA-14: Ultrasonic shear modulus of 90010 and PBX 9404.  
Fig. IIIA-15: Ultrasonic Poisson's ratio of 90010 and PBX 9404.  
Fig. IIIA-16: Uniaxial stress-strain under high rate loading for 90010.  
Fig. IIIA-17: Uniaxial constant strain rate tensile test for 90010.  
Fig. IIIA-18: Compressive stress at 7% strain and stiffness parameter at 2% strain as a function of strain rate for RM-04-BG mock explosive.  
Fig. IIIA-19: Compressive stress-strain curves for RM-04-BG at various rates.

Table IIIA-1. Formulations of mock explosives.

Mock	Explosive	Property	Composition (wt %)	Molecular formula (b)
90010	PBX 9404	Mechanical properties	Pantek (c) 48.0 Ba(NO <sub>3</sub> ) <sub>2</sub> 46.0 NC(d) 2.8 CEP(e) 3.2	C <sub>1</sub> .89H <sub>4.44</sub> N <sub>0.38</sub> O <sub>2.62</sub> Ba <sub>0.18</sub> Cl <sub>0.03</sub> P <sub>0.01</sub>
90505	PBX 9404	Atomic composition	Cyanuric acid 60 Melamine 32 NC(d) 4 CEP(e) 4	C <sub>2.32</sub> H <sub>3.18</sub> N <sub>2.96</sub> O <sub>1.60</sub> C <sub>0.04</sub> F <sub>0.01</sub>
LM-04	LX-04-1	Atomic composition	Cyanuric acid 59.7 Melamine 23.5 Viton A 16.8	C <sub>2.34</sub> H <sub>2.66</sub> N <sub>2.51</sub> O <sub>1.39</sub> F <sub>0.63</sub>
RM-04-BG	LX-04-1	Mechanical properties, static and dynamic	Cyanuric acid 70.5 Barium nitrate 14.5 Viton 15	C <sub>2.02</sub> H <sub>1.86</sub> N <sub>1.75</sub> O <sub>1.97</sub> F <sub>0.54</sub> Ba <sub>0.06</sub>

(a) = 0.05% of a red pigment is also added to these formulations.

(b) Molecular weights of these mixtures are arbitrarily taken as 100.

(c) Pentacerythritol

(d) Nitrocellulose

(e) Triis-*n*-chloroethyl phosphate

(f) Although designed as an atomic composition mock, LM-04 can also be used as an approximate mock of the mechanical properties of LX-04-1 at ambient conditions.

Table IIIA-2. Mechanical properties of mock explosives.

Mock	Density (g/cc)	Compressive Strength (psi)	Tensile Strength (psi)	Shear
90010	1.842	2000 at 70°F	1050 at -65°F 350 at +68°F 60 at +165°F 1780 at -65°F 1190 at 0°F 370 at +62°F 140 at +165°F 1800 at -65°F 1130 at 0°F 350 at +68°F 91 at +165°F	1335 at +70°F NA
LM-04	1.725	NA		
RM-04-BG	1.870	1490 at 70°F		1488 at +70°F

NA: No data available.

Table IIIA-3. Miscellaneous properties of mock explosives.

Mock explosive	Property
90010	Theoretical maximum density: 1.89 g/cc Nominal density: 1.78 g/cc Linear coefficient of thermal expansion $\alpha = 20.8 \times 10^{-6}$ in./in. °F (-65°F to +68°F) Thermal conductivity: $k = 0.308$ Btu/hr °F ft at 80°F Specific heat: $C_p = 0.30$ Btu/lb °F (-70° to +165°F) Compressive strength: 2016 psi at 70°F Shear strength: 1335 psi at 70°F
90503	Theoretical maximum density: 1.68 g/cc Nominal density: 1.57 g/cc
LM-04	Theoretical maximum density: 1.727 g/cc Nominal density: 1.70 g/cc Cubical coefficient of thermal expansion: $\beta = 19.94 \times 10^{-5}$ cc/cc °C (-30 to +70°C)
RM-04-BG	Theoretical maximum density: 1.892 g/cc Nominal density: 1.87 g/cc Linear coefficient of thermal expansion: $\alpha = 6.8 \times 10^{-6}$ in./in. °F (-30 to +165°F) Heat capacity: 0.223 cal/g °C (+26.9 to +12.8°C) 0.233 cal/g °C (+12.8 to +60.3°C) 0.244 cal/g °C (+60.3 to +73.0°C) Thermal conductivity: 0.663 Btu/hr °F ft (+20 to +80°C) Compressive strength: 1490 psi at 70°F Coefficient of friction: (See Table III(B)-1)

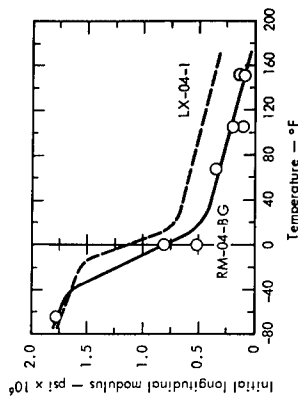


Fig. IIIA-1. RM-04-BG initial longitudinal modulus.

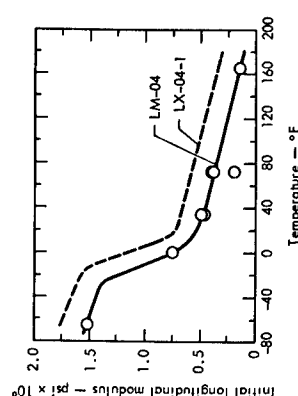


Fig. IIIA-2. LM-04 initial longitudinal modulus.

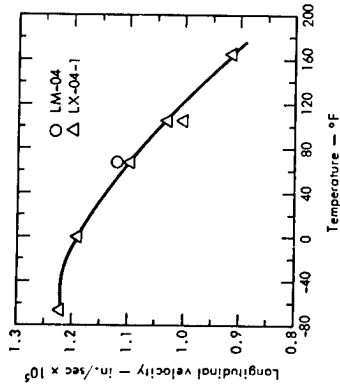


Fig. IIIA-3. Ultrasonic longitudinal velocity of LM-04 and LX-04-1.

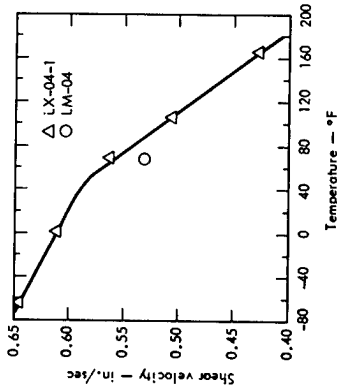


Fig. IIIA-4. Ultrasonic shear velocity of LM-04 and LX-04-1.

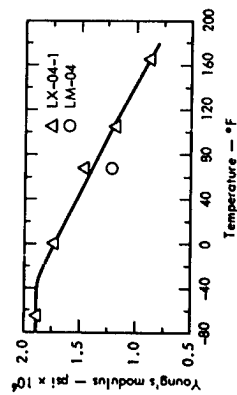


Fig. IIIA-5. Ultrasonic Young's modulus of LM-04 and LX-04-1.

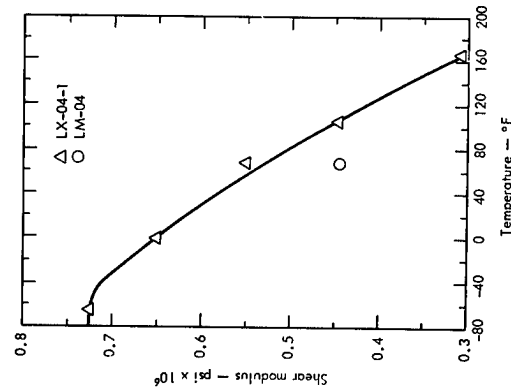


Fig. IIIA-6. Ultrasonic shear modulus of LM-04 and LX-04-1.

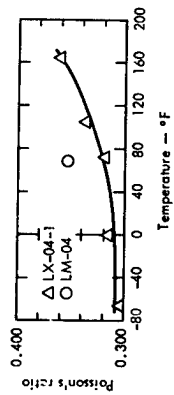


Fig. IIIA-7. Ultrasonic Poisson's ratio of LM-04 and LX-04-1.

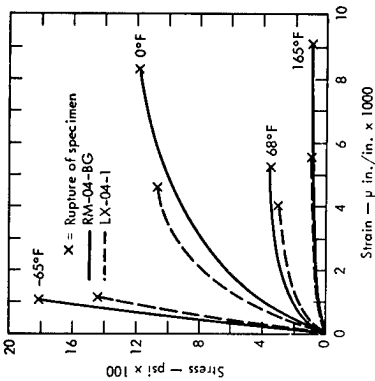


Fig. IIIA-8. Constant rate cross-head deflection test of RM-04-BG. Rate = 0.005 in./min.

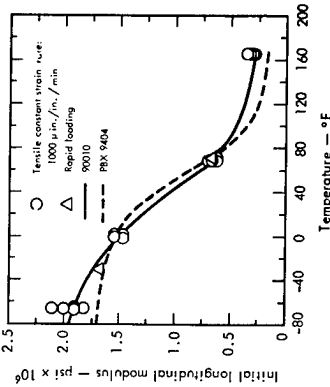


Fig. IIIA-10. Initial longitudinal modulus of 90010.

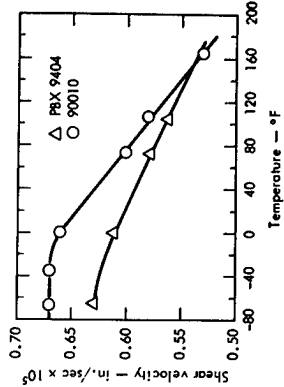


Fig. IIIA-12. Ultrasonic shear velocity of 90010 and PBX 9404.

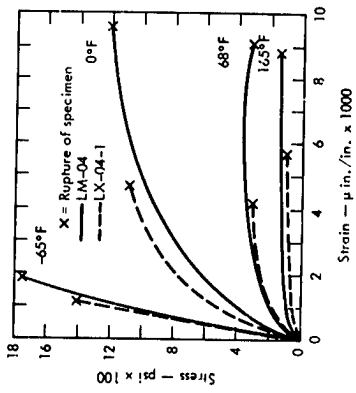


Fig. IIIA-9. Constant rate cross-head deflection test of LM-04. Rate = 0.005 in./min.

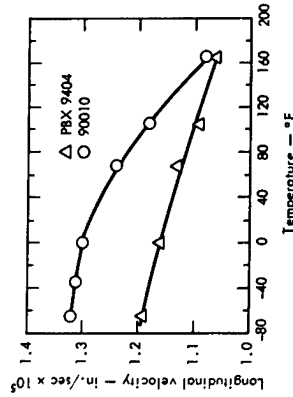


Fig. IIIA-11. Ultrasonic longitudinal velocity of 90010 and PBX 9404.

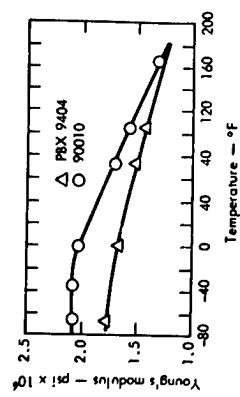


Fig. IIIA-13. Ultrasonic Young's modulus of 90010 and PBX 9404.



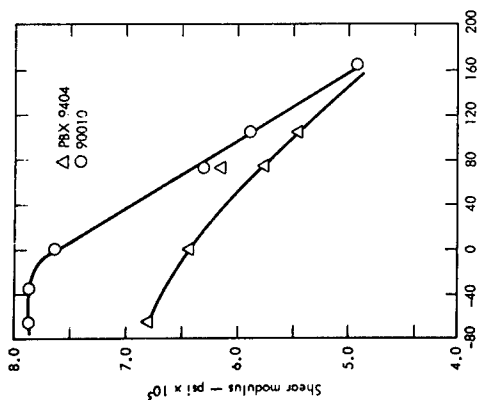


Fig. IIIA-14. Ultrasonic shear modulus of 90010 and PBX 9404.

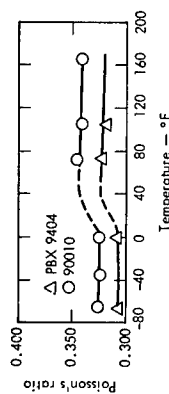


Fig. IIIA-15. Ultrasonic Poisson's ratio of 90010 and PBX 9404.

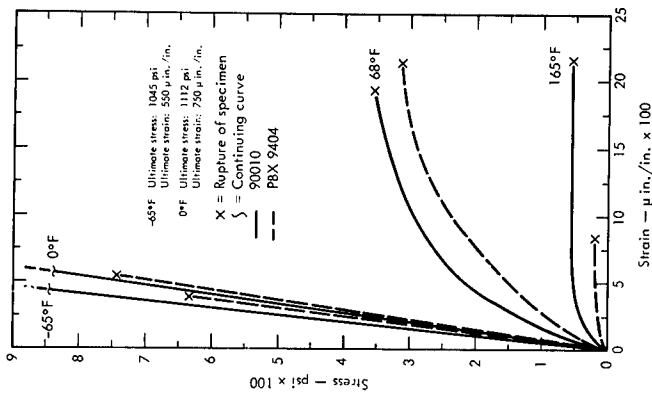


Fig. IIIA-17. Uniaxial constant strain rate tensile test of 90010. Strain rate  $\approx 1000 \mu\text{in./in./min.}$

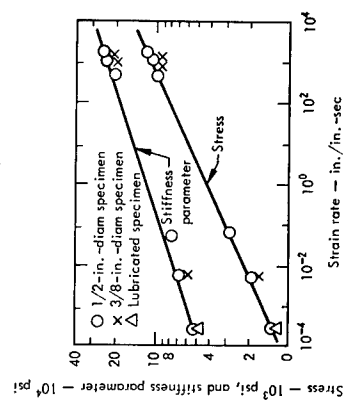


Fig. IIIA-18. Compressive stress at 7% strain and stiffness parameter at 2% strain as a function of strain rate for RM-04-BG mock explosive.

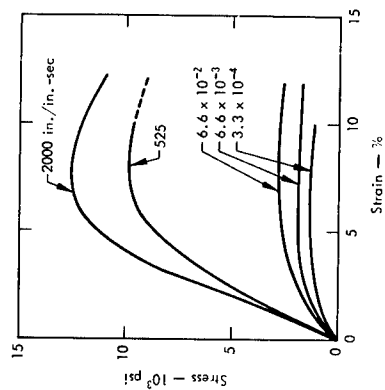


Fig. IIIA-19. Compressive stress-strain curves for RM-04-BG at various strain rates.

### III B COEFFICIENTS OF FRICTION OF HIGH EXPLOSIVES AND MOCK HIGH EXPLOSIVES

All coefficients of friction shown in Figs. IIIB-1 through IIIB-8 of HE's and mock HE's on aluminum were determined by K. G. Hoge of Support Engineering Division at the request of the General Chemistry Division. The results are presented for LX-04-1, PBX 9011, Comp B-3, and RM-04-BG (a strength mock for LX-04-1) in the following figures:

Fig. IIIB-1. LX-04-1 sliding on 6061-T6 aluminum.  
Fig. IIIB-2. LX-04-1 sliding on LX-04-1.  
Fig. IIIB-3. PBX 9011 sliding on 6061-T6 aluminum.  
Fig. IIIB-4. PBX 9011 sliding on PBX 9011.  
Fig. IIIB-5. Comp B-3 sliding on 6061-T6 aluminum.  
Fig. IIIB-6. Comp B-3 sliding on Comp B-3.  
Fig. IIIB-7. RM-04-BG sliding on 6061-T6 aluminum.  
Fig. IIIB-8. RM-04-BG sliding on RM-04-BG.

The coefficients of friction of RM-04-BG are generally lower than those of LX-04-1; therefore, RM-04-BG does not mock the frictional properties of LX-04-1. Moreover, the coefficients for RM-04-BG generally increase with the amount of moisture absorbed, whereas LX-04-1 is relatively insensitive to moisture in the atmosphere. General

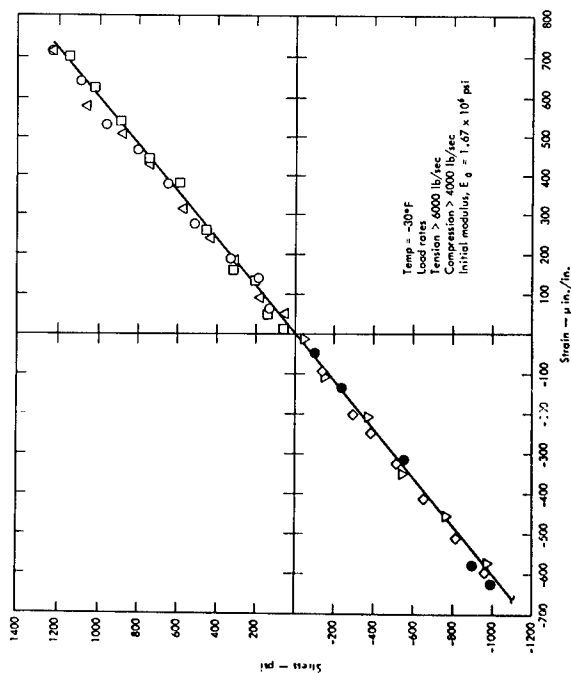


Fig. IIIA-16. Uniaxial stress-strain of 90010 under high rate loading.

Chemistry Division pointed out that RM-64-BG was not intended as a frictional mock.

Data for PBX-9404 was not plotted because specimens tended to shear, causing the data to be unreliable. Most tests for explosives sliding on metals were conducted on 6061-T6 aluminum. The type of metal (aluminum, copper, or steel) had little effect on the friction coefficient as long as the surfaces were clean. Data illustrating the effect of the type of metal and surface finish on LX-04-1 is shown in Table IIIB-1. This table also presents data for some of the constituent materials such as IMX and Viton A.

Other general results are:

- 1) Plastic-bonded explosives have a higher friction coefficient when sliding on explosive material than on metal.

- 2) There is little difference in friction for 16 and 32 surface finishes. However, for a 125 surface finish, friction is greatly increased.
- 3) Plastic-bonded explosives show peaks in the friction/sliding-velocity plots at velocities slightly below 1 in./min.
- 4) Cast or polycrystalline explosives show no definite peaks but indicate an increase in friction with increasing velocities.
- 5) Addition of a lubricant (calcium stearate) to the plastic binder greatly reduces the peak value of the friction coefficient and moderately reduces the steady state value.

For further information, refer to UCRL-50134, The Friction and Wear of Explosive Materials, K. G. Hoge, Sept. 1966, or call K. G. Hoge.

Table IIIB-1. Test data showing the effect of surface finish and type of metal on the coefficient of friction of LX-04-1. Data for some of the filler and plastic binder materials is also shown.

Slider material	Stationary material	Normal pressure, psi	Sliding velocity, in./min	Surface roughness, $\mu$ in., rms	Friction coefficient
LX-04-1	6061-T6 alum.	500	2	16	0.61
LX-04-1	6061-T6 alum.	500	2	32	0.60
LX-04-1	6061-T6 alum.	500	2	125	0.73
LX-04-1	Copper	500	2	32	0.61
LX-04-1	1016 Steel	500	2	32	0.62
LX-04-1	Copper	500	2	125	0.73
LX-04-1	1016 Steel	500	2	125	0.75
Viton A	6061-T6 alum.	125	2	32	1.04
Cyanoacetic acid	6061-T6 alum.	500	2	32	0.25
Cyanoacetic acid	6061-T6 alum.	500	2	125	0.31
IMX	6061-T6 alum.	500	0.2	32	0.42
IMX	6061-T6 alum.	500	2	32	0.42
IMX	6061-T6 alum.	500	0.2	125	0.61
IMX	6061-T6 alum.	500	2	125	0.59

<sup>a</sup> Approximate value.

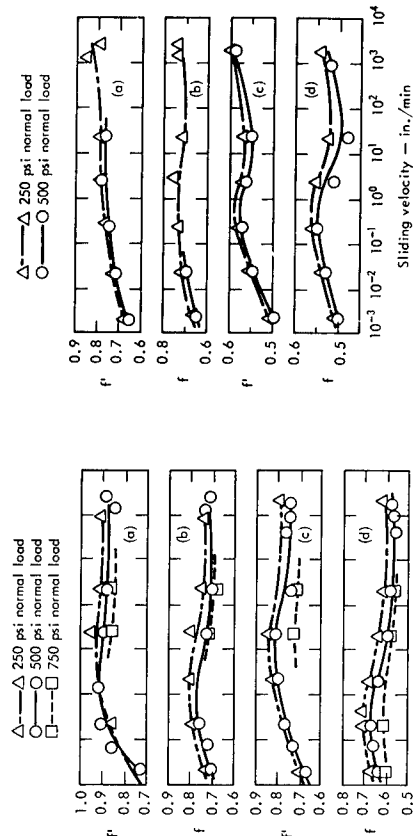


Fig. IIIB-3. PBX 9011 sliding on 6061-T6 aluminum. Surface finish 125 for (a) and (b), 32 for (c) and (d).

Fig. IIIB-1. LX-04-1 sliding on 6061-T6 aluminum. Surface finish 125 for (a) and (b), 32 for (c) and (d).

Note:  $\bar{f}$  is the steady state value of the friction coefficient.  
 $f^*$  is the peak value of the friction coefficient.

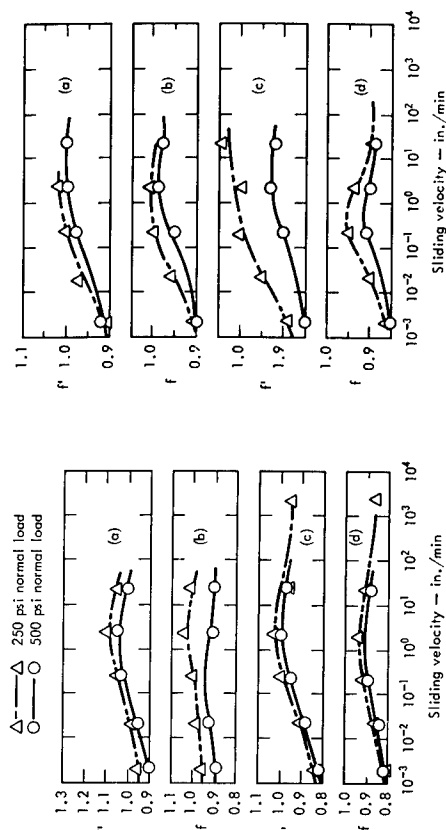


Fig. IIIB-2. LX-04-1 sliding on LX-04-1. Surface finish 125 for (a) and (b), 32 for (c) and (d).

Fig. IIIB-4. PBX 9011 sliding on PBX 9011. Surface finish 125 for (a) and (b), 32 for (c) and (d).

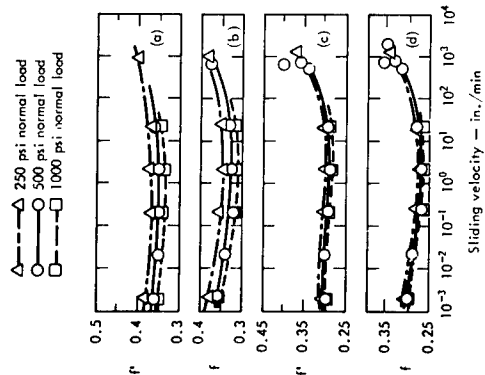


Fig. IIIb-5. Comp H-3 sliding on 6061-T6 aluminum. Surface finish 125 for (a) and (b), 32 for (c) and (d).

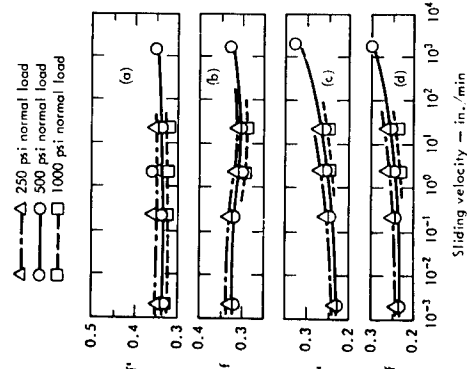


Fig. IIIb-6. Comp H-3 sliding on Comp H-3. Surface finish 125 for (a) and (b), 32 for (c) and (d).

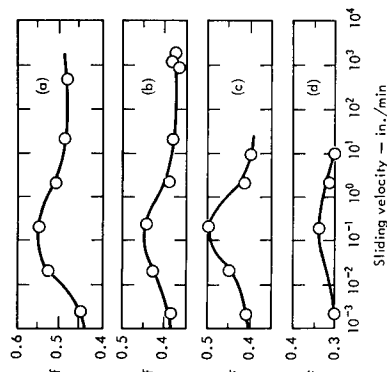


Fig. IIIb-7. RM-04-BG sliding on 6061-T6 aluminum. Specimens exposed to relative humidity of 50% in (a) and (b), 20% in (c) and (d). Surface finish 125 for (a) and (c), 32 for (b) and (d). Normal pressure, 500 psi.

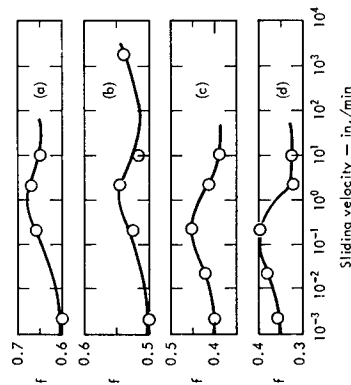


Fig. IIIb-8. RM-04-BG sliding on RM-04-BG. Specimens exposed to relative humidity of 30% in (a) and (b), 20% in (c) and (d). Surface finish 125 for (a) and (c), 32 for (b) and (d). Normal pressure, 500 psi.

#### IV SPECIAL STUDIES OF HIGH EXPLOSIVES

These studies were made either to help achieve a basic understanding of the mechanical behavior of HE's or for specific purposes such as observing aging effects. The HE Group uses many of the results for guidance in its mechanical properties testing. The results are generally interesting and may be useful for design, although fundamental mechanical properties are not usually described.

##### IVA LX-04-1 AGING STUDY

Thirty-six specimens were fabricated from a single pressing in October 1963. The axis of each specimen was made parallel to the axis of the cylindrical pressing. The specimens were stored at room temperature in an air-conditioned magazine until they were tested. The first group of nine were tested in November 1963 and the three subsequent groups of nine were tested a year apart afterwards. The nine specimens of each group were tested with desiccant for 120 hr before testing and were tested three each at 65°F, 68°F, and 165°F at a constant strain rate of 1000  $\mu\text{m./in./min.}$  Data

from the first three groups of specimens are presented in Figs. IVA-1 through IVA-3, as follows:  
LX-04-1 initial modulus dependent on aging at -65°, 68°, and 165°F: Fig. IVA-1.  
LX-04-1 ultimate stress and strain dependent on aging at -65°F: Fig. IVA-2.  
LX-04-1 ultimate stress and strain dependent on aging at 68°F: Fig. IVA-3.  
LX-04-1 ultimate stress and strain dependent on aging at 165°F: Fig. IVA-4.  
LX-04-1 test results at -65°, 68°, and 165°F: Fig. IVA-5.

The data from the -65°F tests indicated that the average fracture strain decreased with time while the ultimate stress decreased only slightly, thereby showing a general stiffening with age. Slight improvements in both failure stress and strain were observed in the 68°F tests. A significant decrease in failure stress and an increase in failure strain was observed in the 165°F tests over the first year of aging; however, no additional changes were observed in the second year.

No firm conclusions on whether aging is detrimental can be made at this time.

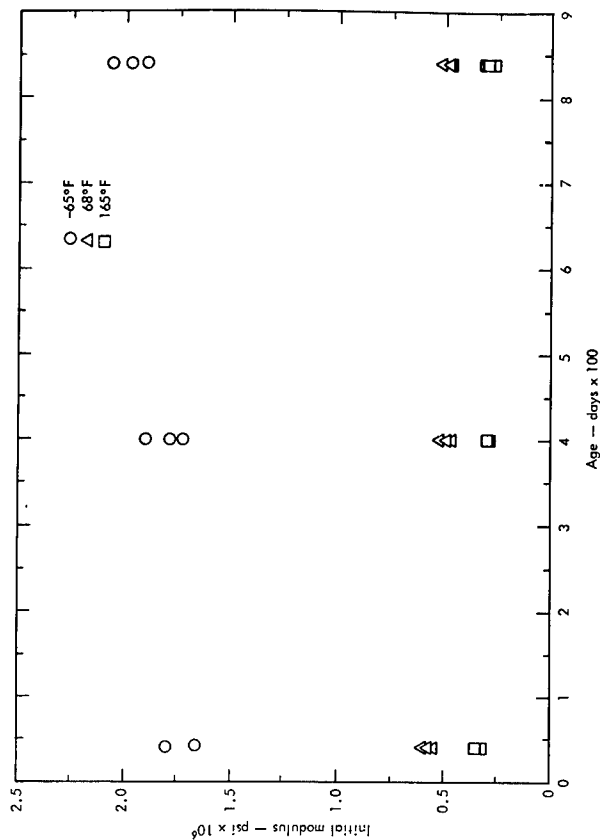


Fig. IVA-1. Aging study of LX-04-1. Initial modulus dependent on age. Test conditions: 1000  $\mu\text{m./in./min.}$

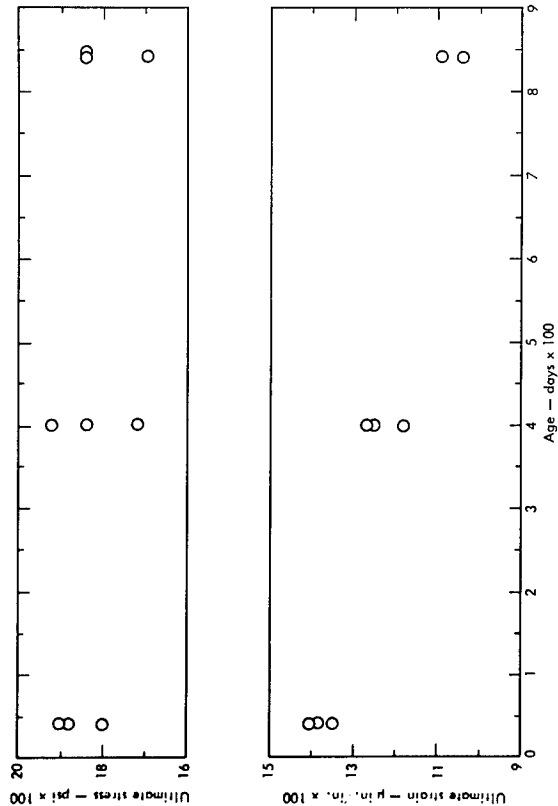


Fig. IVA-2. Aging study of LX-04-1; ultimate stress and strain dependent on age. Test conditions: 1000  $\mu\text{in./in./min.}$ ;  $-65^\circ\text{F.}$

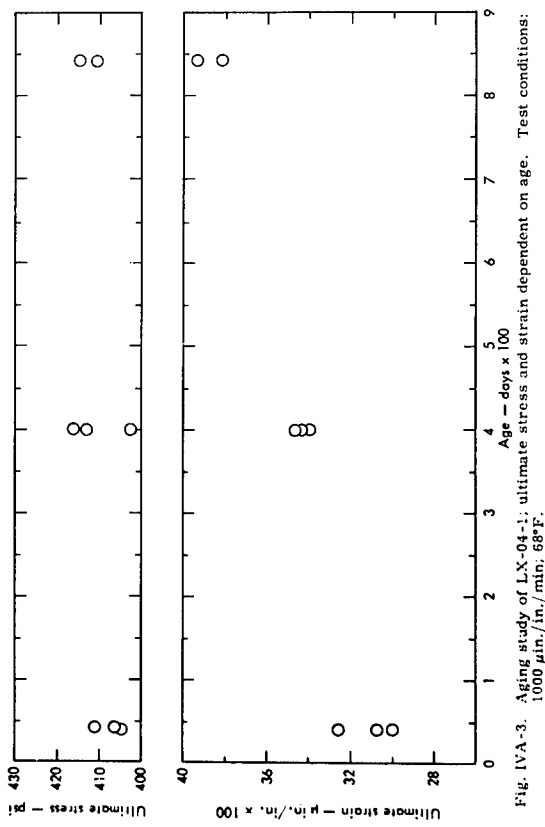


Fig. IVA-3. Aging study of LX-04-1; ultimate stress and strain dependent on age. Test conditions: 1000  $\mu\text{in./in./min.}$ ;  $68^\circ\text{F.}$

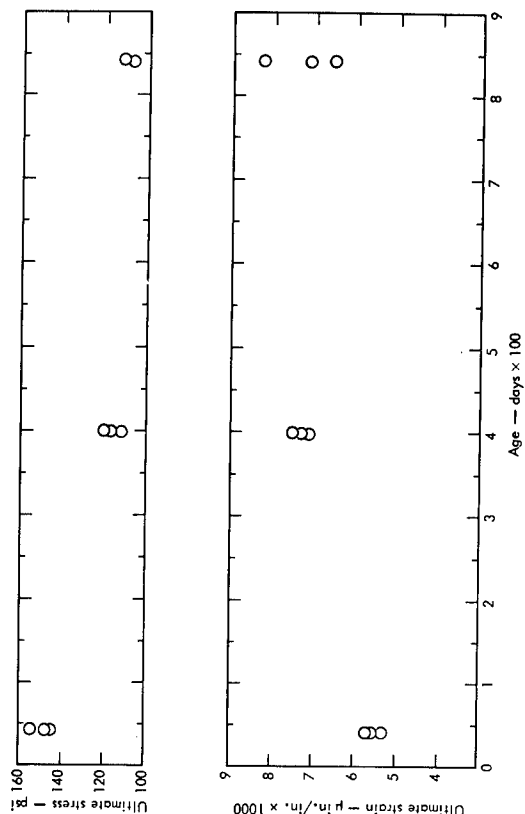


Fig. IVA-4. Aging study of LX-04-1; ultimate stress and strain dependent on age. Test conditions: 1000  $\mu\text{in./in./min.}$ ;  $165^\circ\text{F.}$

# IVB

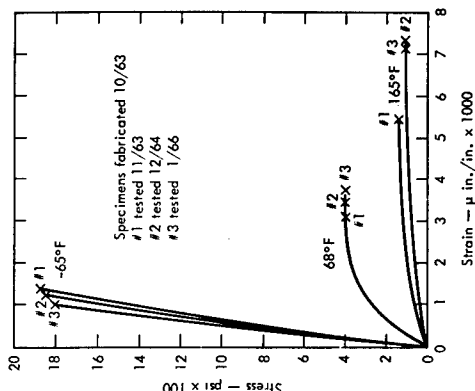


Fig. IVA-5. Aging study of LX-04-1; tensile test. No. 642. Test conditions: 1000  $\mu\text{in./in./min.}$ ; temperature as noted.

**PBX 9404 AGING STUDY**  
 Seventy-two tensile specimens were made from two pressings in September 1963 and stored in open containers in an air conditioned magazine at Site 300. The specimens were tested every 30 days at  $68^\circ\text{F.}$  and a constant strain rate of  $1000 \mu\text{in./in./min.}$  The specimens were dried prior to testing. The initial Young's modulus, and the failure stress and the failure strain as a function of aging are presented in Figs. IVB-1 and IVB-2, respectively. The failure stress increases with age, while the failure strain decreases. A general stiffening with age is observed.

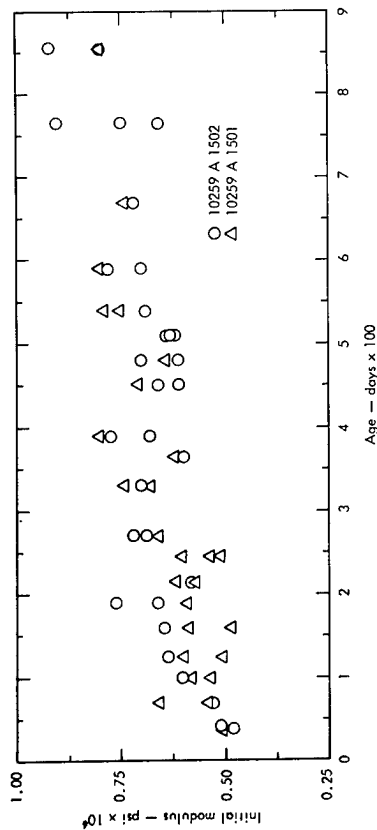


Fig. IVB-1. Aging study of PBX 9404; initial modulus dependent on age. Test conditions: 1000 psi, 1 in., 1 min, 68°F.

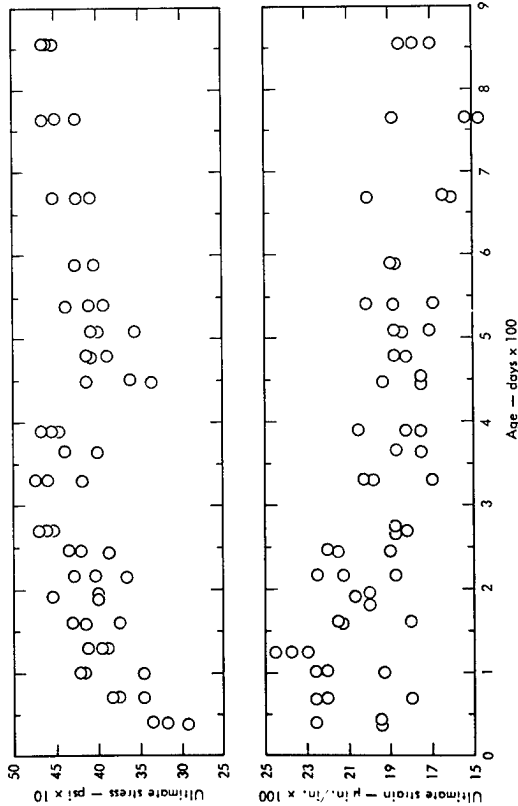


Fig. IVB-2. Aging study of PBX 9404; ultimate stress and strain dependent on age. Test conditions: 1000 psi, 1 in., 1 min, 68°F.

IVC  
STUDIES OF VITON AND HMX  
Viton and HMX are studied to gain a better understanding of the mechanical behavior of various HE's including LX-04-1 and LX-07-1. HMX is elastic over the temperature range -65°F through

165°F with a Young's modulus of approximately  $3.5 \times 10^6$  psi. The viscoelasticity of the HE must therefore be due to the binder; and indeed, the creep curves for LX-04-1 are similar to the Viton creep curves in general shape and rate. Viton

creep curves are presented in Figs. IVC-1 through IVC-5, as follows:  
Fig. IVC-1: Uncured Viton tensile creep; 6 hr plot.  
Fig. IVC-2: Uncured Viton tensile creep; 70 day plot.  
Fig. IVC-3: Uncured Viton tensile creep; 1 yr plot.

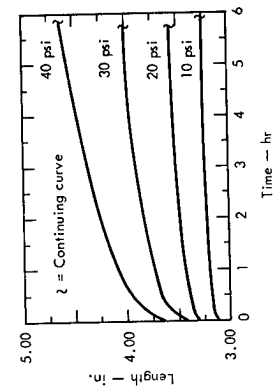


Fig. IVC-1.

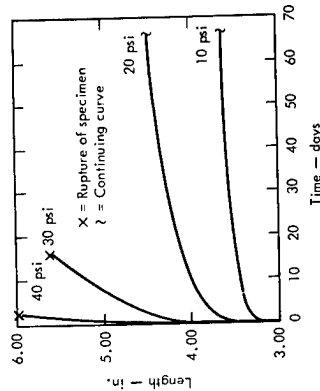


Fig. IVC-2.

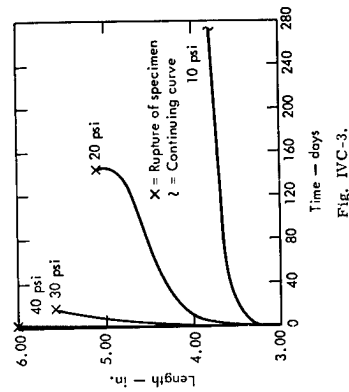


Fig. IVC-3.

Fig. IVC-3: Uncured Viton tensile creep; 1 yr plot.  
Fig. IVC-4: Uncured Viton tensile creep after 200% pre-elongation; 70 day plot.  
Fig. IVC-5: Uncured Viton tensile creep after 200% pre-elongation; 1 yr plot.

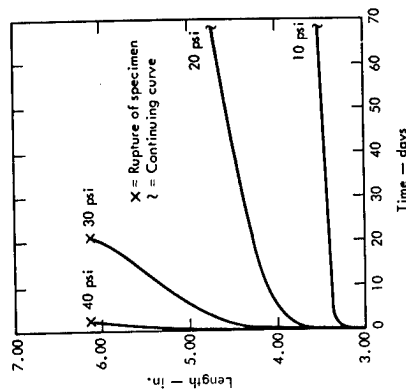


Fig. IVC-4.

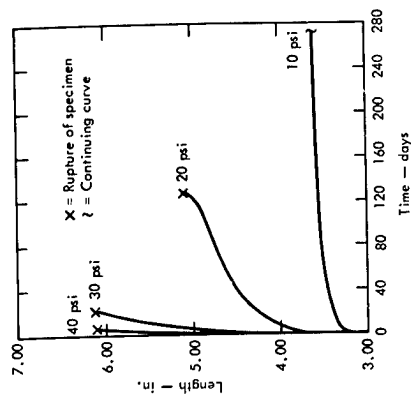


Fig. IVC-5.

Viton molecules resemble long microscopic coiled springs which tend to interlock with each other. They remain interlocked under small strains but when the strains become sufficiently large they uncoil and slip past each other. This implies that small deformations are recoverable but sufficiently large ones are not. Some of our LX-04-1 creep results seem to support such an implication. The Viton molecules are noncrosslinked so that once the molecules uncoil and begin to slip past each other, they will continue to slip for as long as the load is maintained, thereby imparting a behavior similar to that of a very viscous fluid. Some of our creep results are sufficiently high that LX-04-1 and LX-07-1 should have an equilibrium modulus (the ratio of stress to strain when creep finally stops) under small enough loads and will probably never cease to creep under a sufficiently large load. The latter behavior has been observed and the former is yet to be tested.

The coefficient of thermal expansion of Viton is approximately 4.8 times that of HMX. This suggests that rapid heating, even uniformly, could cause mechanical damage in the HE because of mechanical incompatibility between Viton and HMX. Different shapes were obtained in the creep curves for LX-04-1 specimens receiving different soaking times after a change in temperature. This phenomenon may be caused by the differences in the thermal coefficients of expansion.

#### 1VD

#### STRESS AND STRAIN CONCENTRATIONS IN HIGH EXPLOSIVES

Little testing has been done on stress concentration. Results of this testing indicated that stress concentration is reduced by creep. By deduction, if creep does not take place at temperatures near or below the glass-transition temperature or during short-duration loads, then the elastic stress concentration factors commonly found in engineering handbooks can be assumed to hold. This has not been experimentally verified, but it seems to be a reasonable assumption.

Strain concentration is not reduced by creep, and indeed it may be increased. Therefore, if the problem is such that strain concentrations are important, as they might well be under creep failure, then the presence of creep could intensify the problem.

#### IVE

#### FRACTURE SURFACE PICTURES

The following two fracture photographs illustrate the fracture modes and some details of the character of the breaks obtained with LX-04-1.



Fig. IVE-1. Uniaxial tension test of LX-04-1 at 68°F; failed normal to stress; illustrates complete molding powder bonding; 3X magnification.

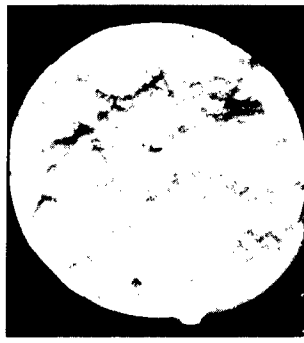


Fig. IVE-2. Uniaxial tension test of LX-04-1 at 68°F; failed normal to stress; more complete molding powder bonding than that shown in Fig. IVE-1; 3X magnification.

#### V

#### REFERENCES

General references to explosives literature may be useful to handbook users and are given below categorized by subject. Most of these references are available in Building T-103, Chemistry, or in the Technical Information Department.

#### VA

#### GENERAL REFERENCE WORKS ON EXPLOSIVES

1. Agard Combustion and Propulsion Panel, *The Chemistry of Propellants*, Pergamon Press, London (1959).
2. Adler, B., Fernbach, S., and Rotenberg, M., *Methods in Computational Physics*, Vol 3: *Fundamental Methods in Hydrodynamics*, Academic Press, N. Y. (1964).
3. Bebie, J., *Manual of Explosives*, Military Pyrotechnics and Chemical Warfare Agents, The MacMillan Co., N. Y. (1943).
4. Berger, J. and Viard, J., *Physique des Explosifs Solides*, Dunod, Paris (1962).
5. Bowden, F. P. and Yoffee, A. D., *Fast Reactions in Solids*, Butterworth's Scientific Publications, London (1958).
6. Bowden, F. P. and Yoffee, A. D., *Initiation and Growth of Explosives in Liquids and Solids*, University Press, Cambridge, England (1952).
7. Bradley, J. N., *Shock Waves in Chemistry and Physics*, Methuen & Co., Ltd., London (1962).
8. Bradley, R. S., *High Pressure Physics and Chemistry*, Vol I and II, Academic Press, N. Y. (1963).
9. Cook, M., *The Science of High Explosives*, Reinhold Publishing Corp., N. Y. (1958).
10. Cook, S. G., Rosen, J. M., and Bernstein, C. N., *Manual for Ammunition Quality Evaluation*, Surveillance Laboratories, U. S. Naval Powder Factory, Research and Development Dept., Indian Head, Md. (1964).
11. Davis, T. L., *The Chemistry of Powder and Explosives*, John Wiley and Sons, Inc., N. Y. (1953).
12. Department of the Army, *Military Explosives*, TM 9-1910, U. S. Government Printing Office, Washington 25, D. C. (1955). (Identical to Department of the Air Force's TO 11A-1-34.)
13. *Blasters Handbook*, 14th edition, E. I. Du Pont Co., Wilmington, Delaware (1958).
14. Evans, B. L., Yoffe, A. D., and Gray, P., *Physics and Chemistry of the Inorganic Azides*, Chem. Rev. 59, 515 (1959).
15. Fedoroff, B. T., *Encyclopedia of Explosives and Related Items*, Vol I and II, Picatinny Arsenal, Dover, N. J. (1960).

16. *Fourth Symposium on Detonation* (preprints), Vol I and II, U. S. Naval Ordnance Laboratory, White Oak, Md. (1965).
17. Hamann, S. D., "The Use of Explosions in High Pressure Research," *Reviews of Pure and Applied Chem.*, 10, 139 (#1960).
18. Hardin, M. C. and Masters, A. I., *The Use of Lithium as a Rocket Propellant*, General Motors Corp., Indianapolis, Indiana (Date unknown).
19. Hayes, T. J., *Elements of Ordnance: A Textbook for Use of Cadets of the United States Military Academy*, John Wiley and Sons, N. Y. (1938).
20. Jacobs, S., "Recent Advances in Condensed Matter Detonations," A. R. S. Journal 30, 151 (1960).
21. Jaffee, B. A., *Principles in Pyrotechnics and Pyrotechnical Ceramics*, Cleveite Corp., Cleveland, Ohio (1960).
22. Khatrin, L. N., *Physics of Combustion and Explosion*, National Science Foundation, Washington, D. C. (1962).
23. Ribaud, G., *Les Ondes de Detonation*, Centre National de la Recherche Scientifique, Paris (1962).
24. Levich, V. G., *Physicochemical Hydrodynamics*, Prentice-Hall, Inc., Englewood Cliffs, N. J. (1962).
25. Lewis, B. and Von Elbe, G., *Combustion, Flames, and Explosions of Gases*, Academic Press, Inc., N. Y. (1951).
26. Marshall, A., *Explosives*, 2nd edition, Vol I and II (1917), Vol III (1932), J. and A. Churchill, London.
27. Ninth Symposium (International) on Combustion (Summer 1962), Academic Press, N. Y. (1963).
28. Orlova, Ye. Yu., *The Chemistry and Technology of High Explosives* (English Translation), Part I and II, USSR, Moscow (1960). Translation prepared by Technical Documents Liaison Office, MCLTD, Wright-Patterson AFB, Ohio (1961).
29. Paushkin, Ya. M., *The Chemistry of Reaction Fuels*, Wright-Patterson AFB, Ohio, Foreign Technology Division, Air Force Systems Command (Nov 1962).
30. Pokrovsky, G. I., *The Explosion and Its Utilization*, (English Translation), USSR, Moscow (1940).
31. *Third Symposium on Detonation* (At James Forrestal Research Center, Princeton University, Sept 26-28, 1960), Rpt. ACR-32, Vol I and II, Office of Naval Research, 18th St. and Constitution Ave., NW., Washington, D. C.
32. Urbanski, T., *Chemistry and Technology of Explosives*, Vol I and II, The MacMillan Co., N. Y. (1964).
33. Urbanski, T., *International Symposium on Nitro Compounds*, Warsaw, 1953, The MacMillan Co., N. Y. (1964).

34. Warren, F. A., Rocket Propellants, Reinhold Publishing Corp., N. Y. (1958).
35. Welch, R. and Straus, R., Fundamentals of Rocket Propulsion, Reinhold Publishing Corp., N. Y. (1960).

#### VB COMPILATIONS OF EXPLOSIVE PROPERTIES

36. Blatt, A. H., Compilation of Data on Organic Explosives, Rpt. GORD 2014, Office of Scientific Research and Development, Washington, D. C. (1944), (Cont.).
37. Pedoroff, B., Encyclopedia of Explosives and Related Items (Vol. I), Interscience Publishers, Inc., N. Y. (1960).
38. GAX Division, Explosives Handbook, LASSL, Los Alamos, N. M. (Date unknown).
39. Lewis, B. von Elbe, G. and Brinkley, S. R. Jr., Survey of Military Explosives, Rpt. WADC-TR-55-176, Air Development Center, Wright-Patterson AFB, Cleveland, Ohio (1956), (Cont.).
40. Punch Card Recording of Data on Explosives, A. D. Little, Inc., Mass. (1954), Supplement A (1955), Supplement B (1956), Supplement C (1957), and Supplement D (1958).
41. McGarry, W. F. and Stevens, T. W., Detonation Rates of the More Important Military Explosives and Several Different Temperatures, Picatinny Arsenal, Dover, N. J. (1958).
42. Ordnance Technical Intelligence Agency, Encyclopedia of Explosives, AD-274026, Ordnance Liaison Group, Durham, N. C. (1960).
43. Tomlinson, W. R. Jr., Properties of Explosives of Military Interest, PA-TR-1740, Picatinny Arsenal, Dover, N. J. (1958).
44. Urizar, M. J., James, E., and Smith, L. C., "Detonation Velocity of Pressed TNT," Phys. Fluids 4, 262 (1961).

#### VC DETONATION THEORY

45. Chaiken, R. F., "Comments on Hypervelocity Wave Phenomena in Condensed Explosives," J. Chem. Phys. 33, 760 (1960).
46. Christian, E. A. and Snay, H. G., Analysis of Experimental Data on Detonation Velocities, NAVORD Rpt. 1508, U. S. Naval Ordnance Laboratory, White Oak, Md.
47. Cole, R., Underwater Explosions, Princeton University Press, Princeton, N. J. (1948).
48. Cowan, R. D. and Fickett, W., "Calculation of the Detonation Properties of Solid Explosives with the Kistiakowsky-Wilson Equation of State," J. Chem. Phys. 24, 932 (1956).
49. Courant, R. and Friedrichs, K. O., Supersonic Flow and Shock Waves, Interscience Publishers, Inc., N. Y. (1948).

50. Evans, M. W. and Ablow, C. M., "Theories of Detonation," Chem. Rev. 61, 129 (1961).
51. Fickett, W., "The Stability of Detonation," Chem. Rev. 45, 69 (1949).
52. Fickett, W., Detonation Properties of Condensed Explosives Calculated with an Equation of State Based on Inter-molecular Potentials, Rpt. LA-2712, LASSL, Los Alamos, N. M. (1962).
53. Fickett, W. and Wood, W., "A Detonation-Product Equation of State Obtained from Hydrodynamic Data," Phys. Fluids 1, 528 (1958).
54. Kandiner, H. J. and Brinkley, S. R., "Calculation of Complex Equilibrium Relations," Ind. Chem. 42, 850 (1949).
55. Levine, H. B. and Sharples, R. E., Operator's Manual for Ruby, Rpt. UCRL-6815, California Univ., Livermore, Lawrence Radiation Lab. (1962).
56. Mader, C., "Detonation Performance Calculations Using the Kistiakowsky-Wilson Equation of State," 3rd Symposium on Detonation, Rpt. ACR-52, Office of Naval Research, 18th St. and Constitution Ave., NW, Washington, D. C. (1960).
57. Pack, D. C., "The Reflection of a Detonation Wave at a Boundary," Phil. Mag. 2, 182 (1957).
58. Selberg, H. L., The Dependence of the Detonation Velocity on the Shape of the Front (Publisher unknown, date unknown).
59. Strange, F., Equation of State for Six Explosives, Document No. 4500-95-2-R8, Brobeck and Associates, Berkeley, Calif. (1964).
60. Taylor, G., "The Dynamics of the Combustion Products Behind Plane and Spherical Detonation Fronts in Explosives," Proc. Roy. Soc. (London) A 200, 235 (1950).
61. Taylor, J., Detonation in Condensed Explosives, Clarendon Press, Oxford, England (1962).
62. Villars, D. S., "A Method of Successive Approximations for Computing Detonation Equilibria on a High Speed Digital Computer," J. Am. Chem. Soc. 83, 321 (1961).
63. White, W. B., Johnston, S. M., and Dantzig, G. B., "Chemical Equilibrium in Complex Mixtures," J. Chem. Phys. 28, 751 (1958).
64. Wilson, D. H., Hydrodynamics, Edward Arnold Publishers, London (1959).
65. Wilkins, M., French, J., and Giroux, R., A Computer Program for Calculating One-Dimensional Hydrodynamic Flow, (KO code), Rpt. UCRL-6919, California Univ., Livermore, Lawrence Radiation Lab. (July 1962).
66. Wilkins, M. L. and Giroux, R., The Calculation of Stress Waves in Solids, Rpt. UCRL-7271, California Univ., Livermore, Lawrence Radiation Lab. (1963).

67. Wilkins, M. L., Squier, B., and Halpern, B., The Equation of State of PBX-9404 and LX-94-01, Rpt. UCRL-7797, California Univ., Livermore, Lawrence Radiation Lab. (April 1964).
68. Wood, W. W. and Kirkwood, J. G., "The Relation Between Velocity and Radius of Curvature of the Detonation Wave," J. Chem. Phys. 22, 1920 (1954).
69. Wood, W. W., Existence of Detonations for Large Values of the Rate Parameter, Internal Report, LASSL, Los Alamos, N. M. ( $\approx 1962$ ).
70. Zeldovich, I. B. and Kompaneets, A. S., Theory of Detonation, Academic Press, N. Y. (1960).

#### VD INITIATION AND SENSITIVITY

71. Bowden, F. P., et al., "A Discussion on the Initiation and Growth of Explosions in Solids," Proc. Roy. Soc. (London) A 246, 145 (1958).
72. Bowden, F. P. and Chadderton, L. T., "Molecular Disarray in a Crystal Lattice Produced by a Fission Fragment," Nature 192, 31 (1961).
73. Bowden, F. P. and Yoffe, A. D., Fast Reactions in Solids, Butterworths Scientific Publications, London (1958).
74. Bowden, F. P. and Yoffe, A. D., Initiation and Growth of Explosion in Liquids and Solids, University Press, England (1952).
75. Campbell, A. W., et al., "Shock Initiation of Solid Explosives," Phys. Fluids 4, 511 (1961).
76. Campbell, A. W., Davis, W. C., Travis, J. R., "Shock Initiation of Liquid Explosives," Phys. Fluids 4, 498 (1961).
77. Chace, W. G. and Moore, H. K., Exploding Wires, Plenum Press, N. Y. (1959).
78. Enig, J. W. and Petrone, F. J., An Equation of State and Derived Shock Initiation Calculating Conditions for Liquid Explosives, Informal Report, U. S. Naval Ordnance Laboratory, White Oak, Md. (1964).
79. Enig, J. W. and Petrone, F. J., On Equations of State in Shock Initiation Problems, Informal Report, U. S. Naval Ordnance Laboratory, White Oak, Md. (1964).
80. Evans, M. W., "Detonation Sensitivity and Failure of Detonators in Homogeneous and Failed Materials," J. Chem. Phys. 36, 193 (1962).
81. Fickett, W., F. P. F. P. Technique Studies of the Initiation of Solid Explosives, Informal Report, LASSL, Los Alamos, N. M. (1960).
82. Hubbard, H. W. and Johnson, M. H., "Initiation of Detonations," J. Appl. Phys. 30, 765 (1959).
83. Jacobs, S. J., Liddard, T. P., and Dummer, B. E., The Shock-to-Detonation Transition in Solid Explosives, Informal Report, U. S. Naval Ordnance Laboratory, White Oak, Md. ( $\approx 1962$ ).

84. Macek, A., "Sensitivity of Explosives," Chem. Rev. 62, 41 (1962).
85. Mader, C., A Hydrodynamic Hot Spot Calculation, Rpt. LA-2703, LASSL, Los Alamos, N. M. (1962).
86. Price, D., "Dependence of Damage Effects Upon Detonation Parameters of Organic High Explosives," Chem. Rev. 59, 801 (1959).
87. Zinn, J. and Mader, C. L., "Thermal Initiation of Explosives," J. Appl. Phys. 31, 323 (1960).

#### VE MEASUREMENT OF DETONATION PROPERTIES

88. Campbell, A. W., "Precision Measurement of Detonation Velocities in Liquid and Solid Explosives," Rev. Sci. Instr. 27, 567 (1956).
89. Cook, M. A., Keyes, R. L., and Ursenbeck, W. O., Measurement of Shock and Detonation Pressures, University of Utah, Salt Lake City, Utah (1961).
90. Deal, W. E., "Measurement of Chapman-Jouguet Pressure for Explosives," J. Chem. Phys. 27, 706 (1957).
91. Deal, W. E., "Measurement of the Reflected Shock Hugoniot and Isentrope for Explosive Reaction Products," Phys. Fluids 1, 523 (1959).
92. Duff, R. E. and Houston, E., "Measurement of the Chapman-Jouguet Pressure and Reaction Zone Length in a Detonating High Explosive," J. Chem. Phys. 23, 1268 (1955).
93. Garn, W. B., "Detonation Pressure of Liquid TNT," J. Chem. Phys. 32, 653 (1960).
94. Goodman, H. J., Compiled Free-Air Blast Data on Bare Spherical Perforated BRL-1092, Ballistic Research Lab., Aberdeen Proving Ground, Md. (1960).
95. Hayes, B., "On the Conductivity of Detonating High Explosives," 3rd Symposium on Detonation, Rpt. ACR-52, 139-149, Office of Naval Research, 18th St. and Constitution Ave., NW, Washington, D. C. (1960).
96. Leger, E. G. and Park, K., A Zig-Zag Oscilloscope Presentation for Detonation Velocity Measurements in Explosives, CARDE-TM-170/58, Canadian Armament Research and Development Establishment, Valcartier, Quebec (1958).
97. Urizar, M. J., Loughran, E. D., and Smith, L. C., "The Effects of Nuclear Radiation on Organic Explosives, Explosivstoffe No. 3, pp. 55-66 (1962), EQUATION-OF-STATE MEASUREMENTS WITH EXPLOSIVES
98. Bancroft, D., Peterson, E. L., and Minshall, S., "Polymorphism of Iron at High Pressure," J. Appl. Phys. 27, 291 (1956).
99. Christian, R. H. and Yarger, F. L., "Equation of State of Gases by Shock Wave Measurements, I. Experimental Method and Hugoniot of Argon," J. Chem. Phys. 23, 2042 (1955).

#### VF

100. Christian, R. H., Daif, R. E., and Yarger, F. L., "Equation of State of Gases by Shock Wave Measurements, II. The Dissociation Energy of Nitrogen," *J. Chem. Phys.* **23**, 2045 (1955).
101. Davis, R. S., and Jackson, K. A., On the Deformation Associated With Compression Shocks in Crystalline Solids, Paper presented at Symposium on Plasticity, April 1960.
102. Deal, W. E., "Shock Hugoniot of the Isentropes of Several High Explosives," 3rd Symposium on Detonation, *Rep. ACR-52*, pp. 336-395, Office of Naval Research, 18th St. and Constitution Ave., NW, Washington, D. C. (1960).
104. Deal, W. E., "Measurement of the Reflected Shock Hugoniot and Isentropes for Explosive Reaction Products," *Phys. Fluids* **1**, 523 (1958).
105. Drummond, W. E., "Explosive Induced Shock Waves, Part I. Plane Shock Waves," *J. Appl. Phys.* **28**, 1437 (1957).
106. Drummond, W. E., "Explosive Induced Shock Waves, Part II. Oblique Shock Waves," *J. Appl. Phys.* **29**, 167 (1958).
107. Durl, R. E., and Minshall, F. S., "Investigation of a Shock-Induced Transition in Bismuth," *Phys. Rev.* **102**, 1207 (1957).
108. Duvall, G. E., "Shock Waves in the Study of Solids," *Appl. Mech. Rev.* **15**, 849 (1962).
109. Eng, J. W., A Complete E. P. V. I. Metals Based on the P. V. I. Micro-Range Concept, NOLIR 62-14, U. S. Naval Ordnance Laboratory, White Oak, Md. (1962).
110. Etkin, J. O., Hydrodynamic Theory and High Pressure Flow in Solids, SPI-114-59, Pulver Laboratories, Stanford Research Institute, Palo Alto, Calif. (1961).
111. Fowles, G. R., Shock Wave Compression of Quartz, *Rev. 003-61*, Pulver Laboratories, Stanford Research Institute, Palo Alto, Calif. (1961).
112. Goranson, R. W., et al., "Dynamic Determination of the Compressibility of Metals," *J. Appl. Phys.* **26**, 1472 (1955).
113. Grimsal, E. G., The Elastic Constants and Moduli and Their Interdependence, Informal Report, Armour Research Foundation of Illinois Institute of Technology, Chicago, Illinois (Date unknown).
114. Halpin, W. J., Jones, O. E., and Graham, R. A., Submicrosecond Technique for Simultaneous Observation of Input and Propagated Impact Stresses, Informal Report, Sandia Corp., Albuquerque, N. M. (1962).

115. Hater, S. C., An Account of the Dynamic Properties of Solids, *KADE Memo Report* (NAN Aug 1959).
116. Ludwig, C. D., The Hugoniot in the Study of Metals, *Aluminum at High Pressures*, Sandia Corp., Albuquerque, N. M. (Aug 1962).
117. Martin, R. L., A Technique for Determining Stress, Strain, and Strain Rate Properties of Materials at High Strain Rates, Internal Report 1-58-45, California University, Livermore, Lawrence Radiation Lab (1961).
118. McQueen, R. G., and Marsh, S. P., "Equation of State for Manganese Metallic Elements from Shock Wave Measurement to Two Megabars," *J. Appl. Phys.* **31**, 1253 (1960).
119. Minshall, F. S., "Properties of Elastic and Plastic Waves Determined by Pin Composites and Crystals," *J. Appl. Phys.* **26**, 463 (1955).
120. Neilson, F. W., et al., Electrical and Optical Effects of Shock Waves in Crystalline Quartz, Preprint SCR-416, Sandia Corp., Albuquerque, N. M. (June 1961).
121. Rice, M. H., and Walsh, J. M., "Equation of State of Water to 250 kilobars," *J. Chem. Phys.* **25**, 324 (1957).
122. Simmons, J. A., Hauser, F., and Dorn, J. E., Mathematical Theories of Plastic Deformation Under Impulsive Loading, Minerals Research Laboratory, Series No. 133, Issue No. 1, University of California, Berkeley (Apr 1959).
123. Sternberg, H. M., One Dimensional Acceleration of Metals Under Explosive Loading, Informal Report, U. S. Naval Ordnance Laboratory, White Oak, Md. (Date unknown).
124. Taylor, G. R., and Quimby, H., "The Plastic Distortion of Metals," *Royal Society of London Philosophical Transactions, A Vol CCXXX*, 323 (1931).
125. von Neumann, J., and Richtmyer, R. D., A Method for the Numerical Calculation of Hydrodynamic Shocks, *J. Appl. Phys.* **21**, 232 (1950).
126. Walsh, J. M., and Christian, R. H., "Equation of State of Metals from Shock Wave Measurements," *Phys. Rev.* **97**, 1544 (1955).
127. Walsh, J. M., and Rice, M. H., "Dynamic Compression of Liquids from Measurements on Strong Shock Waves," *J. Chem. Phys.* **26**, 815 (1957).
128. Walsh, J. M., et al., "Shock Wave Compressions of Twenty-Seven Metals, Equation of State of Metals," *Phys. Rev.* **108**, 196 (1957).
129. Wasley, R., "Elastic Stress Disturbances in Extended Solids," (A lecture series presented at California Univ., Livermore, Lawrence Radiation Lab, in the spring of 1963).

130. Wasley, R., "Plastic Stress Disturbances in Bounded Solids," (A lecture series presented at California Univ., Livermore, Lawrence Radiation Lab, in the winter of 1965).
131. Wasley, R., "Stress Disturbances in Solids, Propagation in Elastic Bounded Media," (A series of notes prepared for possible future presentation in a lecture series at the California Univ., Livermore, Lawrence Radiation Lab).

#### VG MISCELLANEOUS REFERENCES

132. Dordill, J. P., et al., An Evaluation of Safety Devices for Laboratories Handling Explosive Compounds, Redstone Arsenal, Huntsville, Alabama (1961).
133. McGill, R., Explosives, Propellants, and Pyrotechnic Safety Covering Laboratory, Pilot Plant, and Production Operations, NOL-TR-61-138, U. S. Naval Ordnance Laboratory, White Oak, Md. (Feb 1962).

134. Talbot, L., Recent Research on the Shock Structure Problem, Paper presented at spring 1961 meeting of the Combustion Institute held at the University of California.
135. Scribner, K. J., A Physical Properties Mock for LN-01-1, Internal Report GCTN 187, California Univ., Livermore, Lawrence Radiation Lab. (June 1965).
136. Peterman, K. A., Thermal Conductivity of LX-04-1 and PBX-9404, Internal Report ENW-334, California Univ., Livermore, Lawrence Radiation Lab (Sept 1964).
137. Dunagan, F. L., and Kubo, B. A., Dynamic Modulus of High Explosives by Use of Ultrasonics, Internal Report ENS 219, California Univ., Livermore, Lawrence Radiation Lab (Jan 1966).
138. Hoge, K. C., Preliminary Friction Tests on RM-04 Block High Explosive, Memo to R. J. Wasley (LRL) dated June 18, 1965.



## SQUIBS AND PRIMACORD

## I SQUIBS

## 1A

## DEFINITIONS

1) A squib is a flame-producing device with no brisance, primarily used to ignite deflagrating materials such as propellant grains, black powder, metal-oxidant mixtures, fuses, or other combustible or flammable materials.

2) Squib is also used as a general name for other class "C" explosive devices, such as dimple motors, bellows motors, explosive switches, and some explosive actuator assemblies. Gas actuators of the squib type generate moderate pressures to activate pistons, releases, and similar items; sometimes commercial squibs can be used for this type of work depending on the action required.

## CAUTION

Most common squibs require less than 1 V/amp to fire. Special handling is required. Continuity checks can be made only with a blasting galvanometer or a specially designed and approved meter. Handling and use should be done only by personnel fully familiar with and trained in shooting, shunting, and grounding procedures.

## IB

## TIME DELAY ELEMENTS

Time delay elements ranging from milliseconds to 30 sec or more may be built into an explosive train. These delay elements consist of fuse potter columns which are varied in composition to give various burning times per inch of second. The time delays are normally made with separate delay elements, whereby one can build up the time delay desired. The delay element is essentially gasless so it is not necessary to vent the element.

## IC

## INSTANTANEOUS SQUIBS

Instantaneous squibs are those that normally function in a few milliseconds or less when recommended current is used. Some typical types of this kind of squib are:

- 1) Open match type, end flash.
- 2) Thin-bottom type, end flash.
- 3) Side burning type.

The above three types of squibs can be obtained that will have one of the following characteristics:

- 1) Coruscating: A flame burst containing hot-flaming or slag particles.
- 2) Flash: A quick short burst of flame.
- 3) Flame: A longer burst of flame than a flash.
- 4) Jet flame: A directional burst.
- 5) Hot slag: Burning or incandescent particles that persist in their ignition action.

## ID

**EXPLOSIVE ACTUATOR TYPE SQUIB**  
This group includes squibs of the slower acting pusher types, and use powdered loads of metal-oxidant mixtures and small loads of smokeless powder and black powder.

The slow action squib will build up to 1000 psi pressure from 10 to 35 msec; the faster acting type will build a peak pressure of 1600 psi over a period of 2 msec. For faster action and higher pressures, or where more brisance is required, primers or detonators are used.

## II PRIMACORD

## DEFINITION

Primacord is a linear detonating cord or fuse with a small core of explosive, usually PETN. It consists of a braided textile core containing the PETN covered by some suitable reinforcement: textile, water proofing material, plastic, rubber, or wire. The detonating fuse is designed to initiate charges of high explosives by means of the exploding core. The core must be initiated by a detonator or suitable booster. A number of sizes and types are manufactured in the standard and special type primacords.

## IIB

**STANDARD TYPES AND THEIR CHARACTERISTICS.** Table IIB-1.

Table IIB-1. Standard primacord types and their characteristics.

Type	Grating per ft*	o. d., in.	Tensile strength	Color
Plain	50	0.198 ± 0.006	125 lb	Gray-yellow pattern
Reinforced	50	0.202 ± 0.008	125 lb	Yellow, red strand
Plastic reinforced	54	0.215 ± 0.003	275 lb	White (plastic)
E-Cord	60	0.238 ± 0.005	300 lb	Red-white barber pole
	25	0.162 ± 0.008	140 lb	Yellow, red and blue strands

\* ±10%.

# BLANK PAGE

# IIC SPECIAL TYPES AND THEIR CHARACTERISTICS: Table IIC-1.

Table IIC-1. Special primacord types and their characteristics.

Type	O. d., in.	Tensile strength	Color
PETN 40, plastic	0.169 ± 0.011	100 lb	White
PETN 80, plastic (HV)	0.200 ± 0.005	110 lb	White
PETN 130, plastic	0.235 ± 0.008	110 lb	White
PETN 170, plastic	0.270 ± 0.010	180 lb	Dark blue
PETN 400, plastic	0.493 ± 0.010	185 lb	White
PETN 50, duplex	0.493 ± 0.028	300 lb	Light green (core same color)
(Twin core) oval	0.478 ± 0.008	170 lb	Vivid red
RDX 70	0.210 ± 0.008	110 lb	Black
RDX 100	0.236 ± 0.013	110 lb	Black

In the special type, the number indicates the grain load/ft ±10%.

## IID

### DETONATION VELOCITY

The average detonation velocity of primacord is between 20,000 and 21,000 ft/sec. Speed-tested primacord having accurately determined velocity is available from the manufacturer.

High velocity (HV) primacord with speeds averaging greater than 22,600 ft/sec is available also from the manufacturer.

The burn rate of PETN 100, plastic primacord is 6.31 mm/4sec ±2%.

## IIE

### AVAILABILITY

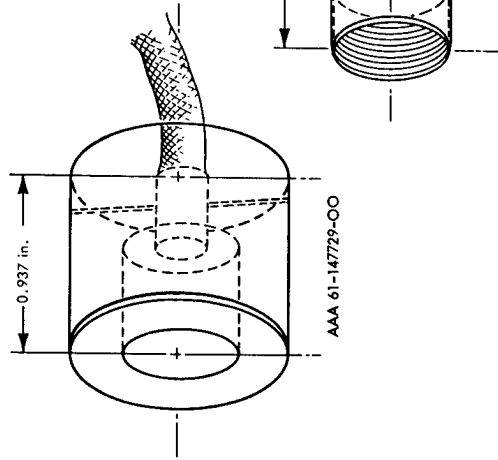
All of the standard type and most of the special type PETN primacords are stock

items with the manufacturer in 500-and 1,000-ft lengths. The PETN 400 plastic is also available in 1-ft lengths, with sealed ends. The only primacord in stock at Site 300 is the special type, PETN 100, plastic.

## USE

The plastic coatings, if undamaged, are almost impervious to water penetration and are unaffected by extremes of winter and summer temperatures normally encountered. The RDX primacords are recommended where temperatures above 284°F are encountered. At temperatures down to -189°F, PETN 100 plastic primacord can be bent to a 3-in. radius without damaging the plastic covering.

The SE-1 detonator can be adapted to the PETN 100 plastic primacord with a SE-1 primacord adapter, Dwg. AAA61-147728-00. Primacord can be adapted to a tetrayl pellet booster with a primacord-pellet adapter, Dwg. AAA61-147729-00. The primacord is fastened to the adapters with a silk pin (regular head pin). Fig. IIF-1 illustrates these adapters.



AAA 61-147728-00

Fig. IIF-1. Primacord adapters. Scale: ≈1.5X.

# IIG MILD DETONATING FUSE (MDF) (ALSO KNOWN AS LOW ENERGY DETONATING CORD, LEDC)

LEDC or MDF consists of a very small, continuous column of explosives in a metal tube. A number of different explosives have been found satisfactory. Core loads in wide range can be prepared and will function. The metal piece can be reinforced with textiles and plastics. The most extensive samples of LEDC made to date have contained one or two grains of PETN in a 0.040-in. o. d. lead alloy tube.

## III

### REFERENCES

1. Primacord Detonating Fuse, What It Is And How To Use It, Fifth printing, The Engin-Bickford Co., Simsbury, Conn., Sept. 1966

The major properties of LEDC are:

- 1) Low brisance. (LEDC has little value as an initiator through its side and will not consistently initiate itself or some explosives laid adjacent to it if unconfined.)
- 2) A detonation velocity in the same velocity range as primacord, approximately 21,000 ft/sec.

## ADHESIVES, FILLERS, AND COATINGS USED WITH EXPLOSIVES

## I

## INTRODUCTION

Adhesives are used to hold together many LRL experimental explosive assemblies because an adhesive causes the least interference with assembly performance.

The subsections herein on adhesives provide the information needed to select an adhesive to meet design criteria, assembly problems, and compatibility requirements for the explosives presently used at LRL. The following is a summary of the four most commonly used adhesives and their best use:

- 1) Adiprene L-100: This adhesive best meets all mechanical and compatibility requirements when explosive bonds are subjected to extended storage periods or temperatures from -65°F to 165°F.
- 2) Eastman 910: This adhesive is ideal where a rapid bond is required and when storage time will be short and at room temperature.
- 3) Gillebreth teflon adhesive: This adhesive is best suited to bond plastics to explosives or to hold small parts in position during assembly.
- 4) Laminac 4116: This adhesive will give good tensile strength within 2 hr. It is usually used for bonding materials other than explosives because it is restricted to the type of explosives it will bond.

NOTE

All the surfaces to be bonded must be free of all foreign matter such as oil, grease, dirt-oxide coatings, and other loose particles. The surfaces must be thoroughly clean and dry.

Use 1, 1, 1-Trichloroethane to clean surfaces to be bonded.

## II

## ADIPRENE L-100

Adiprene L-100 is a liquid urethane polymer which can be cured to a strong rubbery solid. When cured, Adiprene L-100 has a tensile strength of 2700 psi, high resilience, and excellent resistance to abrasion, compression set, oils, solvents, oxidation, ozone, and low temperature embrittlement.

MOCA is a good general purpose curing agent for Adiprene L-100. It provides an excellent balance of cure rate, pot life, vulcanizate properties, and overall handling ease. The best ratio of MOCA for general use is 11 parts per 100 parts by weight of Adiprene L-100. All test and data reported here were made when using 11 parts of MOCA per 100 parts by weight of Adiprene L-100.

## IIA

## WORKING TIME (POT LIFE)

The time required by the mixture to reach a nonpourable viscosity (100,000 cP), measured from the time of addition of curing agent, is the pot life, or working time. MOCA L-100 systems have a pot life of about 10 min at 250°F, 15 min at 212°F, and 3 to 4 hr at 70°F.

The best method of preparing Adiprene L-100 is to heat the MOCA to 212°F or until it is liquid; (DO NOT OVERHEAT). Then add the liquid MOCA to the Adiprene L-100 at room temperature. Mix thoroughly. This method will give a longer pot life and allow longer assembly time.

## IIB

## STORAGE

Storage of Adiprene L-100 is excellent at room temperature in the absence of moisture. Moisture is readily absorbed by Adiprene L-100 and it reacts to form a tough, resilient product, rendering the adhesive useless. Adiprene L-100 should be stored in an inert atmosphere for best shelf life and consistent results.

NOTE

When using Adiprene from the container, it is best to reseal the container with Saran film, discarding the metal cap. This method will provide easy access to the can, provide a far superior seal, and the shelf life will be extended.

## IIC

## ADDITION OF THINNER

It is difficult to get a thin coat of Adiprene L-100 that will flow when applying to metals or explosives. This is especially difficult when assembling components requiring minimum bond-line thickness. The Adiprene L-100 will change from a viscosity of about 10,000 to about 60,000 centipoise (cP) on contact with metal or explosives at 70°F. If 10 parts by weight (pow) of toluene are added to 100 pow of mixed Adiprene L-100, the viscosity is lowered to about 800 and will remain at this consistency for about 2-1/2 hr. The pot life of this mixture is about 5 hr.

The addition of toluene appears to act as a wetting agent. The Adiprene L-100 will flow evenly and can be brushed evenly over metal or explosives. When using toluene as a thinning agent, wait for 20 to 30 min before applying the Adiprene L-100. After application of the adhesive, an open time of several minutes should be used to allow evaporation of the toluene. No tests have been made to determine the effect of toluene on the strength of the Adiprene L-100 system. Preliminary observations indicate there is a decrease in tensile strength.

# BLANK PAGE

## NOTE

The addition of solvents is not recommended where the parts being bonded

will be subjected to environmental tests or long storage periods.

COMPATIBILITY: Table IID-1 and IID-2.

IID

Table IID-1. Chemical reactivity &amp; usage chart for adhesives only

Adhesive	COMP B	TNT	PBX 9404	LX-04-0	RX-04-A-C thru AM	LX-07-0	TETRYL	BARATOL	PBX 9010	PBX 9205	EL 506	RX-12-AB	PBX 9407	PBX 9007
Adiprene L-100	A-1	A-1	A-1	A-1	B-1	A-1	A-1	A-1	A-1	A-1	A-1	B-1		
Adiprene L-167	A-1	A-1	A-1	A-1	B-1	A-1	A-1	A-1	A-1	A-1		B-1		
Adiprene LD-213	A-1	A-1	A-1	A-1	B-1	A-1	A-1	A-1	A-1	A-1		B-1		
Eastman 910	A-2	A-2	A-2	A-2	B-2	B-2	A-1	A-2	A-2	A-2	A-1	B-2		
Laminac 4116	-3	-3	A-1	A-1	B-1	A-1	-3				A-1	B-2		
Gilbreth Teflon			A-2	A-2	B-2	A-2	B-2		A-2		A-1			
Furane X-2	C	C	C	C	C	C	C	C	C	C	C	C	C	C
3M - #465			A-2	A-2					A-2	A-2			A-2	A-2
3M - #466			A-2	A-2					A-2	A-2			A-2	A-2
3M - #Y9146			A-2	A-2									A-2	A-2
Epoxies	C	C	C	C	C	C	C	C	C	C	C	C	C	C

A Compatible. OK for long term storage.

B Compatible. OK for short term storage (less than 30 days).

C Special authorization needed before use.

1 Bond strength equal to explosive.

2 Bond strength below explosive strength.

3 No bond strength.

\* Does not meet environmental test specifications.

A blank space indicates that compatibilities have not been checked.

DO NOT use without written authorization from Hazards Control.

## NOTE

DO NOT MIX explosive fines or powder with any adhesive, filler, or coating without written special authorization from Hazards Control.

Table IID-2. Chemical reactivity &amp; usage chart for fillers &amp; coatings only.

Fillers & coatings	COMP B	TNT	PBX 9404	LX-04-0	RX-04-A-C thru AM	LX-07-0	TETRYL	BARATOL	PBX 9010	PBX 9205	EL 506	RX-12-AB
Silastic RTV <sup>a</sup> 140			A-2	A-2	B-2	A-2						
Silastic RTV <sup>a</sup> 501			A-3	A-3	B-3	A-3			A-3			B-3
Silastic RTV <sup>a</sup> 502			A-3	A-3	B-3	A-3						B-3
Silastic RTV <sup>a</sup> 521			A-3	A-3	B-3	A-3						
Silastic RTV <sup>a</sup> 601				A-3	B-3	B-3						
Silastic Q 90091				A-3		A-3						
Silastic Q 90112			A-3	A-3	B-3	A-3			A-3			B-3
Silastic Q 92009				A-3		A-3						
Silastic Q 93009			A-3	A-3	A-3	A-3						B-3
Epoxy resins	C	C	C	C	C	C	C	C	C	C	C	C
FDA #2 Red			A-3	A-3	B-3	A-3			A-3	A-3		B-3
FDA #2 Green			A-3	A-3	B-3	A-3			A-3	A-3		B-3
DuPont #4817 conductive silver			A-3	A-3	B-3	B-3			B-3			

\* RTV - Room temperature vulcanizing.

A Compatible. OK for long term storage.

B Compatible. OK for short term storage (less than 30 days).

C Special authorization needed before use.

1 Bond strength equal to explosive strength.

2 Bond strength below explosive strength.

3 No bond strength.

A blank space indicates that compatibilities have not been checked.

DO NOT use without written authorization from Hazards Control.

## NOTE

DO NOT MIX explosive fines or powder with any adhesive, filler, or coating without written special authorization from Hazards Control.

### III EASTMAN 910

Eastman 910 is a monomer modified with a thickening agent and plasticizer. It will give rapid and strong bonds between a large number of different materials. This adhesive differs from the conventional adhesive in that it does not require the evaporation of a solvent, does not require pressure, when fasteners are not used. A chemical change occurs when the adhesive film is pressed between the surfaces of two potential adherents, resulting in a strong bond without appreciable change of volume.

The manufacturer reports up to 5180 psi tensile strength for steel-steel bonds, and up to 1,775 psi shear strength for steel-steel bonds; according to his data, Eastman 910 gave exceptional tensile strength through a range of -17°C to 100°C under dry conditions.

Field experience with Eastman 910 has shown that the above tensile values are only applicable when two similar materials are bonded together. When bonding explosives to metal, the bond will age very rapidly, and may fail within a week, unless the bonded parts are maintained at a constant temperature.

#### CAUTION

Do not trust an Eastman 910 bonded joint to be the sole support for holding any explosive charge where the bonded joint is under shear or tension. Even with this restriction, Eastman 910 is used quite extensively in the trim and assembly of explosive components in gyro and device shots.

### III A APPLICATION

1) The adhesive is applied from a container by means of a clean medicine dropper or with a glass rod that is cooled. It is not recommended that Eastman 910 be brushed or rolled onto a surface prior to bonding. The pressure of applying causes partial polymerization on the surface of the adhesive monomer, thereby rendering the adhesive useless.

2) After the adhesive has been spread over one surface, immediately place the mating surface in contact with the adhesive coated surface. Apply manual pressure until bond has set, usually only a few seconds.

3) This adhesive acts similar to pressure sensitive adhesives, and will adhere only when a thin layer is pressed between two parts. Eastman 910 cannot be used for gap filling or where the parts being bonded do not mate. The success of Eastman 910 bond depends on the tolerance between the surfaces

being bonded. Smooth surfaces having intimate contact are more readily bonded. Where intimate contact is found, set-up time or polymerization will take place practically instantaneously. Where the parts to be bonded do not mate perfectly, the adhesive will fill the gaps up to 0.010 in. A thickening agent is set in use. The addition of Santocel-54 to Eastman 910 to increase the viscosity to 300-500 cP will make a good bond possible. When the thickened Eastman 910 is used, it is advisable to use a catalyst, phenyl ethyl ethanamine. Mix 5 to 15 pbw of catalyst to 100 pbw of acetone. Paint the catalyst solution on the surface (the inert material, not the explosive) and then apply the Eastman 910 to the mating surface and assemble. The set up time will be up to 10 sec, depending on the materials being bonded and the amount of catalyst used.

4) On all applications of Eastman 910, do not use excess adhesive. Any excess that oozes out will dissolve the explosive in that area.

5) The Eastman 910 bond is brittle, and shock or thermal expansion of the adherents may break the bond. The addition of 5% by weight of dimethyl sebacate to Eastman 910 will help eliminate the brittle bond joint, but will not lower the bond strength, according to our tests.

#### CAUTION

Do not use Eastman 910 on detonators or tetryl pellets. This adhesive acts as a solvent and will distort the dimensions of the detonators.

If Eastman 910 adhesive will not set up properly, it probably has an over balance of inhibitor. In this case, do one of the following:

- 1) Leave cap off container for a few hours to allow SO<sub>2</sub> to escape.
- 2) Purge with dry nitrogen.
- 3) Stir gently while under slight vacuum.

### IIIB STORAGE

Store in a closed container in a cool place. The moisture in the air will react with the adhesive. Under ideal conditions shelf life can be up to 2 yr.

### IIIC CARE IN HANDLING

Avoid spilling of the adhesive since it adheres tenaciously to skin, clothing, and furniture. If skin contact occurs, the affected parts should be flushed immediately with water. The resulting solid will usually wear off during the course of a day without any ill effects or irritation of the skin.

### APPLICATIONS

The adhesive may be used for bonding most materials and is excellent for gap filling. The manufacturer claims the tensile strength of Laminac 4116 to be 6,800 psi, with good dielectric strength. Tests at LRL indicated a tensile strength of 1,135 psi when bonding beryllium and 482 psi when bonding 9404 explosive formulations to steel. The bond is quite brittle.

For filling voids, making vacuum tight joints, or where a more viscous or putty-like adhesive with short gel time is required, the addition of Santocel-54 to Laminac 4116 will prove quite satisfactory.

Laminac 4116, or most polyesters, are not recommended where bonds will be subjected to long storage or elevated temperatures.

#### CAUTION

Laminac 4116 will produce an exothermic reaction that may exceed 500°F when allowed to cure in large quantities or when poured into a large void.

DO NOT MIX explosive powder or fines with Laminac 4116.

DO NOT use bond lines over 0.125 in. thick.

WORK TIME AND CURING AGENTS  
Laminac 4116 will have a working time, or pot life, of about 10 min when mixed as follows:

MATERIAL	pbw (g)
Resin: Laminac 4116	100.0
Catalyst: methylethylketone (mek) peroxide	1.5
Accelerator: cobalt naphenate (5% metal, by wt)	0.3

#### CAUTION

The accelerator may be added to the resin, and thoroughly dispersed prior to the addition of the required amount of catalyst. DO NOT mix accelerator and catalyst together--A violent reaction may result.

By increasing or decreasing the amount of catalyst, pot life can be varied from 5 min to 2 months. Laminac 4116 as received may contain accelerator, which is indicated by pink color. Tests should be made with each shipment to determine exact gel time. If Laminac 4116 is received in pink color, it is NOT pink if DMA is used as the accelerator, additional accelerator (cobalt naphenate) can be reduced or eliminated from the mix formula.

Eastman 910 is a mild lachrymator (or tear producer) and must be kept away from the eyes and mucous membranes. Use this adhesive in areas with good ventilation.

### IIID CURE TIME

Set time varies from 5 sec to 1 min, depending on material being bonded. For all practical purposes, 5 to 25 sec is maximum working time. The ultimate tensile strength is not reached until 24-48 hr at room temperature have elapsed.

### IIIE COMPATIBILITY

See Tables IID-1 and IID-2.

### IIIF PROPERTIES

Viscosity at 25°C (Brookfield): 100 cP  
Specific gravity: 1.11 g/cm<sup>3</sup>  
Softening point: 165°C  
Solubility: Soluble in N, N-dimethyl formamide

Dielectric constant at 1 Mc (ASTM D-924-49): 3.34

Dissipation factor at 1 Mc (ASTM D-925-490): 2.02

Tensile strength, steel-steel (Fed. Spec. MMM-A-175): 3,800 psi

### IV GILBRETH TEFLON ADHESIVE

Gilbreth teflon adhesive dries to a pressure-sensitive surface that is serviceable from -50°C to 250°C. This cement is ideal for bonding Teflon, rubber, Mylar, polyethylene, silicone glass laminates, and metals where a strong bond or high tensile strength is not required.

### IV A APPLICATION

Brush adhesive over both surfaces. Allow solvent to evaporate for approximately 30 min until adhesive attains an aggressive tack. Components are then pressed together.

To cut down on the 30 min open time by approximately 90%, gently play dry compressed air for 5 min, press one over open surfaces of the adhesive. Do not let a stream of compressed air rip the adhesive surface. If adjustments are to be made after placing surfaces are to be bonded together, do not give full open time.

### IV B COMPATIBILITY

See Tables IID-1 and IID-2.

### V LAMINAC 4116

Laminac 4116 is a room-temperature-cure unsaturated polyester resin. It has a gel time of 5 to 20 min, depending on amount of catalyst and/or accelerator used. Laminac 4116 will have good strength after 2 hr. Maximum strength will be attained in about 24 hr at room temperature. Tests at Picatinny Arsenal indicate tensile values over 1,200 psi on cadmium-plated steel after 2 hr cure at room temperature.

**VC COMPATIBILITY**  
See Tables IID-1 and IID-2.

**VD PROPERTIES**

Viscosity	450 cP
Specific gravity	1.12
Shrinkage during cure	6.5%
Hardness, Barcol	6,000 psi
Tensile strength	22,000 psi
Compressive strength	30,000 psi
Dielectric constant at 60 cps	3.15
Power factor at 60 cps	0.0039
Dielectric strength at 77°F	380 V/mil
Dielectric strength at 212°F	300 V/mil

**VI ADIPRENE LD-213**  
Adiprene LD-213 is a liquid urethane polymer, which when cured with MOCA yields vulcanizates that are harder and more abrasive resistant than those obtainable from Adiprene L-100 or L-167. These vulcanizates also exhibit the typical resilience and resistance to impact and low temperature embrittlement characteristic of elastomers. Adiprene LD-213 hardens to 60 to 75 Shore D.

**VIA CURING AGENT**  
MOCA is the preferred curing agent because it combines maximum pot life with excellent vulcanizate properties. The best balance of properties for general use is obtained when 25 pbw of MOCA is added to 100 pbw of LD-213. Heat MOCA to 212°F or to a liquid; then add to Adiprene LD-213.

Table IVA-1. Curing conditions for LD-213.

Mix temp	Pot life	Cure temp	Cure time
175°F	3 min	212°F	1 hr
175°F	3 min	285°F	1/2 hr
75°F	8 min	75°F	24 hr (min)

**VIB STORAGE**  
Same as for Adiprene L-100 (See Sec. IIB).

**VIC COMPATIBILITY**

See Tables IID-1 and IID-2.

**VII**

**ADIPRENE L-167**  
Adiprene L-167 is a liquid urethane rubber which can be cured like Adiprene L-100 to a strong rubbery solid. The vulcanizate is hard and abrasive resistant. It has great resistance to deformation and high load-bearing capacity. Adiprene L-167 is normally used hardens to 90 to 95 Shore A.

**CAUTION**  
Adiprene L-167 contains a small amount of volatile isocyanate. Use with adequate ventilation. Avoid skin contact. If accidentally spilled on skin, remove promptly.

**CURING AGENT**  
MOCA is the preferred curing agent for Adiprene L-167 because it provides maximum pot life with good physical properties. Sixteen pbw of MOCA to 100 pbw of Adiprene L-167 is a good mix for general use. Heat MOCA to 212°F or to melting point; then add to Adiprene L-167.

**STORAGE**  
Same as for Adiprene L-100 (See Sec. IIB).

**COMPATIBILITY**

See Tables IID-1 and IID-2.

**EPONY RESINS**

Uncured (liquid) epoxy-resin aliphatic-amine systems are not compatible with most explosives and propellants. However, epoxy resin and aliphatic and/or aromatic amine systems are considered compatible if they are in the fully cured condition (i. e., epoxy laminates, etc.).

Furane X-2 has been found to be quite reactive with most explosives used by LRL. Any use of Furane X-2, with or without catalyst, must have prior written approval from Hazards Control.

**TRANSFER ADHESIVES**

The following lists of tapes have been found to be compatible with the various high explosives used for device and hydro assemblies. Any new tape not listed should be referred to Hazards Control before use:

**Manufacturer**

**Trade Name**

**Number**

**Color**

3M	Scotch Brand Electrical Tape	#33	Black
3M	Scotch Brand Mylar	#56	Yellow
3M	Scotch Brand Electrical	#57	Yellow
3M	Scotch Brand Masking	#232	Tan
3M	Scotch Brand Photo Tape	#233	Black
3M	Scotch Brand Double Sided Masking	#400	Tan
3M	Scotch Brand Double Sided Masking	#420	Lead
3M	Scotch Brand Double Sided Masking	#468	Tan
3M	Scotch Brand Plastic	#471	Tan
3M	Scotch Brand Plastic	#471	Yellow
3M	Scotch Brand Cellophane Tape	#471	Red
3M	Scotch Brand Cellophane Tape	#600	White
3M	Scotch Brand Cellophane Tape	#850	Clear
3M	Scotch Brand Magic Mending	#810	Clear
3M	Scotch Filament Tape	#880	Clear
Behr-Manning	Scotch Brand Double Sided Masking	#Y9146	pearl
Hampton Mfg. Co.	Bear Tape	#4/1	Tan
Mystic Tape Inc.	Blue Cross Tape	----	Tan
Okonite	Mystic Tape	#5803	Yellow
Permaceel	High Voltage Rubber Tape	----	Black
Permaceel	permaceel	#29	Brown
Permaceel	permaceel	#32	Black
Saunders Engr. Corp.	permaceel Cellophane Tape	----	Red
Tech. Tape Corp.	Teflon Tape	#S15, S16, S18	Clear
Tech. Tape Corp.	Tuck Tape	----	Blue/brown
Tech. Tape Corp.	Tuck Tape	----	Yellow
Tech. Tape Corp.	Tuck Tape	----	Black

**X**

**CRACK-DETECTING FLUIDS**

Food and Drug Administration (FDA) RED #2 and FDA GREEN #3 food coloring have been found to be exceptional crack detecting fluids when mixed in the following proportions:

Materials	phw (g)
FDA powder (red or green)*	0.08
Ethyl alcohol	16.50
Tap water	46.4
Aerosol wetting agent (BKH Catalog #2520)**	0.45

Paint the above solution over the portion of the suspected crack; then wipe area clean with water-wet Kimwipe or lint-free cloth. On close examination, cracks that are undetectable by radiography and visual inspection will appear as very thin colored lines. These cracks can be easily photographed.

\*Available from Site 300.

\*\*Braun, Knecht, Heilmann Co., Div. Van Waters & Rogers, Inc.

The use of two colors will make it possible to determine when cracks occurred if the piece is subjected to repeated tests.

The above formula has proven quite practical because the solution can be easily removed from the test piece to reveal the crack. If excess FDA coloring powder is used, the dye will be difficult to remove from the treated surfaces. Use water to remove excess dye.

**COMPATIBILITY**  
See Table IID-2.

**ADHESIVES BIBLIOGRAPHY**

1. Blasters' Handbook (A manual describing explosives and practical methods of using them.) E. I. DuPont de Nemours and Co., Wilmington, Del., 14th. Ed. (1958).
2. Eastman 910 Adhesives, Bulletin No. R-103, Eastman Chemical Products, Inc., Kingsport, Tenn. (1958).
3. Furane Resinate Adhesive, Type X-2, Epocast Technical Bulletin EP-57-25, Furane Plastics, Inc., Los Angeles, Calif. (June 1957).

## SOLID PROPELLANT GAS GENERATORS

## I INTRODUCTION

Solid propellant gas generators are compact sources of high pressure gas that can be used to drive a wide variety of auxiliary power units and actuators. They have been used at LRL to drive turbines and positive displacement motors. Their chief advantage over pressure vessels as a source of high pressure gas is that they are much more compact. For example, gas generators

weigh 1/3 to 1/2 less than high-strength titanium-alloy pressure vessels that deliver the same amount of gas.

The essential parts of a gas generator, as shown in Fig. I-1, are:

- 1) Solid propellant
- 2) Igniter
- 3) Inhibitor
- 4) Nozzle
- 5) Pressure vessel (case)

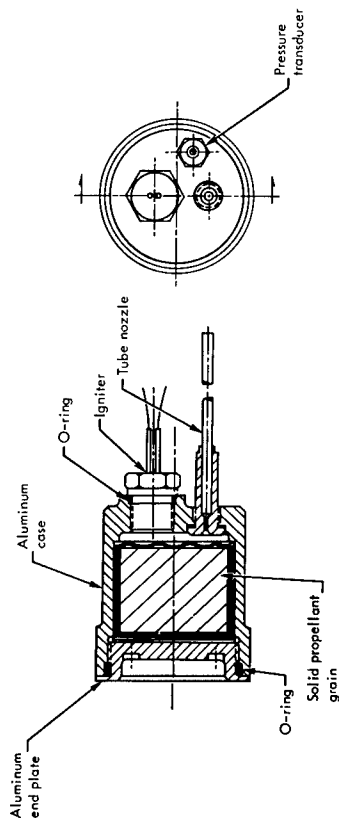


Fig. I-1. Cross section view of a small gas generator.

To operate the gas generator, the igniter is fired by an electric pulse. The igniter pressurizes the pressure vessel chamber up to the optimum burn pressure for the propellant and ignites the propellant. As the propellant burns, the combustion gases pass out through the nozzle. The propellant burns only on the surfaces not covered by the inhibitor.

Gas generators that have been developed for use at LRL are listed in Table I-1. These gas generators have been tested, and test results are available from De-vice Engineering Division. Some of these gas generators are in stock at Site 300. A typical gas generator is shown in Fig. I-2.

# BLANK PAGE

Table I-1. Gas generators developed for LRL.

Item	Propellant type	Flame temp (°F)	Chamber press (psia)	Flow rate (lb/sec)	Burn time
1. LRL Drawing No. L15A 4133	Double-base X-13	3200	1000	0.005	5 sec
2. LRL Drawing No. L114C 3193	"	"	"	.013	"
3. LRL Drawing No. L13H 2313	"	"	"	.026	"
4. LRL Drawing No. L16A 3193	Double-base X-9	"	"	.052	"
5. LRL Drawing No. L16A 3263	"	"	"	.104	"
6. LRL Drawing No. L16A 3233	Ammon. nitrate compos. OMAX 452	2000	"	.006	"
7. LRL Drawing No. L2G 1363	"	"	"	.014	"
8. LRL Drawing No. L12C 1193	"	"	"	.029	"
9. LRL Drawing No. L12C 1303	"	"	"	.057	"
10. LRL Drawing No. L12C 1263	"	"	"	.114	"
11. LRL Drawing No. L12G 1273	Ammon. nitrate compos. APF-176	"	400	.025	4 sec
12. NOTS No. SK-6119-26	Double-base X-9	3200	660	.014	18 sec
13. AiResearch No. 551090 Mod. No. PUA1-1-1-1	Ammon. nitrate compos.	2000	1000	0.055	20 sec

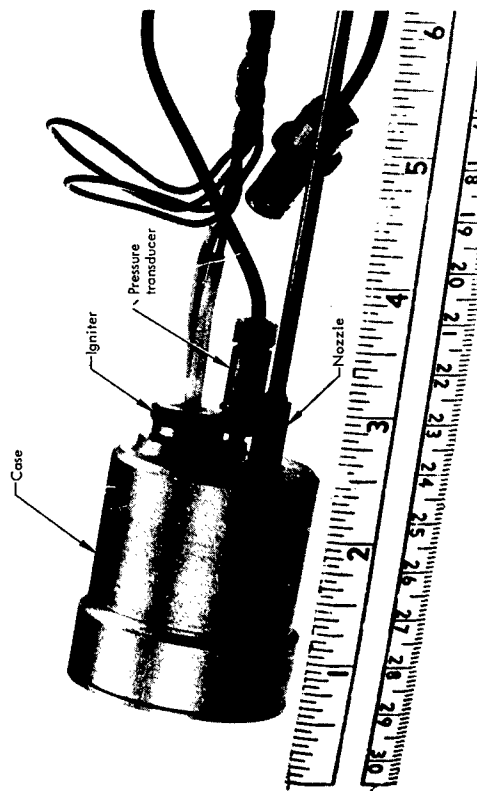


Fig. 1-2. A 5-hp gas generator for auxiliary power use. Weight: 6-1/2 oz.

## II SOLID PROPELLANTS

## IIA TYPES

Two types of solid propellants are used in gas generators: (1) double-base propellants and (2) composite propellants. Double-base propellants are made of nitroglycerin and nitrocellulose. Composite propellants are made of particles of an oxidizer, such as ammonium nitrate or ammonium perchlorate, mixed with an elastomer or plastic which serves as fuel. Both types of propellants contain small amounts of other substances that are added to modify the burning characteristics or to improve the workability, reliability, or storage life.

Solid propellants are cast, molded, or extruded into various shapes called grains. Typical propellant grain shapes are shown in Fig. IIA-1.

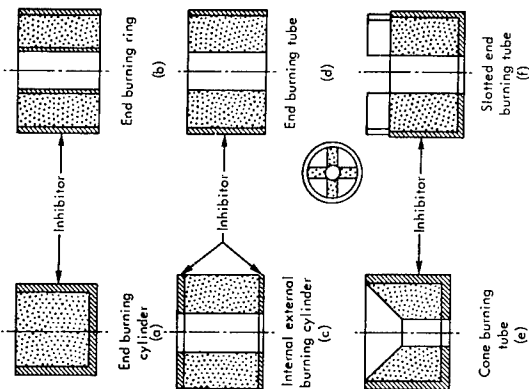


Fig. IIA-1. Some common grain shapes for solid propellants.

## IIIB

## BURNING CHARACTERISTICS

The grain burns only on the uninhibited surface and burning progresses into the grain in a direction normal to the surface except at sharp corners and over complex surfaces. Burning rates of commonly used propellants range from 0.03 to 1.0 in./sec. Increasing the chamber pressure or the grain temperature

causes an increase in the burning rate as shown in Eq. 1.

$$r = aP_c^n \quad (1)$$

where

$r$  = burning rate, in./sec

$a$  = coefficient dependent on grain

$P_c$  = chamber pressure, psia

$n$  = exponent that is characteristic of each specific propellant.

A plot of the burning rate data obtained on a typical composite propellant is shown in Fig. IIB-1. This figure also shows the effect of grain temperature on the burning rate. Burning rates for most propellants will plot as a straight line on log-log paper, but there are some propellants in which there are sharp changes in slope of the burning rate curve. Burning rate curves on this type are shown in Fig. IIB-2.

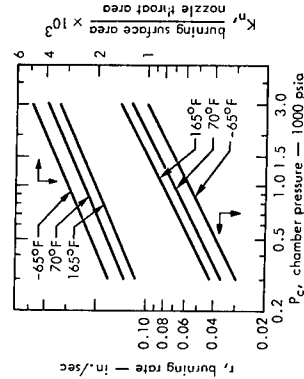


Fig. IIB-1. Burning rate curves for a composite solid propellant.

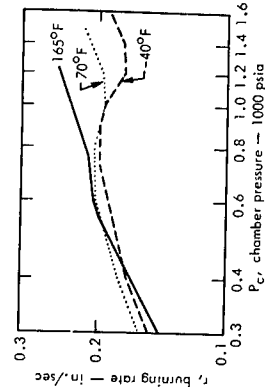


Fig. IIB-2. Burning rate curve for a double-base solid propellant. (Not typical)



In hollow grains, the burning rate is also affected by erosive burning. Part of the grain nearest the exhaust nozzle is eroded by high velocity gases flowing parallel to the burning surface. This erosion causes an unusually high local burning rate. Slow burning propellants are more susceptible to erosive burning than fast burning propellants. When erosive burning is expected, the burning rate equation must be modified empirically.

The rate at which gases are liberated from the burning surface of the propellant may be calculated by the mass flow rate equation:

$$\dot{m} = r A_s \rho_p \quad (2)$$

where

$\dot{m}$  = mass flow rate, lb/sec

$r$  = burning rate, in./sec

$A_s$  = propellant burning surface area, in.<sup>2</sup>

$\rho_p$  = density of propellant, lb/in.<sup>3</sup>

This equation shows that if  $A_s$ , the propellant burning surface area, remains constant, the mass flow rate remains constant. Propellant grains designed to have a burning area that remains constant during the burning time, such as those shown in Fig. IIB-2, are called neutral burning grains. Grain shapes in which the burning surface area increases with burning time are progressive burning grains and those in which the burning surface area decreases with burning time are regressive burning grains.

Theoretically, the chamber pressure,  $P_c$ , should not increase when a neutral grain is burned. However, with small neutral grains, the mass and specific heat are so small that the grain will be heated appreciably during burning, and the burning rate

will increase with a consequent increase in chamber pressure. With small regressive grains, this heating effect may cause the grain to burn as a neutral grain. The pressure profiles for a neutral grain and a regressive grain that exhibit these effects are shown in Figs. IIB-3 and IIB-4.

Other factors that may affect the burning characteristics of the propellant are cracking of the grain and separation of the inhibitor. If the grain cracks because of a cyclic environmental temperature, the burning surface area of the propellant will change and its performance will be unpredictable. Likewise, cyclic temperatures may cause the inhibitor to separate from the grain with a resultant increase in the burning surface area.

Many propellants will not sustain combustion at atmospheric pressure. If the chamber is opened to atmospheric pressure, combustion will stop. Thus characteristic is often used to make gas generators safer by providing them with a disk that ruptures when the design pressures are exceeded.

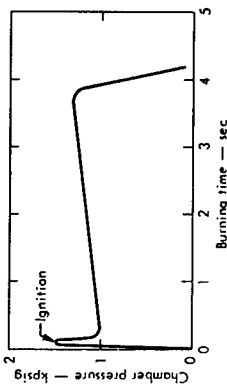


Fig. IIB-3. Pressure profile for a 5-hp gas generator using a double base, neutral grain, solid propellant.

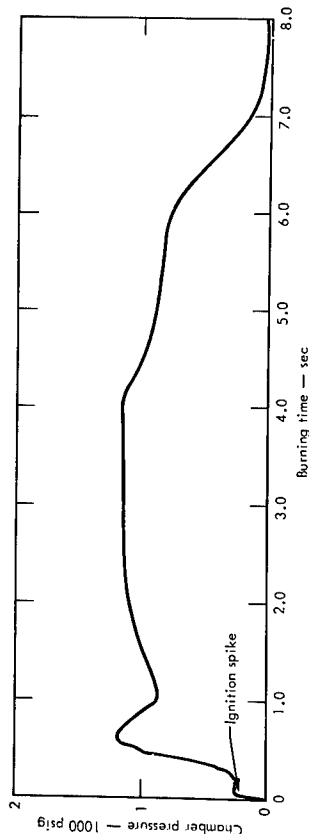


Fig. IIB-4. Pressure profile for a 5-hp gas generator using a composite, regressive grain, solid propellant.

## IIC

### STORAGE LIFE

The storage life of solid propellants is quite variable. Some propellants may be stable for less than a year while others can be stored for as long as ten years. The nitroglycerin-nitrocellulose double-base propellants slowly decompose, and the decomposition products catalyze the decomposition reaction. Various substances are added to compensate for this reaction, but double-base propellants must be selected with care if they are going to be stored for long times, especially at temperatures above 140°F.

Some of the composite propellants are hygroscopic and should not be exposed to air of greater than 40% relative humidity. Ammonium nitrate, which is used in many composites, goes through a phase change at 39°F, which causes a significant increase in volume. If an ammonium nitrate composite propellant is stored where the temperatures will fluctuate above and below 39°F, there may be some problems caused by the alternate expansion and contraction of the propellant.

In some propellant formulations, one of the chemicals may migrate during storage and react with other chemicals in the grain or in the inhibitor. With some double-base propellants, the adhesive used to bond the inhibitor to the grain reacts with the inhibitor and causes a local change in the ballistic properties of the propellant.

## IID

### PROPERTIES

The properties of propellants are not listed here because it is impossible to select a typical propellant and because new and better propellants are being formulated every year as the knowledge of propellant chemistry increases. Before designing a solid propellant gas generator, the designer should call propellant manufacturers or consult the Propellant Manual, SP1A-M2, 1 for the latest information on the properties of solid propellants. The Propellant Manual, published by the Chemical Propulsion Information Agency, is revised annually and contains the following information:

- 1) Composition
- 2) Ballistic properties
  - a) Burning rate curves
  - b) Specific impulse
  - c) Characteristic exhaust velocity
  - d) Burning rate sensitivity to temperature at constant pressure
  - e) Combustion pressure sensitivity to temperature
- 3) Thermodynamic properties of propellant
  - a) Heat of explosion
  - b) Specific heat
  - c) Heat of formation
  - d) Flame temperature

## 4) Thermodynamic properties of combustion products

- a) Composition
- b) Mean molecular weight
- c) Temperature
- d) Enthalpy
- e) Entropy
- 5) Physical and mechanical properties
  - a) Modulus of elasticity
  - b) Tensile strength
  - c) Strain at maximum stress
  - d) Strain at break
  - e) Poisson's ratio
  - f) Density
  - g) Coefficient of linear thermal expansion
  - h) Coefficient of volume thermal expansion
  - i) Thermal conductivity
  - j) Stability and sensitivity
  - 7) Manufacturing processes
  - 8) Current status

## III

### IGNITERS

The purpose of igniters is twofold:

- 1) To pressurize the gas generator to the pressure at which the solid propellant will reliably support combustion.
- 2) To produce a hot flame which will ignite the solid propellant grain.

Most igniters are initiated by an electric squib or electrically heated wire surrounded by a small charge of primary explosive (primer). The primer ignites either a main charge or a booster charge which ignites a sustaining charge. Two types of igniters are shown in Figs. III-1 and III-2.

The igniter is the most critical part of a gas generator system and must be carefully designed to insure that the system is reliable. Most gas generator development problems stem from improper igniter design.

Some of the factors which must be considered when designing an igniter are:

- 1) Composition of grain: Double-base propellants are easier to ignite than composite propellants. Some propellants have a higher threshold ignition pressure than others. Some propellants are difficult to ignite when stored a long time.
- 2) Shape of grain: End-burning grains are easier to ignite than internal-burning grains.
- 3) Location of igniter with respect to grain: If the igniter is too close to the grain, it may blow part of the grain away and increase the burning surface area.

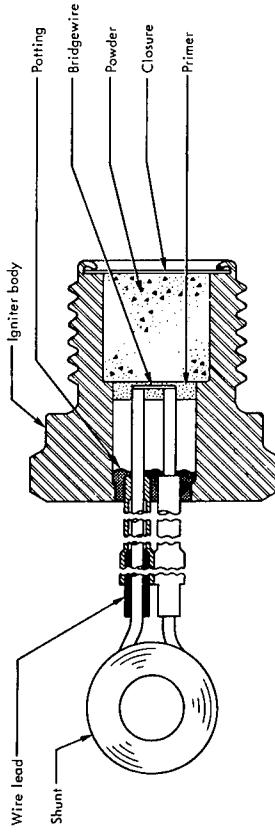


Fig. III-1. Igniter for a composite solid propellant.

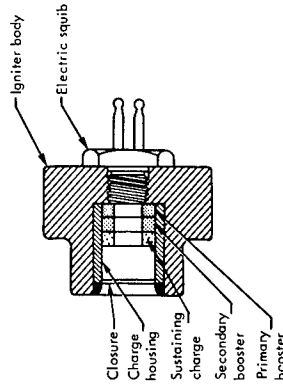


Fig. III-2. Igniter for a double-base solid propellant.

4) Electrical energy required to fire igniter: For reliable ignition, the available electrical energy must be greater than the minimum electrical signal that will cause firing. For safety, the minimum electrical signal that will fire the igniter should be high enough so that static electricity or induced currents from stray electromagnetic radiation (radar, radios, etc.) will not fire the igniter.

5) Ignition pressure rise time: If the ignition pressure rises too rapidly or too high, the grain may crack or the rupture disc may fail. If it rises too slowly, the grain may burn erratically before proper ignition is established.

6) Sealing: Most igniters must be hermetically sealed. Seal materials must be carefully selected because debris from the seals may inhibit burning or delay ignition of the grain.

7) Compatibility of materials: Sometimes it is necessary to separate the igniter charge materials with thin shims. For detailed information on the design of igniters, refer to the Solid Propellant Igniter Design Handbook.<sup>2</sup>

#### IV INHIBITORS

Inhibitors (restrictors) are materials which prevent burning on the surface of a solid propellant grain. They are used to restrict burning to the desired surface area of the grain. Inhibitors for double-base propellants are made of ethyl cellulose or cellulose acetate. Inhibitors for composite propellants are made of the same elastomer or resin that is used as fuel in the propellant. Usually an inorganic salt is mixed with the elastomer or resin.

It is important to match the thermal coefficient of expansion of the inhibitor with that of the propellant and to get a good bond between the inhibitor and the propellant. If this is not done, the inhibitor may separate from the propellant, causing an increase in the burning surface area with a resultant decrease in burn time and increase in chamber pressure.

During burning of the propellant, the inhibitor may also burn or it may decompose by pyrolysis. The decomposition products of some inhibitors contain tars and gummy residues. If a clean gas is desired, inhibitors of this type should be avoided.

#### V NOZZLES

Nozzles are used to control the flow rate of the gases evolved from the burning of solid propellant. When designing nozzles for gas generators, the ballistic characteristics of the solid propellant must be considered. For stable operation, the mass flow rate from the nozzle exit must equal the mass flow rate from the burning propellant. As shown in Eq. (2), the

mass flow rate from the burning propellant is

$$\dot{m} = r A_s \rho \quad (3)$$

and

$$r = a P_c^n \quad (4)$$

therefore

$$\dot{m} = a P_c^n A_s \rho \quad (5)$$

(Refer to Table V-1 for nomenclature)

Table V-1. Nomenclature for solid propellant gas generators.

Symbol	Description	Dimensions
a	Burning rate coefficient	in./sec psi
A <sub>s</sub>	Propellant burning surface area	in. <sup>2</sup>
A <sub>t</sub>	Nozzle throat area	in. <sup>2</sup>
C <sub>g</sub>	Characteristic exhaust velocity	ft/sec
C <sub>D</sub>	Nozzle discharge coefficient	sec <sup>-1</sup>
g	Gravitational constant	ft/sec <sup>2</sup>
k <sub>n</sub>	Burning surface area: nozzle area ratio	dimensionless
M	Mean molecular weight	lb M
n	Mass flow rate: burning rate pressure exponent	lb/sec dimensionless
P <sub>c</sub>	Chamber pressure	psia
R	Gas constant	ft-lb/lb-mole °R
r	Burning rate	in./sec
ρ	Propellant density	lb/in. <sup>3</sup>
T <sub>p</sub>	Propellant flame temperature	°R
t <sub>b</sub>	Burn time	sec
V <sub>p</sub>	Volume of propellant	in. <sup>3</sup>

The mass flow rate through the nozzle is

$$\dot{m} = C_D P_c A_t \quad (6)$$

If the mass flow rates are equal,

$$a P_c^n A_s \rho = C_D P_c A_t \quad (7)$$

or

$$P_c = \left( \frac{a A_s \rho}{C_D A_t} \right)^{\frac{1}{1-n}} \quad (8)$$

Quite frequently Eq. (7) is written as

$$P_c = \left( \frac{a A_s \rho C_g^{1-n}}{A_t g} \right)^{\frac{1}{1-n}} \quad (9)$$

where

$$C_g^* = \frac{g}{C_D} \quad (10)$$

C<sub>g</sub><sup>\*</sup>, the characteristic exhaust velocity, is always given in any compilation of solid propellant data.

Equations (9) and (10) show that the chamber pressure, P<sub>c</sub>, is dependent on the ratio A<sub>s</sub>/A<sub>t</sub> as well as the characteristics of the propellant and the nozzle. The ratio A<sub>s</sub>/A<sub>t</sub> is called k<sub>n</sub>, the ratio of the propellant burning surface area to the nozzle area. The effect of k<sub>n</sub> on chamber pressure and its consequent effect on propellant burning rate is shown in the upper curves of Fig. III-1. These curves show that if k<sub>n</sub> decreases slightly because of erosion of the nozzle, there will be a large decrease in chamber pressure and a consequent decrease in burning rate.

After the solid propellant has been selected and the grain designed, the nozzle throat area, A<sub>t</sub>, can be calculated by using Eq. (9) or by selecting a value of k<sub>n</sub> from the propellant burning curve.

In large gas generators, which are not considered here, the design of the nozzle is complicated and the effects of nozzle erosion must be considered. However, in small gas generators, the simple tube nozzle or orifice has proven to be reliable. One such tube nozzle that has been used at NRL is shown in Fig. I-1. Because erosion of the tube nozzle occurs only near the entrance end, the controlling diameter of the nozzle does not change. For this reason, tube nozzles can be cleaned and reused several times. The controlling diameter of tube nozzles should be accurately machined, however, because diameter variations of 1 mil will cause changes in chamber pressure as high as 22%.

When using a solid propellant that has a high ignition pressure, it may be necessary to provide a frangible nozzle closure to prevent the escape of gas during ignition. The closure material should be carefully selected because debris from the closure may damage the power unit being driven by the gas generator.

When the gas generator is not integrated with the power unit, some sort of plumb- ing is required to connect the nozzle with the power unit. If tubing is used, it should have good high temperature strength. Thin-walled titanium or molybdenum tubing has been used successfully. Stainless steel tubing should be relatively thick-walled except when the mass flow rates are low. The diameter of the tubing should be at least 1-1/2 times the nozzle diameter to avoid choking the gas generator.

Tube fittings should also have good high temperature strength. If threaded fittings are used in the nozzle area, they may loosen because of the vibrations in this area. Welded fittings are preferred over brazed fittings because the strength of brazing alloys is marginal at exhaust gas temperatures.

#### PRESSURE VESSEL

The pressure vessel or case must be designed to withstand the peak pressures that may develop in the combustion chamber. If there is any uncertainty as to what peak pressures may develop under varying environments, the case is equipped with a rupture disc. Rupture of the disc reduces the chamber pressure to a level at which propellants do not burn or burn slowly.

Selection of the case material depends on the type of propellant grain used. If an external burning grain is used, the material with good high temperature strength, such as aluminum or stainless steel, must be selected. If an internal burning grain is used, aluminum alloys or glass-reinforced plastics can be used. Sometimes an insulator or ablative material is wrapped around the propellant grain to keep the case temperatures low.

Threaded closures are often used to seal the case. If the closures are located where the peak temperature occurs near the end of the burning time, rubber O-rings may be used as seals for the closures. Experience at LRL has shown that these O-rings can often be re-used.

#### VII

##### DESIGN PROCEDURE

Before an engineer can design a gas generator, he needs to know:

- 1) How much energy is required?
- 2) At what rate is the energy required?
- 3) How much space is allowed for the gas generator?
- 4) Must the gas be exceptionally clean?
- 5) What is the maximum allowable flame temperature?
- 6) What are the temperature and pressure extremes of the environment?
- 7) How long will it be stored?

When all these questions are answered, contact the solid propellant manufacturers, some of which are listed under "References." They may have the required gas generator in stock.

If it is necessary to design a new gas generator, some trial calculations must first be made before a propellant can be selected. In a typical design problem the following requirements are listed:

- 1) Horsepower, hp
- 2) Burn time,  $t_b$ , sec
- 3) Size of generator (volume)

#### IX

##### SAFETY

Because solid propellant gas generators contain explosives, Hazards Control must be consulted to establish proper procedures for handling them in the areas where the generators are to be used.

#### VIII

##### QUALITY CONTROL

To insure a high degree of reliability of gas generators, the quality of the solid propellant must be carefully controlled. In a gas generator development program conducted by Sandia, it was necessary to x-ray the solid propellant grains because voids, low density areas, and inhibitor separations would cause the burning rate or chamber pressure to fall outside of the design specifications. In addition, it was necessary to test fire the first and last grains made from each lot of propellant.

#### X

##### REFERENCES

1. Propellant Manual, SPIA/M2 (Conf.), Chemical Propulsion Information Agency, Applied Physics Laboratory, Johns Hopkins University, Silver Springs, Maryland (revised periodically).
2. Solid Propellant Igniter Design Handbook (Conf.), CPIA Publication No. 14, Chemical Propulsion Information Agency, Applied Physics Laboratory, Johns Hopkins University, Silver Springs, Maryland (1963).
3. Solid Propellant Gas Generators Data Pak, Sixth Edition, Associated Products Operations, Olin Mathieson Chemical Corp., East Aton, Illinois (1966).
4. Solid Propellant Ballistic Data (Conf.), Rev. D, Amoco Chemicals Corp., Propellants Division, Seymour, Indiana (1962).
5. Explosive Ordnance Technical Data Book, McCormic Selph, Hollister, Calif. (1964).
6. Propellant Products Data Pak, Holes, Inc., Hollister, Calif. (1964).
7. Ray, G. A., Jr., Characteristics and Development Report for the MC-1557 Gas Generator, SCDR 306-62, Sandia Corp. (1962).
8. Pollard, F. B. and Arnold, J. H., Jr., Aerospace Ordnance Handbook, Proutice-Hall, Inc., Englewood Cliffs, N. J. (1966).

**END**

**DATE FILMED**

**9 / 28 / 67**